Neuronal IL-17 controls *C. elegans* developmental diapause through CEP-1/p53

Abhishiktha Godthi[1,2,], Sehee Min[1,2,], Srijit Das[1], Johnny Cruz-Corchado[1,2], Andrew Deonarine[1], Kara Misel-Wuchter[3], Priya D. Issuree[3] and Veena Prahlad[1,2] *

Affiliations: [1]Department of Cell Stress Biology
Roswell Park - Comprehensive Cancer Center
Elm and Carlton Streets
CGP-BLSC L3-307
Buffalo, New York 14263

[2]Department of Biology,
338 Biology Building East,
143 Biology Building, Iowa City, IA 52242-1324.

[3]Department of Internal Medicine,
503 Eckstein Medical Research Building,
431 Newton Road, Iowa City, IA 52242

* Corresponding author email: : veena.prahlad@roswellpark.org

Abstract. How metazoan development is coordinated with nutrient availability remains unclear. Here, we show that the activity of CEP-1, the *C. elegans* ortholog of the tumor suppressor p53, switches organismal development between reproductive growth and dormancy by responding to nutrient availability signaled by neuronal cytokine, ILC-17.1. Specifically, ILC-17.1 is released from amphid neurons upon food availability and promotes glucose utilization and represses CEP-1/p53: CEP-1/p53 repression promotes growth. In the absence of ILC-17.1, CEP-1/p53 is activated, accumulates in post-embryonically dividing progenitor blast cells, upregulates cell-cycle inhibitors, decreases cytochrome C levels, and causes larvae to arrest as stress-resistant, quiescent dauers. We propose a model whereby ILC-17.1 signaling links nutrient availability and energy metabolism to cell cycle progression and cell fate decisions during development through CEP-1/p53. These findings also suggest that the developmental function of the p53-gene family could have shaped their evolution and are relevant to our understanding of neuroimmune mechanisms in cancer.

15 **Main**

16 During metazoan development, nutrient availability is coordinated with the division, growth and
17 metabolic activity of individual cells through cell-cell communication. This is also the case in the
18 invertebrate *C. elegans*, a free-living bacterivore, which displays a dramatic developmental
19 plasticity to ensure that its growth and reproduction match available resources[1-10]. When *C.*
20 *elegans* larvae hatch under optimal conditions (e.g., in the laboratory at 20°C, at low population
21 densities, on abundant food provided by lawns of the *E. coli* strain, OP50) they continue
22 development into reproducing adults. However, if they hatch under suboptimal conditions, such
23 as in the paucity of food, at high population densities, or high ambient temperatures, larvae
24 implement an alternative developmental program and arrest as quiescent, stress-resistant larvae
25 called 'dauer' larvae. Dauer larvae display metabolic and organismal phenotypes specialized for
26 dispersal and survival, and can remain for months in an arrested state to resume development
27 into reproductive adults when conditions become favorable again[1-10]. Studies from several labs
28 have identified molecular pathways that mediate the dauer decision, showing that growth
29 promoting molecules, the best-characterized of which are the insulins, the transforming β growth
30 factor (TGFβ/DAF-7) and lipid based dafachronic acid hormones, are released by sensory
31 neurons and other cells to license continued growth and development; adverse environments
32 inhibit these growth promoting signals and trigger dauer arrest[1-11]. In addition, a number of
33 quantitative trait loci (QTL) also modulate dauer arrest[12]. Yet, how the dauer entry decision results
34 in a coordinated change in cell fates across different tissues and is linked with the systemic shut-
35 down of anabolic pathways still remains poorly understood.

36

37 An important group of proteins that mediate cell-cell communication and metabolism in metazoa
38 are secreted proteins called cytokines[13,14]. The IL-17 cytokines are one such evolutionarily
39 conserved family of proinflammatory cytokines that are released by specialized immune cells at
40 the interface between an organism and the outside world to activate immune surveillance, barrier

function and wound healing, but in humans, also promote cancers and autoimmune disease such as psoriasis[15,16]. More recently IL-17s have been shown to play key immunometabolic roles in modulating mammalian physiology and disease[17]. Here, we show that the *C. elegans* IL-17 ortholog, ILC-17.1, is released from amphid neurons in response to food, and coordinates cell division and cell fate decisions with metabolism by controlling the activity of the *C. elegans* tumor suppressor p53 ortholog, CEP-1. Specifically, ILC-17.1 release that occurs in the presence of food suppresses CEP-1/p53. CEP-1/p53 is activated upon the loss of ILC-17.1, and remarkably, this switches whole organism development from continuous growth to dormancy. The p53-like tumor suppressor genes are found in all multicellular animals where they prevent the transmission of damaged DNA by activating a multifaceted program that controls cell cycle checkpoints, mediates reversible growth arrest or apoptosis, and controls metabolic flux in cells [18-21]. Our studies show that these functions of CEP-1/p53 also act to control developmental quiescence of a whole organism, *C. elegans*, suggesting that the developmental function of the p53- gene family could have shaped their evolution[22-24].

Results

ILC-17.1 is released by *C. elegans* amphid neurons in response to food and prevents dauer arrest.

C. elegans express three IL-17 orthologs[25,26]. Of these, ILC-17.1, which has been shown to act as a neuromodulator, is expressed by a subset of specialized neurons with epithelial properties called amphid neurons that are exposed to the outside and sense information from the environment[25-27]. We discovered that a deletion of *ilc-17.1,* syb5296*,* that removes almost all the coding sequence (2173bp out of 2980 bp; Supplementary Fig. S1a) and abolishes mRNA expression (Supplementary Fig. S1b) caused larvae to constitutively enter the dauer state even under optimal growth conditions (Supplementary Fig. S1c-d). Dauer larvae can be identified by their growth arrest, distinct morphology that includes specialized cuticular structures called alae,

67 a constricted pharynx, and arrested germline, as well as decreased pharyngeal pumping rates
68 and detergent (1% SDS) resistance[3-9]. *ilc-17.1*(syb5296)X dauer larvae displayed all these
69 characteristic morphological and physiological features (Supplementary Fig. S1e-j). Under
70 optimal growth conditions at 20°C, *ilc-17.1* deleted larvae entered the dauer state transiently:
71 approximately 30% (31.2 ±5%) were SDS-resistant 48 hours post-hatching on OP50 bacteria,
72 and most larvae exited dauer and become reproductive adults by 72 hrs (Supplementary Fig.
73 S1c, d). Under the same conditions, none of the wildtype larvae were detergent resistant, nor did
74 any larvae arrest as dauers (Supplementary Fig. S1c, d). However, as with other mutations that
75 promote dauer entry[3,4,28], the dauer arrest of *ilc-17.1* deletion mutants was dramatically
76 accentuated at the slightly more stressful ambient temperature of 25°C, which still supported the
77 growth of all wildtype larvae into reproductive adults, but caused practically 100% of larvae lacking
78 *ilc-17.1* to enter and persist in the arrested dauer state (Fig.1a-d).
79
80 Because the molecular basis for dauer regulation has been the target of extensive genetic
81 screens that are considered to be saturated[3,5,29-31], and IL-17.1 had not been previously implicated
82 in the regulation of dauer, we confirmed the role of *ilc-17.1* in dauer entry by (i) examining the
83 developmental phenotype of another independently generated CRISPR deletion in *ilc-17.1,*
84 syb5297 (loss of 2188 bp of 2980 bp; Supplementary Fig. S1a), (ii) by backcrossing *ilc-17.1,*
85 syb5297, and (iii) by downregulating *ilc-17.1* and its receptor[25,26] in wildtype (N2) larvae using
86 RNA interference (RNAi). Like *ilc-17.1* (syb5296), *ilc-17.1* (syb5297) created using a different
87 guide RNA (see Materials and Methods) also displayed a completely penetrant dauer arrest at
88 25°C (Fig. 1a,b). In *C. elegans* there have been no off-target effects observed using CRISPR
89 even after whole genome sequencing by several labs[32-34]. Nevertheless, due to reviewer's
90 skepticism, we considered whether a similarly large CRISPR-mediated deletion of any gene
91 could, in itself, predispose larvae to enter dauer, and examined whether of the deletion of a related
92 gene *F25D1.3,* syb7367(loss of 1475 bp of 1642 bp) also triggered dauer arrest. This did not

93 (Supplementary Fig. S1k). *ilc-17.1* (syb5296) larvae, however, continued to arrest as dauers even
94 after they were backcrossed 2X time into a wildtype background (Supplementary Fig. S1k). In
95 addition, RNAi-mediated downregulation of *ilc-17.1* in wildtype (N2) animals, but not control RNAi
96 treatment, also caused a small but significant number of larvae to arrest as SDS-resistant dauer
97 larvae at 25°C, (Supplementary Fig. S1l). ILC-17.1 signals though cytokine receptors which in *C.*
98 *elegans* consists of ILCR-1/ILCR-2[25,26]. The ILCR-2 subunit is widely expressed, as determined
99 using a bicistronic SL2 cassette to tag the *ilcr-2* receptor at its endogenous locus with GFP
100 (Supplementary Fig. S2a). Downregulation of *ilcr-2* in wildtype (N2) animals through RNAi caused
101 over one-third, 39.6% ± 4%, of the wildtype larvae to arrest as dauers and did not alter the dauer
102 entry of *ilc-17.1* deleted larvae (Fig. 1e). RNAi, being a partial downregulation of mRNA levels,
103 is generally insufficient to induce dauer arrest with even known dauer pathway genes[3]. Therefore,
104 the RNAi-induced dauer entry of larvae exposed to *ilc-17.1* or *ilcr-2* RNAi for less than 48 hrs.
105 post-hatching, (see Materials and Methods) was not only statistically significant, but also provided
106 additional support for the role of *ilc-17.1* in dauer entry. Thus, together, these observations
107 indicated that during normal development, ILC-17.1 signaling, likely through the ubiquitously
108 expressed ILCR-2 receptors, was required for growth of larvae to reproducing adults; in the
109 absence of ILC-17.1, or the ILCR-2 receptor, larvae arrested growth and entered the dauer state,
110 transiently, or for prolonged durations.
111
112 The dauer phenotype of *ilc-17.1* deletion mutants could be rescued by re-expressing *ilc-17.1*
113 under the control of its own promoter and 3' UTR regions (Fig.1b; see Supplementary Fig. S2b
114 for expression levels of rescue construct in comparison to the endogenous gene). The extent of
115 rescue varied based on the animal's diet (ILC-17.1 re-expression caused an approximately 32.8%
116 rescue on OP50 bacteria, Fig 1b, but 63.6% rescue on HT115 bacteria, Supplementary Fig. S2c;
117 Chi-squared = 121, df = 1, p-value <2e-16), suggesting that the role of ILC-17.1 signaling in dauer
118 might be related to food, a prominent modulator of the *C.elegans* dauer decision[3-9]. The systemic

119 effects of the *ilc-17.1* deletion and rescue were surprising because previous studies using
120 transgenic *ilc-17.1* reporter constructs had shown that *ilc-17.1* mRNA expression is restricted to
121 a small subset of neurons, a pair of amphid sensory neurons (ASE) and two pairs of interneurons
122 (AUA and RMG)[25]. The expression of the endogenous *ilc-17.1* gene was also restricted to a few
123 neurons: mCherry expressed as a bicistronic SL2 cassette along with *ilc-17.1* mRNA from the
124 endogenous *ilc-17.1* locus was also only visible in a few dye-filling amphid neurons
125 (Supplementary Fig. S2d). Therefore, to understand how ILC-17.1 acts systemically, we re-
126 expressed *ilc-17.1* ectopically in *ilc-17.1* deleted larvae, remote from its normal site of expression,
127 using the muscle-specific *unc-54* promoter (Supplementary Fig. S2e), and asked whether ILC-
128 17.1 could act in a cell non-autonomous manner to promote development, or whether its only
129 functioned cell autonomously in amphid neurons. Our expectation was that if ILC-17.1 controlled
130 developmental pathways by acting in a cell-autonomous manner in the amphid neurons, ectopic
131 expression would not rescue the dauer arrest, whereas a cell non-autonomous or endocrine mode
132 of activity could result in a rescue. Consistent with a cell non-autonomous mode of action, and as
133 was the case for the previously reported effects of ILC-17.1 on behavior[25], ILC-17.1 expressed
134 ectopically from the *unc-54* promoter rescued dauer arrest of *ilc-17.1* deleted larvae (Fig.1b and
135 Supplementary Fig. S2c). The rescue from this ectopic expression did not vary with bacterial diet
136 (Fig 1b vs Supplementary Fig. S2c), perhaps because of its non-neuronal expression and/or
137 higher expression levels when compared to that from the endogenous promoter (Supplementary
138 Fig. S2b, f). RNAi mediated downregulation of *ilcr-2* reduced the percentage of *ilc-17.1* larvae that
139 were rescued from dauer arrest by re-expressing ILC-17.1 either under its own promoter, or from
140 the muscle promoter (Fig. 1e). This effect was significant, but only ~10%, reflecting our limited
141 understanding of the stoichiometry of ILC-17.1 ligand-receptor interactions as they relate to the
142 timing of dauer arrest that occurs in the absence of ILC-17.1. Nevertheless, these studies
143 indicated that ILC-17.1 signaling was required for continuous growth and suggested that ILC-17.1
144 might normally be secreted to act cell non-autonomously to promote development.

145

146 Therefore, to more directly examine whether ILC-17.1 is normally secreted from amphid neurons,
147 we immunolocalized ILC-17.1 protein in *C. elegans* larvae using strains expressing ILC-17.1
148 tagged at its endogenous locus using a HA-tag. Suspecting that food played a role in ILC-17.1
149 signaling, we conducted these studies on larvae that were hatched in the absence or presence of
150 food (OP50; Fig. 1f). While *ilc-17.1* mRNA localization was not altered by food availability, and
151 remained restricted to the amphid neurons both in the presence and absence of food as detected
152 by mCherry expressed from the endogenous *ilc-17.1* locus (Fig. 1f; left), ILC-17.1 protein was
153 present outside the amphid neurons, concentrated in the pharynx when larvae were exposed to
154 food (OP50), but not when larvae hatched in the absence of food (Fig.1f; right, quantification in
155 Supplementary Fig. S2g). This suggested that ILC-17.1 protein was secreted and either retained,
156 stabilized, or taken up by the pharynx in response to food signals [we could not reliably detect
157 ILC-17.1 protein in distal tissues such as the intestine or coelomocytes]. The secretion of ILC-
158 17.1 protein was also supported by immunolocalization studies on the muscle-expressed ILC-
159 17.1 protein which, although expressed under a well-characterized muscle-specific promoter (i.e.
160 *unc-54* ; Supplementary Fig. S2e), could be constitutively detected outside muscle cells,
161 throughout the animal (Supplementary Fig.S2h). Thus, the presence of ILC-17.1 protein in regions
162 outside its cellular sites of mRNA synthesis provided strong support that ILC-17.1 is secreted,
163 and in the case of the endogenous ILC-17.1 protein, secretion occurs in response to food
164 availability.

165

166 Sequencing total RNA (RNA-seq) extracted from bleach synchronized larvae grown for 32-36
167 hours at 25°C when *ilc-17.1* mutant larvae were *en route* to dauer arrest, and wildtype larvae were
168 in their late L2/early L3 stage *en route* to developing into reproducing adults, showed that *ilc-17.1*
169 mutant larvae expressed the molecular signatures of dauer larvae[6,35-37] that were distinct from
170 wildtype larvae and from *ilc-17.1* deletion mutants that re-expressed ILC-17.1 (Supplementary

171 Figure S3a; Supplementary Table 1-3). Thus, anabolic processes such as DNA replication and
172 ribosome biogenesis were downregulated (Fig. 1g), and catabolic processes and stress
173 responses such as autophagy, fatty acid metabolism, glutathione metabolism, and xenobiotic
174 defense pathways were upregulated (Fig. 1h). In addition, *ilc-17.1* deleted larvae expressed
175 dauer-specific collagen genes that differ from the collagens of larvae undergoing continuous
176 development[38] (Fig. 1i; Supplementary Table 4). To evaluate the extent to which the *ilc-17.1*
177 deleted dauers were similar to previously described *C. elegans* dauers that accumulate in the
178 population upon starvation or crowding, we compared the global gene expression changes of *ilc-*
179 *17.1* mutant larvae with previously published gene expression changes in larvae entering dauer
180 in response to starvation[37], or pheromone treatment[37] (Supplementary Fig. S3 b,c; Supplementary
181 Tables 5, 6). Consistent with a role for ILC-17.1 in signaling nutrient availability, the expression
182 profile of *ilc-17.1* deleted larvae was more closely correlated to dauer larvae generated by
183 starvation[37] (Supplementary Fig. S3b), compared to ascaroside induced dauers[36] (Supplementary
184 Fig. S3c). These differences were surprising and suggest that the trigger and route of dauer entry
185 determines the gene expression profile of *C. elegans* dauer larvae[39,40].
186

187 **ILC-17.1 loss activates CEP-1/p53 to trigger dauer entry through the activation of DAF-**
188 **16/FOXO, DAF-3/SMAD-DAF-5/Ski complex and steroid hormone pathways.**

189 To understand how the loss of ILC-17.1 was triggering dauer entry we first considered the
190 possibility that, through its role as a neuromodulator[25], the secretion of ILC-17.1 modulated the
191 animals' sensory perception of food or feeding behavior, and the lack of *ilc-17.1* prevented larvae
192 from finding or ingesting food. However, this did not seem to be the case (Supplementary Fig.
193 S4a): *ilc-17.1* deleted animals did not exhibit decreased chemotaxis towards lawns of OP50, or
194 towards organic molecules like lysine or diacetyl thought to mimic the presence of bacteria[41].
195 Animals lacking ILC-17.1 were also able to feed like wildtype animals, and the rate of pharyngeal
196 pumping, a measure that is typically correlated with food uptake, was the same in wildtype animals

197 and animals lacking ILC-17.1, both in the presence and absence of food (Supplementary Fig.
198 S4b). Also, prior to their dauer entry, *ilc-17.1* deletion mutants accumulated slightly, but not
199 significantly fewer numbers of red latex beads in their intestinal lumen that served as a proxy for
200 rates of bacterial ingestion (Supplementary Fig. S4c). These data suggested that *ilc-17.1* deficient
201 larvae arrested development and entered a dauer diapause state despite being able to find and
202 ingest nutrients.
203
204 Therefore, to answer how the loss of ILC-17.1 triggered dauer entry we next adopted a genetic
205 approach, leveraging the wealth of studies on *C. elegans* dauer formation[2-11,28]. In *C. elegans*,
206 insulins released in the presence of optimal food activate or inhibit the sole insulin receptor
207 ortholog, DAF-2, to modulate the function of the Forkhead transcription factor DAF-16. DAF-2
208 signaling supports continuous growth programs: loss of DAF-2 signaling leads to the activation of
209 DAF-16 and promotes dauer entry[2-11,28]. Likewise, TGFβ/DAF-7 ligands released under optimal
210 growth conditions antagonize the activity of the transcription factor complex, DAF-3/SMAD-DAF-
211 5/Ski, to permit continuous growth: inhibition of DAF-7 activates DAF-3/SMAD-DAF-5/Ski and
212 leads to dauer formation[2-11,28]. Both insulins and TGF-β result in the production of the sterol based
213 dafachronic acid hormones that act through DAF-12, a nuclear hormone receptor, to support the
214 development of adult reproductive physiology[2-11,28]. The absence of dafachronic acid pathway
215 components also triggers dauer arrest, and providing exogenous dafachronic acids to mutant
216 animals deficient in insulin or TGFβ signaling, or decreasing DAF-12 activity, can bypass their
217 dauer arrest[3,42]. Finally, a mutation in a transmembrane guanylyl cyclase *daf-11,* that causes
218 chemosensory defects also triggers dauer arrest[3,43]. *ilc-17.1* deletion mutants lacked obvious
219 chemosensory defects (Supplementary Fig. 4a-c), and continued to arrest as dauers on 5mM 8-
220 Bromo-cGMP, which is known to rescue *daf-11*-associated dauer formation[3,43] (Supplementary
221 Fig. 4d). Therefore, to identify signal transduction pathways through which the loss of ILC-17.1

222 might act to control the dauer decision, we examined whether the other dauer effectors, *daf-16,*
223 *daf-5*, or dafachronic acid signaling, modulated dauer formation of *ilc-17.1* mutant larvae.
224
225 A *daf-16* loss of function mutation, mu86[44], completely suppressed dauer formation in animals
226 lacking ILC-17.1, indicating that activation of DAF-16 was one mechanism responsible for their
227 dauer arrest (Fig. 2a). The activation of DAF-16 in animals lacking ILC-17.1 could be quantified
228 by an increase in the proportion of larvae with DAF-16::GFP[45] positive intestinal nuclei even at
229 20°C (Fig. 2b), and the upregulation of DAF-16 target genes[46,47] both at 20°C (Supplementary
230 Fig. S4e) and 25°C (Fig.2c). DAF-16 activation could be suppressed by re-expressing ILC-17.1
231 in *ilc-17.1* deletion mutants under its endogenous promoter, or ectopically, under the muscle-
232 specific promoter (Fig.2c). Similarly, a loss of function mutation in *daf-5*, e1386[48] also completely
233 suppressed the dauer arrest of *ilc-17.1* mutant larvae (Fig. 2d). Finally, and consistent with the
234 role of the DAF-12 pathway downstream of DAF-16 and DAF-5/DAF-3, downregulating *daf-12* by
235 RNAi significantly decreased the number of larvae that arrested as dauers (Supplementary Fig.
236 S5a), and exposing *ilc-17.1* deficient larvae to exogenous Δ7-dafachronic acid at concentrations
237 of 50 nM[42], partially but significantly suppressed their dauer arrest and only ~65% instead of
238 ~100% of the larvae were dauers (Fig 2e). The activation of DAF-16/FOXO and DAF-3/SMAD-
239 DAF-5/Ski by the loss of ILC-17.1 was not simply because *ilc-17.1* deleted larvae were deficient
240 in the expression of insulin signaling and TGFβ/ DAF-7 signaling pathway components. The
241 expression levels of *daf-2* mRNA and the 28 insulin ligands[49,50] were not decreased in *ilc-17.1*
242 deletion mutants, (Supplementary Fig. S5b *daf-2* boxed; Supplementary Table 7), and the
243 expression of *ins-4* was even slightly higher (Supplementary Fig. S5c). The expression of insulin
244 peptides INS-4 and DAF-28[50] were also not altered in larvae deficient in *ilc-17.1*, as seen using
245 GFP translational reporters of these insulin ligands (Supplementary Fig. S5d, e). In addition, the
246 dauer arrest of a mutation in the insulin receptor, *daf-2* (e1370)[51], could not be rescued by ILC-
247 17.1 overexpression, suggesting that ILC-17.1 did not act genetically downstream of *daf-2*

248 (Supplementary Fig. S5f). Similarly, the mRNA expression levels of the main TGFβ components
249 were mostly unaltered in *ilc-17.1*, and *daf-5* levels were even downregulated (Supplementary
250 Fig. S5g; Supplementary Table 8). Thus, these data together indicated that ILC-17.1 acted
251 upstream of DAF-16/FOXO, DAF-3/SMAD-DAF-5/Ski, and the DAF-9/DAF-12 endocrine
252 pathways to modulate dauer entry.
253
254 In wildtype animals, DAF-16/FOXO and DAF-3/SMAD-DAF-5/Ski complex are thought to act
255 independently, and in parallel to modulate the dauer decision[3,5]. Therefore, to identify
256 mechanism(s) that led to the activation of both these pathways in *ilc-17.1* deleted larvae, we used
257 RNAi to downregulate genes known to interact with these dauer effectors[52-59] (Supplementary Fig.
258 S5a). Intriguingly, amongst the possible candidates, we found that the downregulation of *cep-1*,
259 the *C. elegans* ortholog of p53[60,61] (Supplementary Fig. S5a), or a deletion in *cep-1*, gk138,
260 completely rescued the dauer arrest of *ilc-17.1* deletion mutants and nearly all (98%) of *cep-1;ilc-*
261 *17.1* double mutant larvae grew into reproductive adults (Fig 2f-h).
262
263 Although p53 is best studied as a tumor suppressor, p53-like proteins modulate vertebrate
264 development through as yet poorly understood mechanisms[18-24]. The *C. elegans* p53 ortholog,
265 *cep-1* has not been previously implicated in *C. elegans* development. Nevertheless, as could be
266 predicted by the dauer rescue of *ilc-17.1* larvae upon *cep-1* deletion, the overexpression of CEP-
267 1 alone was sufficient to arrest growth and promote an almost completely penetrant dauer
268 phenotype in larvae that developed at 25°C (Fig. 3a, b; see Supplementary Fig. S6a for mRNA
269 levels). CEP-1 overexpression was achieved by expressing a functional, fluorescently tagged
270 CEP-1 under its own promoter, CEP-1::GFP, that was able to complement a *cep-1* deletion, *cep-*
271 *1*(*lg12501*),[62-64] as a genomically integrated multicopy array in a wildtype background. CEP-
272 1::GFP did not induce dauer arrest in the background of the *cep-1* deletion, *cep-1*(*lg12501*),
273 (Figure 3c), indicating that it was the higher expression levels of *cep-1* (Supplementary Fig. S6a),

274 and not the GFP tag on CEP-1/p53, that was responsible for the dauer arrest of CEP-1::GFP
275 overexpressing larvae. CEP-1/p53 overexpression not only caused dauer arrest at 25°C, but also
276 prompted larvae to transiently enter dauer at 20°C, as seen by their SDS-resistance
277 (Supplementary Fig. S6b), phenocopying the *ilc-17.1* deletion. RNA-seq analysis showed that
278 genes differentially expressed in CEP-1/p53 overexpressing larvae *en route* to their dauer arrest
279 significantly overlapped with those expressed in larvae lacking ILC-17.1 (65% of the 15,443
280 differentially expressed genes overlapped, padj.< 0.05; Supplementary Fig. S6c; Supplementary
281 Tables 9, 10). CEP-1/p53 overexpressing larvae also upregulated dauer-specific collagens
282 (Supplementary Fig. S6d; Supplementary Table 4), downregulated genes involved in anabolism
283 (Supplementary Fig. S6e), and upregulated genes involved in catabolism (Supplementary Fig.
284 S6f). In addition, between 15 hours to 32 hours post-hatching at 25°C, CEP-1/p53 overexpressing
285 larvae and *ilc-17.1* deletion mutants showed a remarkably constant level of gene expression, and
286 only 340 and 34 genes respectively changed expression (p<0.05), compared to the > 10,000
287 genes that were either upregulated or downregulated in wildtype larvae and *cep-1;ilc-17.1* double
288 mutant larvae that were in the process of developing into reproductive adults (PCA analysis;
289 Supplementary Fig. S6g; Supplementary Table 11), suggesting that the dauer decision was
290 implemented by 15 hrs post-hatching.
291
292 Like in the ILC-17.1 deficient animals, the completely penetrant 25°C-dauer arrest of larvae
293 overexpressing CEP-1 was dependent on DAF-16, DAF-5 and the steroid hormone pathway.
294 Downregulating *daf-16* expression by RNAi (Fig. 3d; we could not generate CEP-1/p53
295 overexpressing and *daf-16* double mutant larvae, perhaps because of the site of integration of
296 CEP-1::GFP transgene into the genome) or crossing CEP-1/p53 overexpressing larvae into *daf-*
297 *5*, e1386, suppressed their dauer arrest (Fig. 3e). Treatment with 50nM exogenous Δ7-
298 dafachronic acid also allowed a significant proportion of CEP-1/p53 overexpressing larvae to
299 bypass dauer arrest (Fig. 3e). In accordance, DAF-16 target genes were also upregulated in

300 larvae overexpressing CEP-1/p53 at both 25°C (Fig 3f) and 20°C (Supplementary Fig. S7a). In
301 addition, and most convincing, the upregulation of *daf-16* target genes in *ilc-71.1* deletion mutant
302 larvae was *cep-1* dependent at both 25°C and 20°C (Fig 3f; Supplementary Fig. S7a). As we
303 showed for ILC-17.1, CEP-1/p53 induced dauer entry appeared to be somewhat specific to
304 reduced ILC-17.1 signaling, as the 25°C-dauer arrest of *daf-2*(e1370) III larvae that occurred due
305 to reduced insulin signaling did not depend on *cep-1* (Supplementary Fig. S7b). Moreover, in
306 agreement with previous reports[65,66], *cep-1* was not required for dauer induction at high
307 temperatures as *cep-1* (gk138) I larvae could enter dauer at 27°C just like wildtype animals
308 (Supplementary Fig. S7c).
309
310 To confirm that CEP-1/p53 was indeed activated in the absence of ILC-17.1, we tested whether
311 known targets of CEP-1/p53, the BH3-only proteins *egl-1* and *ced*-13[67-70], were upregulated in *ilc-*
312 *17.1* deleted larvae in a CEP-1/p53 dependent manner. As could be expected, *egl-1* and *ced-13*
313 mRNA levels were upregulated upon CEP-1/p53 overexpression in larvae both at 25°C (Fig 3g)
314 and 20°C (Supplementary Fig. S7d). *egl-1* and *ced-13* were also upregulated in a CEP-1/p53-
315 dependent manner in *ilc-17.1* deletion mutants at both 25°C and 20°C, and could be suppressed
316 by rescuing *ilc-17.1* deletion mutants with ILC-17.1 re-expressed under its endogenous-, or
317 muscle-specific promoters (Fig 3g; Supplementary Fig. S7d). In addition, Chromatin
318 Immunoprecipitation followed by quantitative PCR (ChIP-qPCR) using animals carrying an
319 endogenous CRISPR/Cas9 FLAG tagged *cep-1* showed that more CEP-1/p53 was bound to the
320 promoter regions of *egl-1* and *ced-13* in larvae lacking *ilc-17.1* when compared to wildtype larvae,
321 and the increased occupancy was abrogated when *ilc-17.1* deletion mutants were rescued from
322 dauer arrest by re-expressing ILC-17.1 (Fig. 3h).
323
324 In mammalian cells, activation of p53 in response to stress increases p53 protein levels due to its
325 escape from constitutive degradation mediated by the E3 ubiquitin ligase MDM2[18,20]. *C. elegans*

326 genome lacks MDM2 orthologs, but CEP-1/p53 is controlled through translational and
327 posttranslational modifications[62,71], although the mechanisms of activation remain incompletely
328 understood. Western analysis of FLAG-tagged endogenous CEP-1/p53 in *C. elegans* showed
329 that CEP-1::FLAG expression was increased in larvae lacking *ilc-17.1* (Fig 3i). As a positive
330 control we used gamma irradiation at doses known to activate CEP-1/p53 in the germline, and
331 this also increased CEP-1::FLAG levels (Fig 3i)[67,69]. These results together showed that CEP-
332 1/p53 was activated upon loss of ILC-17.1 signaling and triggered the dauer arrest of *ilc-17.1*
333 deletion mutants through the DAF-16/FOXO and DAF-3/SMAD-DAF-5/Ski (and likely DAF-12)
334 pathways. Thus, it appeared that ILC-17.1-CEP-1/p53 could act as a node to integrate and
335 coordinate the diverse cellular, physiological and metabolic effects of the DAF-2/Insulin signaling-
336 and TGFβ/DAF-7-growth hormone signaling pathways that normally act in parallel to control dauer
337 arrest. However, as we showed for DAF-2, these transcription complexes also likely receive
338 independent information through the insulin receptor, DAF-2, and the TGFβ/DAF-7 receptors.
339

340 **ILC-17.1 modulates CEP-1/p53 activity in ventral blast cells (P cells) of larvae and directly**
341 **or indirectly controls cell cycle progression and cell fate programs.**

342 During *C. elegans* development, most cell divisions are completed during embryogenesis, but a
343 subset of somatic and germline cells divide post-embryonically during and beyond the L1 stage,
344 to generate adult tissues[72-77]. Previous studies have shown that upon dauer entry these cells
345 maintain or re-establish multipotency to be able to continue development when conditions
346 become favorable again[78,79], and this is mediated by the known dauer signaling pathways that act
347 to different extents, in different post-embryonically developing tissues, to modulate their cell cycle
348 G1/S transition, natural re-programming, and/or differentiation[80-87]. Because of its conserved
349 functions in promoting reversible cell cycle arrest and stem cell differentiation[19-21,88], we
350 speculated that CEP-1/p53 activated by the loss of ILC-17.1, was also restraining cell cycle
351 progression and suppressing adult fates in post-embryonically developing cells when nutrients

352 were scarce. To test this possibility, we (i) examined the localization of CEP-1/p53 in developing
353 *ilc-17.1* deleted larvae and *cep-1* overexpressing larvae during their dauer entry, (ii) examined
354 whether CEP-1/p53 activity in *ilc-17.1* deletion mutants (and CEP-1/p53 overexpressing larvae)
355 altered cell fate or increased the expression of cell cycle inhibitors [89,90], and (iii) examined whether
356 decreasing the expression of the cell cycle inhibitors that may be upregulated could systemically
357 rescue dauer arrest.
358
359 Previous studies have shown that CEP-1/p53 is expressed in the adult germline, and in a subset
360 of larval pharyngeal muscle and neuronal cells[60,62]. This has been visualized by other groups
361 using the same functional, fluorescently tagged CEP-1, CEP-1::GFP which complements the *cep-*
362 *1* deletion, *cep-1*(*lg12501*), where endogenous CEP-1 protein is not expressed[62]. We found that
363 in addition to these cells, CEP-1/p53 was also expressed in the ventral somatic progenitor blast
364 cells (P cells) early during larval development (15-20 hours post-hatching; Fig. 4a). The ventral P
365 blast cells are multipotent progenitor cells that divide post-embryonically during larval stage 1 (L1)
366 to generate neuroblasts, hypodermal blast cells and vulval precursor cells which later form adult
367 tissue [72,73,77,91]. These cells express the Paired-box gene *pax*-3, the sole *C. elegans* PAX-3
368 transcription factor homolog, during these early stages of development[92]. CEP-1::GFP colocalized
369 with approximately 50% of *pax*-3-driven mCherry that can be used to mark P cells, 15 hours post-
370 hatching at 20°C, and accumulated in more *pax-3* expressing cells under dauer inducing
371 conditions of 25°C (Fig. 4a, b). In addition, CEP-1::GFP expression levels in P blast cells
372 increased at 25°C in larvae overexpressing CEP-1/p53 or lacking ILC-17.1, when compared to
373 larvae at 20°C, or when compared to CEP-1::GFP expression in *cep-1* (lg12501) larvae that do
374 not arrest as dauers (Fig. 4c). Notably, CEP-1::GFP expression in blast cells of *cep-1* (lg12501)
375 larvae did not vary between 20°C and 25°C (Fig. 4c), indicating that increased CEP-1/p53 levels
376 in blast cells of larvae overexpressing CEP-1/p53, or lacking ILC-17.1, was likely related to their
377 dauer entry and not due to changes in temperature *per se*. Thus, during dauer arrest of *ilc-17*

378 deletion mutants, or CEP-1/p53 overexpressing larvae, CEP-1/p53 appeared to be activated in
379 the ventral P blast cells that would arrest lineage progression as dauers.
380
381 Larvae overexpressing CEP-1/p53 and *ilc-17.1* deleted larvae also upregulated cell cycle
382 inhibitors that are known to be direct or indirect targets of CEP-1/p53[90]: one of the two p21
383 homologs, *cki-1,* and *phg-1,* the *C. elegans* homologue of Growth arrest-specific 1 or Gas1 were
384 upregulated (Fig. 4d). *phg-1,* but not *cki-1,* was a direct target of CEP-1/p53, as *ilc-17.1*
385 deletion mutants displayed increased occupancy of CEP-1/p53 at the promoter of the *phg-1*
386 gene (Fig. 4e), but not the *cki-1* gene (Supplementary Fig. S7e). The increased expression of
387 these genes and occupancy at *phg-1* promoter was restored to wildtype levels upon re-
388 expressing ILC-17.1 (Fig. 4d, e). For technical reasons we could not localize *phg-1* or *cki-1*
389 mRNA in larvae during these early stages of development and therefore do not know whether
390 the increased expression occurred in the P blast cells. Nevetheless, the increased expression
391 of *phg-1* and *cki-1* played a causal role in dauer arrest: downregulation by RNAi was sufficient
392 to significantly, but modestly rescue dauer arrest in *ilc-17.1* deletion mutants and CEP-1/p53
393 overexpressing larvae, and promote their development into adults (Supplementary Fig. S7f).
394 Crossing *ilc-17.1* deletion mutants into *phg-1* deletion mutants, ok2741, resulted in a greater
395 rescue and ~40% escaped dauer arrest and grew into reproductive adults, but surprisingly, over
396 60% of the *ilc-17.1;phg-1* double mutants still remained arrested as dauers (Fig. 4f;
397 Supplementary Fig. S7g), suggesting that CEP-1/p53 activity might be acting in cooperation
398 with other cell cycle or dauer pathway genes. In addition, a proportion of *ilc-17.1* deletion
399 mutant and CEP-1/p53 overexpressing larvae that appeared morphologically dauer, displayed
400 modest but significant non-dauer physiological traits on *phg-1* and *cki-1* RNAi such as increased
401 rates of sporadic pumping (Supplementary Fig. S7h; wildtype larvae at larval stage 2, L2, were
402 used as controls), suggesting there there may also occur a wider, albeit incomplete, dauer
403 rescue in some tissues. The dauer arrest of *daf-2* mutant larvae which did not depend on *cep-*

404 *1,* was also not rescued upon downregulating *phg-1* or *cki-1*, nor were the pumping rates of *daf-*
405 *2* dauers altered, and these remained even lower than in *ilc-17.1* deleted or CEP-1/p53
406 overexpressing dauers (Supplementary Fig. S7f, h). These data together showed that cell cycle
407 inhibitors that were CEP-1/p53-targets were upregulated upon loss of ILC-17.1 signaling or
408 overexpressing CEP-1/p53 and downregulating these inhibitors was sufficient, at least in part, to
409 cause a systemic rescue from dauer arrest.
410
411 Given these observations, we asked whether overexpressing CEP-1/p53 in P blast cells alone,
412 under the *pax-3* promoter, might drive larvae to arrest as dauers. This expectation turned out to
413 be too simplistic, and was not supported, as the majority (85.7 ± 5%; n=6 experiments, 122 larvae
414 total) of *pax-3p::CEP-1* expressing larvae grew into adults at 25°C, although 14.3 ± 4.5% did not
415 complete development and arrested at various early larval (<L4) stages. However, CEP-1/p53
416 expression in the P blast cells caused anteroposterior patterning defects in larvae and 11.8 ±2.9%
417 of larvae displayed dorsalization, vulvaless and dumpy phenotypes (representative example; Fig.
418 4g) suggesting that CEP-1/p53 expression could alter the cell fates of the P blast cell lineages[76,93-
419 95]. Consistent with these observations, in larvae lacking ILC-17.1 or overexpressing CEP-1/p53,
420 HOM-C homeobox genes required for anterio-posterior body patterning[76,93-95] were differentially
421 expressed compared to wildtype or *ilc-17.1; cep-1* double mutant larvae (Fig 4h; $p < 0.05$). This
422 included *lin*-39 (Scr/Dfd/Hox3–5) which maintains P cells competent to respond to later inductive
423 signals and prevents aberrant cell fusions, and *mab-5* (Antp/Hox6–8) and *egl*-5 (Abd-A/Abd-
424 B/Hox9–13), involved in mid- and posterior body patterning, which were maintained at modestly,
425 but significantly higher levels when compared to larvae continuously developing into adults
426 (compare expression levels between 15 hr and 32 hr larvae in Supplementary Table 12). Thus,
427 while further studies are required to better understand how CEP-1/p53 activity in *ilc-17.1* deleted
428 larvae triggers dauer arrest, these data together indicate that CEP-1/p53-induced increase in cell
429 cycle inhibitors such as *phg-1* (in P cells or other cells), and its ability to directly or indirectly

430 modulate cell fate in the ventral P cell lineage during development, where CEP-1/p53
431 accumulates during dauer arrest, may collaborate to pause growth programs of the animal.
432
433 **ILC-17.1 links glucose metabolism to CEP-1/p53 activity in progenitor blast cells (P cells)**
434 **of larvae.**
435 The release of ILC-17.1 from amphid neurons in response to food suggested the intriguing
436 possibility that ILC-17.1 signaling linked CEP-1/p53-mediated cell fate decisions to energy
437 metabolism, since limited nutrient availability, glucose starvation or energy deprivation are all
438 known to activate p53 in mammalian cells[88,96]. Indeed, the dauer arrest of *ilc-17.1* mutant larvae
439 appeared related to an impairment in their ability to utilize glucose normally available through their
440 diets: decreasing glucose availability by downregulating *fgt-1,* the main Glucose transporter
441 (GLUT) responsible for glucose absorption in *C. elegans*[97], decreased the extent of dauer-rescue
442 conferred by ILC-17.1 re-expression in *ilc-17.1* mutant larvae (Fig. 5a). Similarly, *fgt-1* RNAi
443 increased the numbers of *ilc-17.1* deletion mutant larvae that arrested as dauers under optimal
444 conditions at 20°C (Fig. 5b). Promoting glucose utilization and/or metabolism by providing extra
445 glucose[98] rescued the dauer arrest of *ilc-17.1* deficient larvae (Fig. 5c; Supplementary Fig. S8a).
446 This effect of glucose supplementation also depended on glucose utilization and metabolism.
447 Impairing glucose import through *fgt-1* RNAi decreased the percentage of larvae that were
448 rescued by the extra glucose (Supplementary Fig. S8b), and no rescue was observed on the non-
449 hydrolyzable glucose analog 2-Deoxy-d-glucose (2-DOG; Supplementary Fig. S8c) which cannot
450 undergo glycolysis and does not enter the metabolic pathway. We ruled out the involvement of
451 mitochondrial reactive oxygen species, ROS, known to be increased under glucose-rich diets[98]
452 by using mitochondria-targeted antioxidant, Mito-Tempo, that scavenges ROS (Supplementary
453 Fig. S8c). The rescue also did not appear to be due to the non-specific effect of nutritional
454 supplementation (e.g. L-glutamine, another important carbon source for metabolism, or skim milk
455 powder that can be ingested by *C.* elegans[99]; Supplementary Fig. S8d). Downregulating *fgt-1* in

456 wildtype larvae, while not sufficient to trigger dauer arrest, modestly increased the expression of
457 CEP-1/p53 target *egl-1* (but not *ced-13*; Supplementary Fig. S8e). Thus, these data supported
458 the possibility that the activation of CEP-1/p53 upon the loss of ILC-17.1 could, at least in part,
459 occur due an impairment in the *ilc-17.1* deleted larvae's ability to utilize glucose.
460
461 If glucose impairment was responsible for CEP-1/p53 activation, glucose supplementation should
462 also rescue the dauer arrest of larvae overexpressing CEP-1/p53. This was the case (Fig 5c;
463 Supplementary Fig. S8a), also arguing that decreased glucose intake in the absence of ILC-17.1
464 was not a consequence of CEP-1/p53 activation, but instead acted logically upstream of CEP-
465 1/p53 activation. In agreement, providing extra glucose decreased the levels of CEP-1::GFP that
466 accumulated in the ventral P blast cells (Fig. 5d), suppressed the increased expression of *phg-1*
467 the direct target of CEP-1/p53, which was in part responsible for dauer arrest of *ilc-17.1* deleted
468 animals (Fig. 5e), and decreased DAF-16/FOXO activation (Fig.5e). Surprisingly, not only did
469 CEP-1/p53 appear to be activated by the inability of *ilc-17.1* to utilize glucose normally, but CEP-
470 1/p53 activity, in turn decreased the expression levels of key metabolic enzymes involved in
471 glucose metabolism[100]: phosphofructokinase-1.2 (*pfk-1.2*), the rate limiting enzyme in glycolysis,
472 and cytochrome *c* (*cyc-2.2*), the subunit of complex IV of the electron transport chain responsible
473 for the final transfer of reducing equivalents to O_2. This was visible in the RNA-seq data
474 (Supplementary Figure S9 a-f; Supplementary Table 13) and confirmed by qRT-PCR
475 (Supplementary Figure S9g, Fig. 5f). In mammalian cells, p53 activity is known to decrease the
476 expression of enzymes required for glycolysis[88] and indeed, the decrease in mRNA expression
477 of *pfk-1.2* was a consequence of CEP-1/p53 activation in the *ilc-17.1* deleted larvae: the deletion
478 of *cep-1* rescued the low mRNA levels (Supplementary Figure S9g). Surprisingly, the decrease
479 in *cyc-2.2* expression was also dependent on CEP-1/p53, but also on DAF-16/FOXO, as the
480 deletion of *cep-1* or *daf-16* rescued the low *cyc-2.2* mRNA levels in *ilc-17.1* deleted larvae (Fig.
481 5f). Moreover, although the downregulation of *pfk-1.2* or *cyc-2.2* alone was not sufficient to induce

482 dauer in wildtype animals, RNAi induced downregulation of *cyc-2.2* in *ilc-17.1* deleted larvae
483 increased the percentage of larvae that arrested as dauers under optimal conditions at
484 temperatures of 20°C, suggesting that CEP-1/p53-dependent decrease of *cyc-2.2* could feedback
485 onto *ilc-17.1* loss to increase dauer propensity (Supplementary Figure S9h). These data,
486 together, strongly suggested that the loss of ILC-17.1 resulted in an impairment in glucose
487 utilization and thus activated CEP-1/p53, which, upon activation, could further limit glucose
488 utilization by downregulating genes important for glycolysis and OXPHOS. Thus, ILC-17 secretion
489 from amphid neurons that occurred in response to food availability appeared to link cell fate
490 decisions with energy metabolism through CEP-1/p53.
491
492 **ILC-17.1 suppresses CEP-1/p53 in *C. elegans* and human epithelial cells.**
493 Since our data pointed towards a model whereby ILC-17.1 signaling that occurred constitutively,
494 under favorable conditions in the presence of food, suppressed CEP-1/p53 to promote continuous
495 development, we directly examined whether IL-17 suppressed CEP-1/p53 activity. As was shown
496 in B lymphoma cells[101], stimulation of untransformed human epithelial cells with human
497 recombinant IL-17A also induced a modest but significant downregulation of p53 expression
498 levels (Fig. 6a). This was similar to the decrease in CEP-1/p53 levels seen in *C. elegans* upon
499 overexpression of ILC-17.1 (Fig. 3i). For the experiments in mammalian cells, IL-17A stimulation
500 of epithelial cells was confirmed by measurement of secreted CXCL5, a key cytokine downstream
501 of IL-17A signaling[102] (Supplementary Fig. S10a).
502
503 In *C. elegans* too, increased ILC-17.1 levels suppressed CEP-1/p53 activation: overexpressing
504 ILC-17.1 in animals also overexpressing CEP-1/p53 inhibited their dauer arrest (Fig. 6b),
505 inhibited the increase in mRNA levels of CEP-1/p53 target genes, *egl-1*, *ced-13* in CEP-1/p53
506 overexpressing animals (Fig 3g; Supplementary Fig S7d), *cki-1* and *phg-1* (Fig. 4d), and
507 partially restored the decreased *cyc-2.2* mRNA levels that resulted from CEP-1/p53

508 overexpression (Fig 5f). In *C. elegans* the activity of CEP-1/p53 has been best studied in the
509 adult germline where CEP-1/p53 controls germline apoptosis in response to genotoxic
510 insults[60,62,67,68]. Therefore, we used gamma irradiation to cause DNA damage in day-one adult
511 animals, and measured the number of germline apoptotic corpses that result 24 hr. later, to
512 determine whether increased ILC-17.1 levels could also inhibit this canonical activity of CEP-
513 1/p53 (Fig 6c). As has been previously shown[68], and consistent with the role of p53 in
514 controlling DNA-damage induced-, but not physiological apoptosis, *cep-1 (gk138)* adults lacking
515 functional CEP-1/p53 displayed only a mild decrease in the rates of physiological apoptosis
516 when compared to wildtype animals (Fig. 6c). However, as also shown previously[68], in these
517 animals gamma irradiation did not increase apoptosis (Fig. 6c). CEP-1/p53 overexpression,
518 surprisingly, caused a significant increase in physiological apoptosis, and a marked increase in
519 irradiation-induced apoptosis, both of which were decreased upon also overexpressing ILC-17.1
520 in these animals (Fig 6c). Overexpressing *ilc-17.1* alone also decreased both physiological or
521 irradiation-induced apoptosis compared to that in wildtype animals, but this effect was mild and
522 did not reach significance (average nos. of cells undergoing physiological apoptosis in N2 v ILC-
523 17.1 overexpressing animals were 3.56 ± 1.3 and 2.53 ± 1.1 cells, and upon irradiation, these
524 increased to 7.1 ± 1.8 in N2, and 5.72 ± 2.2 in IL-17 overexpressing animals). Also, for reasons
525 we do not understand, *ilc-17.1* deletion mutants did not display changes in apoptosis when
526 compared to wildtype animals, suggesting perhaps that the functions of ILC-17.1 in adult tissue,
527 and/or germline cells may be more nuanced when compared to its developmental function.
528 Nevertheless, these data confirmed that, consistent with our working model (Fig. 6d), ILC-17.1
529 could inhibit CEP-1/p53. In addition, they suggested the possibility that the roles of *ilc-17.1*
530 signaling and CEP-1/p53 activity might diverge post-development.
531
532 **Discussion**

533 Here we show, for the first time, a role for the cytokine IL-17, and p53 in the development of an
534 invertebrate species, *C. elegans*. Specifically, we show that CEP-1/p53 repression during early
535 larval development ensures the continuous growth of the animal into reproductive adults, and this
536 repression is mediated by ILC-17.1 released by amphid neurons upon food availability. Reduced
537 ILC-17.1 signaling, expected to occur when food is scarce, activates CEP-1/p53, which then
538 triggers dauer arrest through the well characterized dauer activating pathways, DAF-16/FOXO,
539 DAF-3/SMAD-DAF-5/Ski and also, perhaps also through steroid hormone signaling. In its role in
540 promoting dauer arrest CEP-1/p53 accumulates in multipotent P blast cells that differentiate
541 postembryonically into adult tissues, restrains cell cycle progression, and alters cell fate decisions.
542 In addition, while promoting dauer arrest, CEP-1/p53 alters metabolic flux by directly or indirectly
543 controlling the levels of phosphofructokinase (*pfk*-1) and cytochrome C (*cyc-2.2*). Notably, these
544 are functions of p53 in its role as a tumor suppressor. We propose a working model whereby ILC-
545 17.1 secretion from amphid neurons that occurs in response to food availability links cell fate
546 decisions with energy metabolism through the conserved, multifaceted program of CEP-1/p53
547 (Fig. 6d). Our data also support the possibility that this ancient function of p53, conserved in all
548 multicellular animals and shown here to modulate an invertebrate developmental program, could
549 have been the driving force in the evolution of the p53 gene-family.

550

551 It is intriguing that during normal *C. elegans* development CEP-1/p53 appears to modulate the
552 fate of multipotent P blast cells. In mammals too, normal p53 activity is essential for maintaining
553 stem cell quiescence in the hematopoietic system and other organs during steady state tissue
554 homeostasis[103,104], and unrestrained p53 activity is associated with a developmental syndrome
555 resembling CHARGE (coloboma, heart defects, atresia choanae, growth retardation, genital
556 abnormalities, and ear abnormalities), through its effects on cell cycle progression, apoptosis
557 and the migration of neural crest cells[24]. Cytokines such as IL-17 modulate glucose metabolism

558 in mammalian models, and glucose deprivation can, in turn, activate p53[88,96]. Thus, as seen in
559 *C. elegans*, the ability of p53-proteins to link metabolic control with cell cycle progression and
560 stem cell fate could be a conserved mechanism leveraged by several signaling pathways similar
561 to IL-17s to coordinate metazoan development with nutrient availability.
562
563 The specific mechanisms by which ILC-17.1/CEP-1 axis promotes dauer entry remain to be better
564 explored. In addition, we are yet to dissect the temporal requirements, sites of action, and
565 mechanisms and consequences of ILC-17.1 signaling required to control CEP-1/p53 activation,
566 as well as its effects on adult traits such as longevity and stress resistance--traits linked to other
567 dauer-activating pathways. While the discovery of new *C. elegans* dauer pathway genes is
568 surprising given the extensive genetic screens that have been conducted[3,5,29-31], genes that
569 require a complete deletion to confer a dauer phenotype, QTLs that interact in complex ways to
570 limit the discovery of dauer phenotypes, or genes that show functional redundancy and tolerance
571 to quantitative variation such as seen with CEP-1/p53 overexpression, could have been missed.
572 Indeed, a previously characterized *ilc-17.1* mutation *ilc-17.1*(tm5218), generated through EMS
573 mutagenesis and in the background of a linked mutation in *npr-1,* itself known to be a modifier of
574 the dauer phenotype, does not trigger dauer arrest under the same conditions (Supplementary
575 Figure S10b). Intriguingly, our RNA-seq data show that gene expression changes between 15 hr.
576 post-hatching and 32 hr. post-hatching are negligible in *ilc-17.1* deletion mutants and CEP-1/p53
577 overexpressing larvae, suggesting that this pathway is one of the very early checkpoints in the
578 larval decision between continuous growth and dauer arrest[3,4]. Thus, it is plausible that ILC-17.1
579 and CEP-1/p53 could even act as early as in the maternal germline, or during embryogenesis, to
580 modulate developmental decisions.
581

582 It is interesting that ILC-17.1 is secreted by *C. elegans* sensory neurons to control CEP-1/p53
583 activity. Neurons control dauer entry also though TGFβ, insulin and steroid hormone signaling. In
584 addition, other stress-responsive transcriptional programs such as the cellular response to protein
585 misfolding that are cell autonomous in individual cells are controlled through neuronal signaling
586 in a metazoan such as *C. elegans*, allowing the nervous system to coordinate tissue-specific
587 transcriptional and epigenetic responses with organismal physiology and behavior[105-108]. Nutrient
588 scarcity has shaped much of evolution, and the ability of cells and organisms to sense nutrient
589 availability and prepare in anticipation to pause cell cycle progression and growth and maintain a
590 quiescent state until resources are optimal, has unquestionable selective advantages. For *C.*
591 *elegans*, like for most organisms, the availability of food is not guaranteed. Neuronal ILC-17.1
592 signaling appears to be one mechanism which allows the animal to match the cell fate programs
593 in the developing larvae and metabolic requirements with resource availability. In mammals,
594 resident neurons and immune molecules in peripheral tissue profoundly influence cell fate
595 decisions to remodel tissue architecture during development, organogenesis, inflammatory
596 responses, and in diseases such as cancer[109,110]. It is therefore not far-fetched to imagine that
597 mammalian neurons control p53 activity, cell quiescence and stem cell fate in response to nutrient
598 availability through IL-17s, as seen in *C. elegans*, although, perhaps in mammals this occurs
599 locally through peripheral innervation and immune cells. Such a control mechanism could open
600 new avenues for therapeutic intervention in cancer and other IL-17-mediated diseases.
601

602 **Materials and Methods**

603 ***C. elegans* strains**

604 *C. elegans* strains used in this study are listed in Table 1. Strains were procured from
605 Caenorhabditis Genetics Center (CGC, Twin Cities, MN), generated in the laboratory or
606 generated by Suny Biotech (Suzhou, Jiangsu, China 215028). All strains will be available upon
607 request, after publication.

Strain Name	**Gene name**	**Source**	**Additional information**
N2, *C. elegans* var *Bristol*	N2, Wild-type	Caenorhabditis Genetics Center	
TJ1	*cep-1* (gk138) I	Caenorhabditis Genetics Center	
CF1038	*daf-16* (mu86) I	Caenorhabditis Genetics Center	
TG12	*cep-1*(lg12501) I*; unc-119* (ed4) III; gtIs1 [CEP-1::GFP + *unc-119* (+)]	Caenorhabditis Genetics Center	Pcep-1::CEP-1(let-585 3'UTR)::GFP; from construct pRH53
CB1370	*daf-2* (e1370) III	Caenorhabditis Genetics Center	
VEP024	praEx021 (*ilc-17.1*p::*ilc-17.1* cDNA::3XFLAG::*ilc-17.1* 3'UTR; p*myo-2*::mCherry::*unc-54* 3'UTR)	Prahlad Lab	ILC-17.1 overexpression under its own promoter and 3'UTR

VEP031	praEx022 (*unc-54*p::*ilc-17.1* cDNA::3XFLAG::*tbb-2* 3'UTR; p*dat-1*::GFP::*unc-54* 3'UTR)	Prahlad Lab	ILC-17.1 overexpression under the muscle promoter and 3'UTR
VEP032	*ilc-17.1* (syb5296) X	Prahlad Lab/ SunyBiotech	*ilc-17.1* deletion, 2173bp deletion, and the 15bp and 127bp sequences were left in the 5' and 3' deletion end, respectively of the 2315 bp *ilc-17.1* gene
VEP033	*ilc-17.1* (syb5296) X; praEx022 (*unc-54*p::*ilc-17.1* cDNA::3XFLAG ::*tbb-2* 3'UTR; p*dat-1*::GFP::*unc-54* 3'UTR)	Prahlad Lab	ILC-17.1 paracrine rescue of *ilc-17.1* deletion
VEP034	*ilc-17.1* (syb5296)X; *cep-1* (gk138) I	Prahlad Lab	
VEP035	*ilc-17.1* (syb5296); *daf-16* (mu86) I	Prahlad Lab	
VEP036	*unc-119* (ed4); gtIs1 [CEP-1::GFP + *unc-119* (+)]	Prahlad Lab	CEP-1 overexpression (ref: [60])
VEP037	*ilc-17.1* (syb5296); praEx022 (*unc-54*p::*ilc-17.1* cDNA:: 3XFLAG::*tbb-2* 3'UTR; p*dat-1*::GFP::*unc-54* 3'UTR);	Prahlad Lab	IL-17.1 overexpression;

	unc-119 (ed4); gtIs1 [CEP-1::GFP + *unc-119* (+)]		CEP-1/p53 overexpression
VEP038	*ilc-17.1* (syb5296); praEx022 (*unc-54*p::*ilc-17.1* cDNA:: 3XFLAG::*tbb-2* 3'UTR; p*dat-1*::GFP::*unc-54* 3'UTR); *daf-2* (e1370) III	Prahlad Lab	
VEP039	*daf-2* (e1370) III; *cep-1* (gk138) I	Prahlad Lab	
VEP040	*cep-1* ((syb6099) [*cep-1*::3XFLAG]) I	Prahlad Lab/ SunyBiotech	Endogenous *cep-1* 3X FLAG tagged at C-terminus
VEP041	*ilc-17.1* (syb5296)X ; *cep-1* (pra02 [*cep-1*::3XFLAG]) I	Prahlad Lab	
VEP042	praEx022 (*unc-54*p::*ilc-17.1* cDNA::3XFLAG::*tbb-2* 3'UTR; p*dat-1*::GFP::*unc-54* 3'UTR); *ilc-17.1* (syb5296) X ; *cep-1* (pra02 [cep-1::3XFLAG]) I	Prahlad Lab	
VEP043	*ilc-17.1* (pra03 [*ilc-17.1*::SL2::mCherry]) X	Prahlad Lab/ SunyBiotech	
VEP044	*ilc-17.1* (pra04 [*ilc-17.1*::3xHA]) X	Prahlad Lab/ SunyBiotech	
VEP045	*ilcr-2* (pra05 [*ilcr-2*::SL2::GFP]) II	Prahlad Lab/ SunyBiotech	
CB1386	daf-5(e1386) II	Caenorhabditis Genetics Center	

VEP061	*ilc-17.1* (syb5297)	Prahlad Lab/ SunyBiotech	*ilc-17.1* deletion, 2188bp deletion, and the 9bp and 118bp sequences were left in the 5' and 3' deletion end, respectively of the 2315 bp *ilc-17.1* gene
RW10645	stIs10645 [pax-3p::HIS-24::mCherry + *unc-119*(+); *unc-119* (ed3)	Caenorhabditis Genetics Center	
VEP062	stIs10645 [pax-3p::HIS-24::mCherry + *unc-119*(+); *unc-119* (ed3); *ilc-17.1*(syb5296)	Prahlad Lab	
VEP059	stIs10645 [pax-3p::HIS-24::mCherry + *unc-119*(+); *unc-119* (ed3); gtIs1[cep-1::GFP + *unc-119*(+)]	Prahlad Lab	
VEP063	praEx026(*pax-3*p::CEP-1A cDNA::3xFLAG::*unc-54* UTR; p*myo-2*::mCherry::*unc-54* UTR)	Prahlad Lab	
AX5690	npr-1(ad609)X; ilc-17.1(tm5218)X	Mario de Bono's lab/ C. elegans National Bioresource Project, Japan	

608 **Generation of CRISPR strains**

609 CRISPR/Cas9 was used to create following *C. elegans* strains:

Background Strain	**Type of editing**	**Description/position of editing**	**Gene**	**Resulting strain**
N2, *C. elegans* var Bristol	Deletion (syb5296)	2173bp deletion, and the 15bp and 127bp sequences were left in the 5' and 3' deletion end, respectively of the 2135 bp *ilc-17.1* gene. **sgRNA used - CCAAAATCACCACACAGGACAAA**	(*ilc-17.1*)X	VEP032
N2, *C. elegans* var Bristol	Deletion (syb5297)	2188bp deletion, and the 9bp and 118bp sequences were left in the 5' and 3' deletion end, respectively of the 2135 bp *ilc-17.1* gene. **sgRNA used- tagGCAAATGCGAATGCGGATGG**	(*ilc-17.1*)X	VEP032
N2, *C. elegans* var Bristol	Insertion; *SL2::mCherry*	C'-terminus	(*ilc-17.1*)X	VEP043
N2, *C. elegans* var Bristol	Insertion; 3X HA	C'-terminus	(*ilc-17.1*)X	VEP044
N2, *C. elegans* var Bristol	Insertion; SL2::GFP	C'-terminus	(*ilcr-2*)II	VEP045

N2, *C. elegans* var Bristol	Insertion; 3X FLAG	C'-terminus	(*cep-1*)I	VEP040
N2, *C. elegans* var Bristol	Deletion (1475bp of 1692 bp)	Prahlad Lab/ SunyBiotech	F25D1.3 (syb7367) V	PHX7367

610

611 **Generation of transgenic strains**

612 **i) Backcrossing of *ilc-17.1* (syb5296) X**

613 The *ilc-17.1 (syb5296)* X strain was crossed to wildtype (N2) males, and the the male F1
614 progeny which harbored the *ilc-17.1 (syb5296)* allele on their X chromosome were backcrossed
615 to the *ilc-17.1 (syb5296)* X strain and homozygous F2s were selected by PCR. This procedure
616 was conducted 2X times to generate the 2X backcrossed *ilc-17.1 (syb5296)* X line.

617 **ii) Generation of *cep-1* overexpression strain**

618 TG12 (*cep-1*(Ig12501) I; *unc-119* (ed4) III; [CEP-1::GFP + *unc-119* (+)]) is a strain that expresses
619 a functional CEP-1 tagged with GFP integrated into its genome, as determined by the rescue of
620 *cep-1*(Ig12501) phenotype[62]. To overexpress CEP-1 we backcrossed the TG12 strain with wild-
621 type (N2) worms and selected F2 progeny that were homozygous for the wild-type *cep-1* gene,
622 lacked the *cep-1*(Ig12501) I mutation (confirmed by PCR), and were homozygous for the CEP-
623 1::GFP transgene (confirmed by 100% GFP expression amongst the F3 and F4 progeny).
624 Overexpression of cep-1 mRNA was verified by qPCR (Supplementary Figure S6d). The CEP-
625 1::GFP construct was PCR amplified from the final transgenic VEP037 *C. elegans* strain, and
626 sequence verified.

627 **iii) Generation of ILC-17.1 overexpression strain under its own promoter and 3'UTR**

628 To generate the strain VEP024 – praEx021 [(*ilc-17.1*p::*ilc-17.1* (cDNA)::3xFLAG::*ilc-17.1*
629 3'UTR); p*myo-2*::mCherry::*unc-54* 3'UTR], which overexpressed *ilc-17.1* under the endogenous
630 *ilc-17.1* promoter and *ilc-17.1* 3'UTR, we first amplified 3 kb of genomic sequence upstream of

631 the translational start site (*ilc-17.1* promotor) and 1 kb of genomic sequence downstream from
632 the translational stop codon (*ilc-17.1* 3' UTR). These regions were cloned using Gateway
633 technology into pDONR221. *ilc-17.1* cDNA fused to C-terminal 3xFLAG sequence was
634 synthesized as a gBlock (Integrated DNA technologies). These three fragments were then
635 submitted for gene synthesis service through GenScript to generate the expression vector
636 pUC57(*ilc-17.1*p:: *ilc-17.1* (cDNA)::3xFLAG:: *ilc-17.1* 3'UTR). All plasmids were sequence
637 verified. The *ilc-17.1* expression vector was then injected at 97.5 ng/ul along with the co-
638 injection marker pCFJ90 (p*myo-2*::mCherry::*unc-54* 3'UTR) at 2.5 ng/ul by InVivo Biosystems
639 injection express service. Animals expressing mCherry were singled, lines transmitting the
640 extrachromosomal array were established, and mCherry positive progeny were PCR verified to
641 ensure they were transmitting *ilc-17.1*p:: *ilc-17.1* (cDNA)::3xFLAG:: *ilc-17.1* 3'UTR. These lines
642 were then harvested for Western blot to verify expression of protein.

643 **iv) Generation of ILC-17.1 overexpression strain under the *unc-54* muscle promoter**
644 **and *tbb-2* 3'UTR**

645 To generate VEP031, we overexpressed ILC-17.1 under muscle promoter by fusing - [(*unc-*
646 *54*p:: *ilc-17.1* (cDNA)::3xFLAG] which was synthesized as a gBlock (Integrated DNA
647 technologies) and *tbb-2* 3' UTR which was amplified from genomic DNA. The two fragments
648 were cloned into pUC19 plasmid as the backbone using Gibson assembly[111] to create the
649 overexpression plasmid [(*unc-54*p:: *ilc-17.1* (cDNA)::3xFLAG::*tbb-2* 3'UTR); p*dat-1*::ssmito] and
650 sequence verified. The construct was injected at 100 ng/ul along with the co-injection marker
651 that expressed GFP in the dopaminergic neurons under a *dat-1* promoter [p*dat-1*], at 10 ng/ul
652 into wildtype (N2) worms. Animals expressing GFP in their dopaminergic neurons were singled,
653 lines were established, and GFP-positive progeny were PCR verified to ensure that they were
654 also transmitting harbored the *ilc-17.1* transgene. These lines were then harvested for Western
655 blot to verify expression of protein.

656 **v) Generation of CEP-1 overexpression strain under the *pax-3* P-cell promoter and**
657 ***unc-54* 3'UTR**

658 To generate the strain VEP063 – praEx026(*pax-3*p::CEP-1A cDNA::3xFLAG::*unc-54* UTR;
659 p*myo-2*::mCherry::*unc-54* UTR)], which overexpressed CEP-1 under the P-cell promotor *pax-3*
660 and *unc-54* 3'UTR, we first amplified 2655 bp of genomic sequence upstream of the
661 translational start site (*pax-3* promotor), 1932 bp of CEP-1A full length cDNA sequence without
662 a stop codon from N2 cDNA, and 851 bp of sequence was amplified from vector pDONRP2r-
663 P3(3xFLAG::*unc-54* 3'UTR). These three sequences were then cloned using a BP reaction into
664 the appropriate DONR vectors for the Multisite Gateway Pro cloning kit (Invitrogen) according to
665 manufacturer's guidelines. An expression vector was created by performing the multisite LR
666 reaction using pDEST R1-R2 with the three entry clones generated above to generate pDEST
667 R1-R2 (*pax-3*p::CEP-1A::3xFLAG::*unc-54* 3' UTR) according to manufacturer's instructions. All
668 plasmids were sequence verified. The CEP-1 expression vector was then injected at 120 ng/ul
669 along with the co-injection marker pCFJ90 (p*myo-2*::mCherry::*unc-54* 3'UTR) at 5 ng/ul into N2
670 wildtype animals. Animals expressing mCherry were singled, lines transmitting the
671 extrachromosomal array were established, and mCherry positive progeny were then harvested
672 for Western blot to verify expression of protein.

673 **vi) Generation of crosses.**

674 Crosses between strains were generated according to standard procedures. The primers used to
675 genotype strains are included in the table below.

	Forward primer	Reverse primer
VEP032	TGAATGAGCAAATCGACCAG	AGTTTTGAGATTGAGGGCAAA
	CAGGTCAAGGGGCTAAAACA	CCCACATTAATACTCGCACCT
CF1038	CGGATCAGGAAGAACCAGAA	CATTCCCCGAGTACGAGCTA
	AAGCTGCTGCCTTCACTCTC	ATGGGACTCGAGTTGAGTGG

TJ1	CGGTCTTTTTGGACGATGAA	GTAAACATTGCCGCGTTTTT
	GCGATTCGAAATCCAAGAAG	AGGAACGCATCCATGAAGAC
TJ12	GCCTTCCTCTATTCACTTGAAAC	ACCGAGAGCTCCATGAAGAA
	TCACTCTTTGAATTGGTTCTTTTG	GCTTACGTTCGATTGGCTTC
	AAAAACGCGGCAATGTTTAC	GAGCTTTGTGGGAAGCAATC
RB2075	GACAGTTACGCTGTGCTTGG	CTCCCGGGGTATTCTGAAAT
	GGTGATTCTCCCGTTGGTAA	AAACGGAAATGGCAGAGAGA
CB1370	TAA ATC TCG GAA TTC TGG TGA A	GGA TGA GAC TGT CAA GAT TGG A
	AAG ATG AAC GAG CTG GAG GA	AGA TTG GAG ATT TCG GAA TGG
VEP040	AGA ATT CGA GAA ACA TAA TGA CAT CTT	AAA AAT GCG ATT ATA AAA AGG AAC A
CB1386	CGG CTT GAT CGG ATA GTG AT	AAG AGC AAG GAG TGC GAA AA
	Wild-type PCR product was digested by BstNI	

Antibodies used:Growth conditions for *C. elegans* strains

All strains were grown and maintained at 20°C unless otherwise mentioned. Animals were grown in 20°C incubators (humidity controlled) on 60mm nematode growth media (NGM) plates by passaging 8-15 L4s (depending on the strain) onto a fresh plates. Extra care was taken to ensure equal worm densities across all strains. Animals were fed *Escherichia coli* OP50 obtained from Caenorhabditis Genetics Center (CGC) that were seeded (OD_{600}=1.5 and this was strictly maintained throughout the experiments) onto culture plates 2 days before use. The NGM plate thickness was controlled by pouring 8.9ml of autoclaved liquid NGM per 60mm plate. Laboratory temperature was maintained at 20°C and monitored throughout. For all experiments, age-

686 matched day-one hermaphrodites, or larvae timed to reach specific developmental stages as
687 mentioned in the figure legend, were used.
688 For all experiments with larvae, the timings were adjusted to account for the differences in growth
689 rates at different temperatures. Thus, at 25°C, larvae were harvested 30-36 hrs. post bleach hatch
690 or egg lay, and at 20°C, larvae were harvested 40 hrs. post bleach hatch or egg lay.
691
692 **Obtaining synchronized embryos by 'bleach-hatching'**
693 Bleach-hatching' was performed as previously described[105]. Populations of 250-300 gravid adults
694 were generated by passaging L4s, as described above. These plates were used for obtaining
695 synchronized embryos by bleach-induced solubilization of the adults. Specifically, animals were
696 washed off the plates with 1X PBS and pelleted by centrifuging at 2665Xg for 30s. The PBS was
697 removed carefully, and worms were gently vortexed in the presence of bleaching solution [250µl
698 1N NaOH, 200µl standard (regular) bleach and 550µl sterile water] until all the worm bodies had
699 dissolved (approximately 5-6 minutes), and only eggs were viable. The eggs were pelleted by
700 centrifugation (2665Xg for 45s), bleaching solution was carefully removed and then embryos were
701 washed with sterile water 3-4 times and counted under the microscope. The desired number of
702 embryos were seeded on fresh OP50 plates and allowed to grow at 20°C or 25°C for specific time
703 periods depending on the experimental need. If >5% eggs remained unhatched, these plates
704 were discarded.
705
706 **Dauer Assay**
707 Embryos were allowed to hatch and grow on OP50 plates at 20°C or 25°C for this assay. Embryos
708 were generated according to one of the following two methods: (i) Day-one gravid adults that had
709 grown under normal culture conditions (on OP50 at 20°C) were bleach dissolved as described
710 above, and ~50-100 embryos obtained from these gravid adults were seeded on fresh OP50
711 plates or (ii) day-one gravid adults were allowed to lay eggs on fresh OP50 (or RNAi) plates for

712 2-4 hours at 20°C, the adults were removed, and then embryos were allowed to develop at 20°C
713 or 25°C under humified condition for 48-72 hrs. The former, bleach-synchronization method was
714 used for RNA-seq method and experiments requiring large numbers of age-matched larvae. The
715 latter, timed-egg lay method was used for all other exeriments. For each of the strains and
716 experiments, when we had to use bleach synchronization, we first ensured that bleaching alone
717 did not alter the percentage of dauers or gene expression profiles by conducting a pilot experiment
718 using both methods side-by-side. This was the case for all experiments, except experiments
719 where glucose rescued the dauer phenotype. Here, although the trends were the same, and
720 glucose resulted in a significant rescue of ilc-17.1 deletion mutants and cep-1 OE larvae that were
721 generated either by bleach-synchronization or timed-egg lay, bleach synchronization caused a
722 lower percentage to be rescued from dauer arrest. To assess dauer entry, the number of larvae
723 that arrested as dauers (determined by phenotype and/or resistance to 1%SDS) and those that
724 developed into L4s or adults were counted and percentage of dauers was calculated. The total
725 number of embryos in each plate was ~50-100. Each experiment was performed in triplicate or
726 more.
727
728 For the *ilc-17.1* deletion mutants, in order to acertain that the dauer phenotype was not simply
729 due to the presence of a background mutation, we also conducted the dauer assay after
730 backcrossing the *ilc-17.1* (syb5296) X animals with wild-type Bristol N2 animals, 2X times. The
731 backcrossed strains also arrested as dauers under that same conditions and 100 ± 0% larvae
732 (n=3 independent repeats, 212 larvae scored), arrested as dauers at 25°C as determined by SDS
733 resistance compared to 0% of wildtype larvae.
734
735 **SDS treatment**
736 Larvae were washed off the dauer assay plates, washed 1X with PBS to remove bacteria, treated
737 with 1% sodium dodecyl sulfate (SDS) for 30 minutes, washed again with M9, and then transferred

738 onto a fresh plate. Larvae could be scored easily as dead/dissolved or as live dauer larvae (based
739 on their phenotype, and movement).
740
741 **RNAi mediated downregulation of genes**
742 All RNAi clones used were verified by sequencing, and plates were seeded with RNAi bacteria
743 for a maximum of two days before being used. Day-one gravid adults grown on OP50 were
744 allowed to lay eggs on RNAi-bacteria seeded plates for 2-4 hours at 20°C. A second generation
745 of RNAi knockdown was performed where necessary by transferring L4's on existing RNAi
746 plates to fresh plates for knockdown in their progeny. The adults were allowed lay eggs and
747 then removed, and the embryos were transferred to 25°C (or kept at 20°C) under humified
748 condition for 48-72 hrs. The number of larvae that arrested as dauers (determined by phenotype
749 and/or resistance to 1%SDS) and those that developed into L4s or adults were counted and
750 percentage of dauers was calculated.
751
752 **Exposure to food [OP50] availability**
753 Gravid day-one *ilc-17.1*(pra03 [*ilc-17.1*::SL2::mCherry]) X adults or *ilc-17.1*(pra04 [*ilc-*
754 *17.1*::3xHA]) X adults were bleach dissolved and embryos were placed either on empty plates
755 with no food or NGM plates seeded with OP50 and allowed to grow for 24-36 hours at 25°C. To
756 observe mRNA expression of *ilc-17.1, ilc-17.1*(pra03 [*ilc-17. 1:*SL2::mCherry]) X larvae were
757 anesthetized with 1mM levamisole, mounted on 1% agarose pads, and imaged using a
758 Confocal SPE microscope using optimal settings. mCherry expression served to mark cells that
759 expressed *ilc-17.1* mRNA. To identify where ILC-17.1 protein was expressed prior to food
760 exposure, and after food exposure, 24-36 hour *ilc-17.1*(pra04 [*ilc-17.1*::3xHA]) X larvae were
761 fixed and immunostained using Bouin's Tube Fixation method (see below).
762
763 **Immunofluorescence**

764 Nematodes were fixed and immunostained using a modification of the Bouin's Tube Fixation
765 method [112]. Worms were fixed for 30 min. at room temperature (RT) in 400 µl Bouin's fix (Sigma
766 Aldrich) + 600 µl methanol and 10 µl β-mercaptoethanol by tumbling, freeze cracked three times
767 in liquid nitrogen and again tumbled for 30 mins at RT. For permeabilization, the fixative was
768 removed and exchanged for borate-Triton-βmercaptoethanol (BTB: 1xBorate Buffer, 0.5% Triton
769 and 2% β-mercaptoethanol) solution. Worms were tumbled 3 times for 1 hour each in fresh BTB
770 solution at RT. Worms were washed with PBS-0.05% Tween and incubated in block-solution
771 (5% BSA). Staining with primary antibody was performed overnight at 4 °C, incubation with
772 secondary antibody (Donkey anti-Mouse Alexa Fluor 488, 1:2000) for 2-4 hours at RT. All
773 antibody dilutions were performed using antibody buffer containing 5% BSA. Samples were
774 mounted onto glass slides using VECTASHIELD antifade mounting medium (Vector
775 Laboratories, Burlingame, CA, USA). Primary antibodies used: (i) Monoclonal ANTI-FLAG M2,
776 Sigma Aldrich, 1:500, (ii) Mouse anti-HA antibody, Thermofisher; 2-2.2.14, at 1:1000), (iii) anti β-
777 Actin, Cell Signaling Technology, #4967, 1:1000.
778
779 **Chemotaxis**
780 Chemotaxis assay was performed on 9 cm petri dishes containing NGM. Two marks were made
781 on the back of the plate at opposite sides of the plate about 0.5 cm from the edge of the agar.
782 About 5 µl of attractant diluted in water was placed on the agar over one mark, and 5 µl of water
783 was placed as the control over the opposite mark. Attractants and concentrations used are
784 listed in drugs and metabolites section. 5 ul sodium azide with the concentration of 1M was also
785 placed at both the attractant source and the control source. This drug could anesthetize animals
786 within about a 0.5-cm radius of the attractant. Age synchronized day-one adult worms were
787 transferred to the middle of the NGM plates at a point equidistant from the middle of each
788 odorant. After 1 hr., the assay was quantified by counting the number of worms that had left the

789 center origin a chemotaxis index was calculated [#Odor - #Control] / [#Odor + #Control]. Each
790 repeat consisted of 50 worms, and experiments were repeated a minimum of three times.
791
792 **Measuring Pharyngeal pumping**
793 Synchronized day-one adults were singled onto NGM plates seeded with OP50, and onto plates
794 without OP50. Pharyngeal pumping rates were determined by recording the pharyngeal region of
795 animals by video using a Leica S9i digital stereo microscope at 5X magnification and slowing
796 down the video to manually count the number of 'pumps' in 10 seconds, three times per animal.
797 The mean of these pumps was determined and the number of pumps/minute calculated. One
798 complete cycle of synchronous contraction and relaxation of the corpus and the terminal bulb was
799 counted as a pump.
800
801 **Feeding of fluorescent latex beads**
802 Overnight 5ml OP50 culture LB was pelleted and resuspended in fresh 0.5ml LB to concentrate
803 bacteria. 1 µl of fluorescent beads of 0.5µm mean particle size that mimic size of *E. coli*. (Sigma
804 L3280, red fluorescence) was added to 1 ml of concentrated OP50 [1:1000 ratio (v/v)], and 100ul
805 of the mixture was seeded onto NGM plates [113]. Synchronized day-one adults were allowed to lay
806 eggs on the bead containing plates for 2 hours at 20°C and then removed. After 40 hours, larvae
807 were picked onto 1% agarose pads on glass slides and anesthetized using 10mM levamisole. Z-
808 stack images of the larvae were taken on Leica TCS SPE confocal microscope and number of
809 beads within a set area near the tail region per larvae was quantified.
810
811 **Drug and metabolite treatment**
812 The following drugs or metabolites were used:

Drug/metabolite	Source	Final concentration

Glucose	Research products International	50/100mM
2-Deoxy-d-glucose	R&D systems	50mM
Mitotempo	Millipore sigma	0.1mM
L-Glutamine	Sigma-Aldrich	0.26mM
Skim Milk powder	HyVee - instant nonfat dry milk	20mM
Diacetyl	Sigma-Aldrich	0.01% v/v
Lysine	Sigma-Aldrich	1M
(25S)-Δ7-Dafachronic Acid	Cayman Chemical	50nM
8-Bromo-cGMP	Cayman Chemical	5mM

813 The drug solution (0.5 ml) was spread onto NGM agar plates containing an OP50 lawn and left
814 for 1 hr. to dry or used for chemotaxis assays as described. Age synchronized day-one adult
815 worms were transferred to the middle of the NGM plates for 4 hrs. and dauer assay were
816 performed as described. Sterile water was used as control.
817 8-Bromo-cGMP solution was first added to standard NGM plates and allowed to dry for 1 hour.
818 1.5 OD op50 was added on top and allowed to grow for 1 day before starting the dauer assay as
819 described.
820 Plates containing D-glucose were prepared as described in published methods [98], except
821 previously except that we seeded live OP50 onto Glocose plates. Stock solutions of 0.1 and 1M
822 Sterile D-glucose was prepared and added into NGM agar to obtain final concentration of 5mM
823 and 50mM, respectively. For control plate, equivalent amount of sterile water was added to
824 NGM agar. The plates were left to dry for 2 days at RT before seeding 1.5 OD OP50 onto them.
825 After drying at RT for another 1day, dauer assays were performed as described.

826

827 **Fluorescence Image analysis**

828 ImageJ (Fiji) v1.53i was used for measuring fluorescence intensity as follows: single planes [,
829 DAF-16::GFP, CEP-1::GFP, TG12] or projections of z-planes [DAF-28, INS-4, fluorescent latex
830 beads,pax-3p::mCherry] were used for measuring fluorescence intensity. The region of interest
831 was circled using the circle selection tool. The mean fluorescence intensity of each circled area
832 was recorded using the measurement tool. When appropriate, the background fluorescence
833 intensity was measured and subtracted. Quantification of measurements was done in Microsoft
834 excel/GraphPad.
835
836 **RNA-sequencing and Data analysis**
837 **a) RNA isolation, library preparation and sequencing**
838 For the Total RNA-seq samples: Day-one adult worms were bleach-hatched and ~3200
839 eggs/genotype (~800 eggs/plate and 4 plates/genotype) were seeded on fresh OP50
840 plates and allowed to grow for 30-34 hrs. at 25°C. Worms were washed with sterile water
841 and total RNA was extracted from biological triplicates using the Direct-zol RNA Miniprep
842 Kits (catalog no. R2050, Zymo Research). Libraries were prepared using the Illumina
843 Stranded Total RNA Prep
844 with Ribo-Zero Plus, for rRNA depletion (catalog no. 20040525, Illumina). Samples
845 were sequenced in one lane of the Illumina NovaSeq 6000, generating 2x150bp paired-
846 end reads.
847 For the mRNA-seq samples : Day-one adult worms were bleach-hatched and ~3200
848 eggs/genotype (~800 eggs/plate and 4 plates/genotype) were seeded on fresh OP50
849 plates and allowed to grow for either 15 hours or 32 hours at 25°C. Worms were washed
850 with sterile water and total RNA was extracted from biological triplicates using the Direct-
851 zol RNA Miniprep. Libraries were prepared using Illumina TruSeq Stranded mRNA kit.

852 Samples were sequenced in one lane of the Illumina NovaSeq 6000, generating 2x100bp
853 paired-end reads.
854
855 **b) RNA-seq analysis**
856 The quality of the RNA sequences was assessed with FastQC. Adapters and sequence
857 reads with a quality lower than Q25 were trimmed by using Trimgalore [114](v0.67).
858 Ribosomal RNA (rRNA) contamination was filtered with sortmeRNA[115] (version 4.3.4).
859 Sequencing reads were aligned to the *C. elegans* genome (WBcel235[116]) using the Star
860 aligner[117] (v2.7.9a) and then the aligned reads were quantified with FeatureCounts
861 v2.0.1 from the R package Rsubread[118] . Differential expression analysis was performed
862 using DESeq2[119] and genes with FDR corrected p-value of < 0.05 were considered
863 significant. Pairwise distance analysis (sample-to-sample) was performed by using
864 normalized counts coupled with the variance stabilization transformation (VST) on the
865 complete set of genes and calculating the Euclidean distance between the replicates.
866 Principal Component Analysis (PCA) was done using the plotPCA function in DESeq2[119]
867 with the VST transformed data. The mRNA-seq was analyzed following a similar
868 protocol as described above, excluding the SortmeRNA step.
869 The microarray data for the *C. elegans* dauer stage was obtained from the
870 Supplementary Table 1 of the study by Wang, J. & Kim (2003)[37]. The expression values
871 of the dauer stage were defined as the dauers expression (fold-change) at 0hr relative to
872 the mixed staged reference RNA. Sequences IDs from the array were converted to
873 standard gene nomenclature using Simplemine in Wormbase[120]. The correlation
874 between the expression at the dauer stage and the fold change in expression in the *ilc-*
875 *17.1* deletion mutant relative to the wild type, was determined by performing a Spearman
876 Rank Test.

877 The expression of C. elegans larvae (L1) treated with ascaroside cocktail was obtained
878 from Cohen, et al. [121]. The correlation between the Fold-Change in expression in the
879 larvae treated with ascaroside relative to N2 larvae and the fold change in expression in
880 the *ilc-17.1* deletion mutant relative to the wild type, was determined by performing a
881 Spearman Rank Test. The differentially expressed genes (DEGs) between N2 and daf-
882 1(m40) was obtained from. Hu, et al. [122] and were presented as Log_2(Fold-Change)
883 values. The overlap between differentially expressed genes (DEGs) in the cep-1
884 overexpression mutant and the *ilc-17.1* deletion mutant was tested using Fisher exact
885 test from the Gene Overlap package[123]. Venn diagram was done using the R package
886 VennDiagram[124].

887 **c) Functional analysis**

888 Gene ontology analysis (GO) and KEGG enrichment analysis was performed on the
889 differentially expressed genes by using ClusterProfiler 4.0[125]. Terms with an FDR
890 corrected p-value <0.05 were considered significant. The annotations were obtained
891 from R package org.Ce.eg.db[126] (version 3.14) and the KEGG database[127]. The
892 annotations of genes as part of the metabolic pathways were obtained from the
893 database Wormpaths[100] and heatmaps were done using the R packages
894 Complexheatmap and pheatmap[128,129].

895

896 **Progenitor blast cell (P cells) imaging and quantification.**

897 Synchronized day-one adults were allowed to lay eggs on OP50 plates for 2 hours at 20°C and
898 then removed. The plates were then placed at 20C or 25°C. After 15 hours, about 10 L1 larvae
899 were picked onto 1% agarose pads on glass slides and anesthetized using 10mM levamisole and
900 imaged on a Leica SP8. Cells expressing pax-3p::mCherry and CEP-1::GFP were scored, and
901 the percent pax-3p::mCherry cells that also expressed CEP-1::GFP was calculated for individual
902 worms.

903

904 **DiO dye filling assay to identify amphid neurons**

905 A stock dye solution containing 2mg/ml DiO (Molecular Probes, catalog # D-275) in dimethyl
906 formamide is made and maintained under dark conditions. Day-one adult worms were
907 transferred into an eppendorf tube with 1 ml of M9, spun down at 2000-3000 rpm and
908 supernatant removed. Worms were resuspended in 1 ml of M9 and 5 microliter DiO stock sol
909 (1:200 dilution) was added and incubated on a slow shaker for 2 hours at room temperature.
910 Worms were spun down and washed with M9 twice before transferring them onto agar pads
911 with 1mM levamisole to visualize by fluorescence using a Leica TCS SPE confocal microscope.

912

913 **Dauer pharyngeal pumping**

914 Synchronized day-one adults were allowed to lay eggs on OP50 plates for 2 hours at 20°C and
915 then removed. The plates were then placed at 25°C, and larvae were allowed to arrest as dauers
916 or grow into L4 larvae (RNAi treatment) . On day 3, larvae that remained arrested as dauers were
917 used to measure pharyngeal pumping rates using Zeiss Axio Observer.A1 at 40X magnification.
918 WT (N2) L2 stage larvae were used to measure pumping rates as controls. Pumping rates were
919 measured by counting the number of grinder movements in the terminal bulb per minute. The
920 average of three biological replicates consisting of 10 dauer larvae each was quantified.

921

922 **Scoring apoptotic nuclei with Acridine Orange**

923 Acridine orange (AO) staining was performed as previously described (Hefel et al. 2021). AO
924 staining to detect apoptotic germline cells was performed by picking 50 L4 animals to a fresh
925 plate and allowing them to grow into day-one adults for 24 hours at 20°C. Day 1 adults were
926 then either exposed to 75 Gy from a Cesium source or left unirradiated. 24 hours later, AO
927 staining was performed.. For each trial, 10 mg/ml AO stain was freshly prepared and then
928 diluted 1:400 with M9 buffer. Worms were then picked to a tube of the diluted AO stain, wrapped

929 tightly with foil, and rotated at room temperature for 1 hour. After mixing, worms were
930 transferred to a fresh OP50 plate and allowed to crawl away from residual AO stain for 1 hour
931 before being picked to a droplet of 10 mM levamisole on a 1% agarose pad. A cover slip was
932 added, and worms were imaged immediately using the Leica fluorescence microscope on 60x
933 magnification. It was important to visualize AO within 10 mins after mounting animals on the
934 pad. The number of AO stain positive cells found in 12 individual gonad arms per experiment
935 were recorded for each sample.
936

937 **Gamma irradiating *C. elegans* to activate CEP-1/p53**

938 100 L4 larvae were picked onto an OP50 seeded plate, allowed to mature into day-one adults
939 and exposed to 75 Gy gamma irradiation, and subsequently harvested for Western blot
940 analysis. To determine the number of AO positive apoptotic nuclei, at least 50 L4 larvae were
941 exposed to 75 Gy gamma irradiation. The number of AO positive cells were scored 24 hrs. later,
942 when animals had matured into day-one adults.
943

944 **Western blot analysis**

945 **i. Western blot analysis of *C. elegans***

946 Western blot analysis was performed with 30–100 adult day-one animals, or approximately 400
947 30-36 hr. larvae as indicated. Animals were harvested in 15 µl of 1X PBS (pH 7.4), and 4X
948 Laemmli sample buffer (catalog no. 1610737, Bio-Rad) supplemented with 10% β-
949 mercaptoethanol was added and samples were boiled for 30 min. Whole-worm lysates were
950 resolved on 12% SDS-PAGE gels and transferred onto nitrocellulose membrane (catalog no.
951 1620115, Bio-Rad). Membranes were blocked with Odyssey Blocking Buffer (part no. 927–50000,
952 LI-COR). Immunoblots were imaged using LI-COR Odyssey Infrared Imaging System (LI-COR
953 Biotechnology, Lincoln, NE). Mouse anti-FLAG M2 antibody (catalog no. F1804,
954 RRID:AB_262044,_Sigma Aldrich) was used at 1:500 to detect CEP-1::FLAG. Mouse anti-HA

955 antibody (Thermofisher; 2-2.2.14), was used at 1:1000 to detect ILC-17.1::HA. Mouse anti-α-
956 tubulin primary antibody (AA4.3, RRID:AB_579793), developed by C. Walsh, was obtained from
957 the Developmental Studies Hybridoma Bank (DSHB), created by the National Institute of Child
958 Health and Human Development (NICHD) of the National Institute of Health (NIH), and
959 maintained at the Department of Biology, University of Iowa. The following secondary antibodies
960 were used: Donkey anti-mouse IgG (H and L) Antibody IRDye 800CW Conjugated (Licor) and
961 Alexa Fluor 680 goat anti-rabbit IgG (H+L) (Invitrogen). LI-COR Image Studio software
962 (RRID:SCR_015795) was used to quantify protein levels in different samples, relative to α-tubulin
963 levels. Fold change of protein levels was calculated relative to wildtype (N2)/ controls.

964 **ii. Western blot analysis of epithelial cell lines**

965 A549 epithelial cells were lysed in a modified M2 buffer containing 20mM
966 tris[hydroxymethyl]aminomethane, 150mM NaCl at pH 7.4, 0.5% NP40, 3mM EDTA, 3mM
967 EGTA, 4mM PMSF, and a cOmplete Mini, EDTA-free protease inhibitor tablet according to the
968 manufacturer's instructions (Roche, #11836170001). Epithelial cells were collected by
969 mechanical dislodgment in lysis buffer at individual time points, incubated for 20 minutes on ice,
970 and spun at 14,000 x g for 5 minutes to remove insoluble material. 25ug protein was resolved
971 by NuPAGE™ 4-12% Bis-Tris gel (Invitrogen) and transferred to PVDF for immunoblotting. Anti-
972 p53 (Cell Signaling Technology, #9282) and β-actin (DSHB, 224-236-1) primary antibodies were
973 used with HRP-conjugated secondary antibodies to anti-rabbit IgG (Jackson ImmunoResearch,
974 #111-035-003) and anti-mouse IgG (Invitrogen, #62-6520). Densitometry was analyzed with
975 ImageJ software.

976

977 **RNA extraction and real-time quantitative reverse-transcriptase PCR (RT-PCR)**

978 Worms were bleach-hatched as described above and ~400-800 eggs/plate (2 plates/strain) were
979 seeded on fresh OP50 plates and were allowed to grow (i) for 30-34 hrs. at 25°C or (ii) for 36 hrs.

980 at 20°C and then harvested for RNA extraction. RNA was extracted as described earlier [130].
981 Briefly, plates were washed with sterile water and centrifuged. Water was carefully removed and
982 300 µl of Trizol (catalog no. 400753, Life Technologies) was added and snap-frozen immediately
983 in liquid nitrogen. Samples were thawed on ice and then lysed using a Precellys 24 homogenizer
984 (Bertin Corp.). RNA was then purified as detailed with appropriate volumes of reagents modified
985 to 300 µl of Trizol. The RNA pellet was dissolved in 17 µl of RNase-free water. The purified RNA
986 was then treated with deoxyribonuclease using the TURBO DNA-free kit (catalog no. AM1907,
987 Life Technologies) as per the manufacturer's protocol. cDNA was generated by using the iScript
988 cDNA Synthesis Kit (catalog no. 170–8891, Bio-Rad). qRT-PCR was performed using PowerUp
989 SYBR Green Master Mix (catalog no. A25742, Thermo Fisher Scientific) in QuantStudio 3 Real-
990 Time PCR System (Thermo Fisher Scientific) at a 10 µl sample volume, in a 96-well plate (catalog
991 no. 4346907, Thermo Fisher Scientific). The relative amounts of mRNA were determined using
992 the $\Delta\Delta C_t$ method for quantitation. We selected *pmp-3* as an appropriate internal control for gene
993 expression analysis in *C. elegans*.
994
995 All relative changes of mRNA were normalized to either that of the wild-type control or the control
996 for each genotype (specified in figure legends). Each experiment was repeated a minimum of
997 three times. For qPCR reactions, the amplification of a single product with no primer dimers was
998 confirmed by melt-curve analysis performed at the end of the reaction. Primers were designed
999 using Primer3 software and generated by Integrated DNA Technologies. The primers used for
1000 the qRT-PCR analysis are listed below:

Gene	**Forward primer (5'-3')**	**Reverse primer (5'-3')**
pfk-1.2	TTGCATCGAATCTGTGAAGC	TCGCTGCAGTCAAAGCTAGA
cyc-2.2	CGGTGGAGCTATTCCAGAAG	GCAACTTGTCCGGATTGTCT
egl-1	TCCAAGCTAGCAGCAATGTG	GCGAAAAAGTCCAGAAGACG

ced-13	GCAACTCAAACACCGTTGAA	CAATGCTGGCATACGTCTTG
phg-1	CAGAGGAGCTTGTACCGACA	TCGTCTCTAGCAGTGCATGT
sod-3	CACTGCTTCAAAGCTTGTTCA	ATGGGAGATCTGGGAGAGTG
mtl-1	TGGATGTAAGGGAGACTGCAA	CATTTTAATGAGCCGCAGCA
lys-7	GCCGTCAAACTTGGCATCTT	GGGTTGTATGCACGAACGAA
pmp-3	TAGAGTCAAGGGTCGCAGTG	ATCGGCACCAAGGAAACTGG
cep-1(a+b isoform)	GCTCACTCTGTCGACTGCTGAGT	AACCCAAGTGTATCTGGGAACTTT
cep-1(a isoform)	GTTGTGCTCGACTCCCAAAAG	GGCACGCTTCTCAATTACAAGTT

1001

1002 **Chromatin immunoprecipitation (ChIP)**

1003 Chromatin immunoprecipitation (ChIP) was performed as described earlier (Das et al., 2020).
1004 Day-one adult worms were bleach-hatched as described above and ~1600 eggs were seeded
1005 (~800 eggs/plate and 2 plates/genotype) on fresh OP5O plates. Plates were kept at 25°C for 30-
1006 34 hrs. and larvae were washed with 1X PBS (pH 7.4) and cross-linked with freshly prepared 2%
1007 formaldehyde (catalog no. 252549, Sigma Aldrich) at room temperature for 10 min followed by
1008 addition of 250 mM Tris (pH 7.4) at room temperature for 10 min. Samples were then washed
1009 three times in ice-cold 1X PBS supplemented with protease inhibitor cocktail and snap-frozen in
1010 liquid nitrogen. The worm pellet was resuspended in FA buffer [50 mM HEPES (pH 7.4), 150 mM
1011 NaCl, 50 mM EDTA, 1% Triton-X-100, 0.5% SDS and 0.1% sodium deoxycholate], supplemented
1012 with 1 mM DTT and protease inhibitor cocktail. The suspended worm pellet was lysed using a
1013 Precellys 24 homogenizer (Bertin Corp.), and then sonicated in a Bioruptor Pico Sonication
1014 System (catalog no. B0106001, Diagenode) (15 cycles of 30 s on/off).

1015 Endogenous CEP-1 was immunoprecipitated with anti-FLAG M2 magnetic bead (catalog no. M-
1016 8823, Sigma-Aldrich). Beads were first pre-cleared with salmon sperm DNA (catalog no. 15632–
1017 011, Invitrogen). Worm lysate was incubated at 4°C overnight with the pre-cleared FLAG beads.
1018 Beads were washed with low salt, high salt and LiCl wash buffers and then eluted in buffer
1019 containing EDTA, SDS and sodium bicarbonate. The elute was then de-crosslinked overnight in
1020 presence of Proteinase K. The DNA was purified by ChIP DNA purification kit (catalog no. D5205,
1021 Zymo Research). qPCR analysis of DNA was performed as described above using primer sets
1022 specific for different target genes. For all ChIP experiments, 10% of total lysate was used as 'input'
1023 and chromatin immunoprecipitated by different antibodies were expressed as % input values. The
1024 primers used for ChIP experiments, and the expected amplicon sizes are as follows:

Gene	**Position**	**Forward primer (5'-3')**	**Reverse primer (5'-3')**	**Amplicon size**
egl-1	TSS +4 to +123)	CTCACCTTTGCCTCAACCTC	CGAGGAGAAGTCCTGAGACG	120 bp
ced-13	Promoter (-428 to -310)	CTATTCTTGGCCGTGCTCAT	AGGCAATCTAGCATGCACCT	119 bp
phg-1	Promoter -428 to -294)	GCCAAACCTTCCAGATTTACA	TTCCTAGATAAGGGTTAGATGATGAGA	135 bp
phg-1	Intron 1 (+223 to +326)	AAGCTGAGCTCCGAAAACAA	TTTCCCGCTAAACGAGACAT	104 bp

cki-1	Promoter (-698 to -722)	TTT TCC ATA CTT CAC TAG TCA AAA CCT	GAC AGT GAG AAG CTT TCG TAT TGA	103 bp
cki-1	Promoter (-542 to -428)	TTC CTC ATA ATC ACG GAG CA	GGA ACC GAA GTG GTC AGA TG	114 bp
cki-1	Promoter (-323 to -217)	TCT CCG ACT GCT GAC CT	CGA GAA GGG GTG GAG TCA TA	106 bp

1025

1026 **Treatment of mouse epithelial cell lines with human IL-17 and Nutlin3A**

1027 A549 epithelial cells were seeded in a 6-well plate overnight and stimulated with 50-100ng/mL
1028 recombinant human-IL-17 (Peprotech, SKU 200-17) or 10uM Nutlin3A (Tocris, 675576-98-4),
1029 and supernatants and cell lysates were harvested 18 hours later.

1030

1031 **QUANTIFICATION AND STATISTICAL ANALYSIS**

1032 Each 'experiment' refers to a set of independent biological samples that undergo treatment
1033 together. No statistical methods were used to predetermine sample size, and experiments were
1034 not randomized, but some were blinded. For the assays where we scored dauers, for each
1035 experiment, independent biological samples of the different strains were allowed to lay eggs and
1036 the eggs were subjected to 'treatment' or 'control' conditions. The results of an experiment
1037 generated counts categorized as either (a) dauers, or (b) non-dauers. The counts of dauers/non-
1038 dauers for the different types of experiments were used to generate a contingency table, and a
1039 chi-squared test was performed to test the independence (whether the results are related or not)
1040 of the experiment. This Chi-square statistic, degrees of freedom (df) and p value for each
1041 experiment is reported. Yates' continuity correction was used to prevent overestimation of

statistical significance for small data. For qPCR or other experiments, the data were analyzed by using Student's t-test and/or one-way ANOVA with Tukey's correction (GraphPad Prism software) as described in respective figure legends. P values are indicated as follows: *p<0.05; **p< 0.01; ***p<0.001, ns, not significant.

DATA AVAILABILITY

The following data sets were generated

Genes differentially expressed in the following *C. elegans* larvae bleach-hatched and allowed to grow for 30-36 hr. at 25°C: wild type (N2), *ilc-17.1*(syb5296) X and praEx022 (*unc-54*p::*ilc-17.1* cDNA::3XFLAG::*tbb-2* 3'UTR; p*dat-1*::GFP::*unc-54* 3'UTR).

Genes deferentially expressed in the following *C. elegans* larvae bleach-hatched and allowed to grow for 15 hr. and 32 hr. at 25°C: wild type (N2), *ilc-17.1*(syb5296) X, *cep-1* (gk138) I, *ilc-17.1*(syb5296) X; *cep-1* (gk138) I, and VEP036 (unc-119 (ed4); gtIs1 [CEP-1::GFP + unc-119 (+)].

The data discussed in this publication have been deposited in NCBI's Gene Expression Omnibus (Edgar et al., 2002) and are accessible through GEO Series accession number GSE218596, , https://www.ncbi.nlm.nih.gov/geo/query/acc.cgi?acc=GSE218596 and GSE229132, https://www.ncbi.nlm.nih.gov/geo/query/acc.cgi?acc=GSE229132

1063 **Figure 1: ILC-17.1 is released by larval amphid neurons in response to food availability and**
1064 **reduced ILC-17.1 signaling causes dauer arrest.**
1065 **a.** Schematic of experiment to assess dauer arrest. For each experiment, independent samples
1066 of 10 day-one adults of each strain laid eggs for two hours at 20°C on 60 mm NGM plates with
1067 OP50 lawns. Adults were removed, and embryos were transferred to 25°C. Approximately 48 hr.
1068 later, larval phenotype was scored and categorized as either dauers, or larvae that continued
1069 development into stage 4 larvae (L4) and/or young adults. If unsure, SDS-resistance was used to
1070 confirm dauer arrest. Extent of crowding on plates was comparable. [Representative average
1071 numbers of embryos/plates from experiments in **b** are 64, 68, 56, 46 and 65 for wildtype (N2), *ilc-*
1072 *17.1*(syb5296) X, *ilc-17.1*(syb5297) X, *ilc-17.1*(syb5296) rescued with *ilc-17.1p::ilc-17.1*, and *ilc-*
1073 *17.1*(syb5296) rescued with *unc-54p::ilc-17.1* respectively]. Pearson's Chi-squared test with
1074 Yates' continuity correction was used to determine significance throughout the manuscript, unless
1075 otherwise stated. Chi-squared values were calculated for whole experiments, and for pair-wise
1076 comparisons. All legends show Chi-squared, df and p values for the whole experiment; p values
1077 for pair-wise comparisons are depicted on graphs using ***$p < 0.001$, **$p < 0.01$, *$p < 0.05$ and ns,
1078 not significant.
1079
1080 **b.** Percentage larvae that arrest as dauers. ***$p<0.001$. (*n*=3-12 experiments; Chi-squared =
1081 2359.6, df = 4, p-value < 2.2e-16.)
1082
1083 **c**, **d**. Representative micrographs 48 hours post-hatching at 25°C. **Top (c):** Wildtype (N2) grew
1084 to L4s. **Bottom (d):** *ilc-17.1*(syb5296) larvae arrested as dauers. Scale bar, 0.5mm.
1085
1086 **e. Top**: Schematic of experiment. **Bottom**: Percentage of wildtype (N2) and *ilc-17.1* larvae that
1087 arrest as dauers on control (L4440) and *ilcr-2* RNAi. ***$p < 0.001$, ns, not significant (n=3-10
1088 experiments. Chi-squared = 1815.1, df = 7, p-value < 2.2e-16.)

1089

1090 **f. Top:** Schematic of experiment to localize *ilc-17.1* mRNA and ILC-17.1 protein in the presence
1091 and absence of food (OP50). Embryos were hatched at 20°C and imaged after 24-36 hours (L1
1092 stage larvae). **Left panels:** Representative micrographs of z-section showing mCherry co-
1093 expressed with *ilc-17.1* mRNA in amphid neurons. **Right panels**: projection of z-sections showing
1094 immunostaining with anti-HA antibody to visualize CRISPR tagged endogenous ILC-17.1::HA
1095 protein. Pharyngeal region of larvae **(top panel)** hatched in the absence of food, and **(middle**
1096 **panel)** in the presence of food (OP50). B**ottom panels:** Controls (N2) that do not express HA or
1097 mCherry used to assess specificity of the fluorescence signal. (n>3 experiments, 4-5 larvae each).
1098 Scale bar, 5µm.

1099

1100 **g.** KEGG enrichments associated with differentially downregulated genes (p.adjust <0.05) in *ilc-*
1101 *17.1* mutant larvae (RNA-seq on 32-36 hr. larvae).

1102

1103 **h**. KEGG enrichments associated with differentially upregulated genes (p.adjust <0.05) in *ilc-17.1*
1104 mutant larvae (RNA-seq on 32-36 hr. larvae).

1105

1106 **i**. Heatmap depicting expression levels (log_2 normalized counts) of the major dauer-specific
1107 collagens in wildtype (N2) as L2-L3 larvae *en route* to development into reproductive adults, *ilc-*
1108 *17.1* deletion mutants *en route* to dauer entry and *ilc-17.1* deletion mutants rescued from dauer
1109 entry with *unc-54p::ilc-17.1.*

1110

1111 Bars show mean ± S.E.M. Individual data points in the bar graphs in **b** and **e** represent the %
1112 dauers/experiment, and the bar graph depicts mean of these percentages.

1113

1114 **Figure 2: Reduced ILC-17.1 signaling acts through DAF-16/FOXO, DAF-3/SMAD-DAF-**
1115 **5/Ski complex, steroid hormone signaling and CEP-1/p53 to control dauer arrest.**
1116 **a.** Percent dauers in *ilc-17.1* deletion mutants and *ilc-17.1;daf-16* double mutant larvae.
1117 ***p < 0.001, (*n*=4-8 experiments, Chi-squared = 497.65, df = 1, p-value < 2.2e-16).
1118
1119 **b. Left**: Percent larvae showing DAF-16::GFP nuclear localization in intestinal cells. Larvae were
1120 grown at 20°C for 36 hrs**.** *n*=3 experiments with 10-15 larvae each. Each data point represents
1121 average no. of larvae with nuclear DAF-16::GFP/experiment. ***p < 0.001, (unpaired t-test). Note:
1122 experiments were conducted at 20°C, since DAF-16::GFP localized constitutively in intestinal
1123 nuclei even in wildtype larvae at 25°C. **Right:** representative micrographs showing intestinal DAF-
1124 16::GFP (boxed) in wildtype and *ilc-17.1* deletion mutant larvae. Scale bar, 5μm
1125
1126 **c.** Average *sod-3, mtl-1, and lys-7* mRNA levels in larvae 32-36 hr. post-hatching at 25°C. mRNA
1127 levels were determined relative to *pmp-3* and normalized to wildtype (N2) values. *n*=4-10
1128 experiments. ***p < 0.001, **p < 0.01, ns=not significant, (unpaired t-test).
1129
1130 **d.** Percent dauers in *ilc-17.1* mutants and *ilc-17.1;daf-5* double mutants. ***p < 0.001, (*n*=3-5
1131 experiments, Chi-squared = 787.3, df = 3, p-value < 2.2e-16).
1132
1133 **e.** Percent dauers in *ilc-17.1* mutants on control (H_2O) and exogenous 50nM Δ7-dafachronic acid.
1134 ***p < 0.001, (*n*=3-5 experiments, Chi-squared = 784.32, df = 3, p-value < 2.2e-16).
1135
1136 **f-h. f,** percent dauers in *ilc-17.1* mutants and *ilc-17.1;cep-1* double mutants. ***p < 0.001, (*n*=3-5
1137 experiments, Chi-squared = 1029.2, df = 3, p-value < 2.2e-16). Representative micrographs of **g,**
1138 *ilc-17.1* deleted larvae arrested as dauers, and **h,** *ilc-17.1;cep-1* double mutants that grew to L4s,
1139 48 hr. post-hatching at 25°C. Scale bar, 0.5mm

1140

1141 Bars show the mean ± S.E.M. Individual data points in bar graphs in **a, d, e, f** represent the

1142 average % dauers/experiment, Pearson's Chi-squaredd test with Yates' continuity correction.

1143

1144 **Figure 3: CEP-1/p53 acts downstream of reduced ILC-17.1 signaling and activates DAF-**
1145 **16/FOXO, DAF-3/SMAD-DAF-5/Ski complex to control dauer entry.**

1146 **a-c. a,** Percent dauers in wildtype (N2), *cep-1 (lg12501)*;CEP-1::GFP animals that do not
1147 overexpress CEP-1/p53, and CEP-1/p53 overexpressing larvae. ***p < 0.001, (n=3-4
1148 experiments, Chi-squared = 569.35, df = 2, p-value < 2.2e-16). For *cep-1* mRNA expression levels
1149 see **Supplementary Fig. S6a**. Representative micrographs 48 hrs. post-hatching at 25°C,
1150 showing in **b,** CEP-1/p53 overexpressing larvae arrested as dauers and **c,** *cep-1 (lg12501)*; CEP-
1151 1::GFP as L4s. Scale bar, 0.5mm.

1152

1153 **d.** Percent dauers in wildtype (N2), and CEP-1/p53 overexpressing larvae on control (Ctrl; L4440)
1154 and *daf-16* RNAi. ***p < 0.001, **p <0.01 (n=3-4 experiments, Chi-squared = 494.22, df = 3, p-
1155 value < 2.2e-16).

1156

1157 **e.** Percent dauers in wildtype (N2), *daf-5* (e1386), CEP-1/p53 overexpressing larvae, CEP-1/p53
1158 overexpressing larvae crossed to *daf-5* (e1386), and N2 and CEP-1/p53 overexpressing larvae
1159 treated with 50nM Δ7-dafachronic acid (DA). ***p < 0.001, **p<0.01, ns, not significant, (n=3-4
1160 experiments, Chi-squared = 982.66, df = 5, p-value < 2.2e-16).

1161

1162 **f**. Average *sod-3, mtl-1, and lys-7* mRNA levels in larvae 32-36 hr. post-hatching at 25°C. mRNA
1163 levels were determined relative to *pmp-3* and normalized to wildtype (N2) values. n=4-10
1164 experiments. ***p < 0.001, **p < 0.01, ns=not significant, (unpaired t-test).

1165

1166 **g**. Average *egl-1* and *ced-13* mRNA levels in 32-36 hr. larvae grown at 25°C. mRNA levels were
1167 determined relative to *pmp-3* and normalized to wildtype (N2) values. n=6-7 experiments.
1168 ***p < 0.001, **p < 0.01, *p < 0.05, ns=not significant, (unpaired t-test).

1169

1170 **h.** CEP-1 occupancy (expressed as percent input) in 32-36 hr. larvae grown at 25°C, measured
1171 at the promoter proximal regions of *egl-1* and *ced-13* (**Top,** schematic). CEP-1 occupancy was
1172 assayed in animals where endogenous *cep-1* was FLAG tagged at its C-terminus using
1173 CRISPR/Cas9, and immunoprecipitated with anti-FLAG antibody. Strains used: CEP-1::FLAG
1174 expressing animals in control wildtype background (Ctrl), in *ilc-17.1* background, and in *ilc-17.1*
1175 rescued from dauer arrest by *unc-54p::ilc-17.1* (*ilc-17.1;unc-54p::ilc-17.1* CDS). n=4 experiments.
1176 ***$p < 0.001$, **$p < 0.01$, *$p < 0.05$. (unpaired t-test).
1177
1178 **i. Top**: Representative Western blot showing CEP-1::FLAG and tubulin when crossed into *unc-*
1179 *54p::ilc-17.1,* and *ilc-17.1* deletion backgrounds. *cep-1* RNAi serves to show specificity. Samples
1180 constitute 32-36 hr. larvae grown at 25°C, except for positive control, irradiated sample (4; adults).
1181 **Bottom**: CEP-1 levels were quantified relative to tubulin and normalized to values from control
1182 animals (Ctrl; CEP-1::FLAG in wildtype background). n=4 experiments. Numbers in data bars
1183 correspond to representative bands on western. ***$p < 0.001$, **$p < 0.01$ (unpaired t-test).
1184
1185 Bars show the mean ± S.E.M. Individual points in bar graphs in **a, d, e** represent the %
1186 dauers/experiment, Pearson's Chi-squaredd test with Yates' continuity correction.
1187
1188

1189 **Figure 4. CEP-1/p53 accumulates in multipotent progenitor cells (P cells) during dauer**
1190 **entry, upregulates cell cycle inhibitors, and modulates cell fate.**
1191 **a.** Representative micrographs of 15 hr. L1 larvae at 25°C, showing *pax-3p::*mCherry marking
1192 ventral postembryonic blast cells (P cells; **top panel**; see schematic above), CEP-1::GFP
1193 expression (**middle panel**), and overlap (**bottom panel**) to show co-localization. Co-localized
1194 cells are marked with *. CEP-1::GFP expressing cells that do not co-localize with *pax-3p*::mCherry
1195 marked with #. Insets: zoom-in on the P blast cells. Scale bar=5um.
1196
1197 **b.** Percent co-localization between *pax-3p::*mCherry-expressing cells and CEP-1::GFP
1198 expressing cells at 20°C and 25°C. n=3 experiments, 10-15 larvae/experiment.***$p < 0.001$,
1199 (unpaired t-test). Each data point represents the percent of *pax-3p;mCherry*-expressing cells that
1200 colocalize with CEP-1::GFP in one animal.
1201
1202 **c.** Fluorescent intensity (arbitrary units; AU) measured in P cells of L1 larvae, 15 hr. post-hatching
1203 at 20°C and 25°C. Strains used: *cep-1* (Ig12501); CEP-1::GFP animals that do not overexpress
1204 CEP-1/p53, CEP-1/p53 overexpressing larvae, and *ilc-17.1* deletion mutants expressing CEP-
1205 1::GFP. n=3 experiments, 5-6 larvae/experiment. ***$p < 0.001$, ns, not significant (unpaired t-test).
1206 Each data point represents the average fluorescence intensity value across five P cells in one
1207 animal (see **Material and Methods**).
1208
1209 **d**. Average *cki-1* and *phg-1* mRNA levels in 32-36 hr. larvae grown at 25°C. mRNA levels were
1210 determined relative to *pmp-3* and normalized to wildtype (N2) values. n=4-6 experiments.
1211 *$p < 0.05$. (unpaired t-test).
1212
1213 **e**. CEP-1 occupancy (expressed as percent input) in 32-36 hr. larvae grown at 25°C, measured
1214 at the promoter proximal region of *phg-1* (**Top,** schematic). CEP-1 occupancy was assayed in

1215 animals where endogenous *cep-1* was FLAG tagged at its C-terminus using CRISPR/Cas9, and
1216 immunoprecipitated with anti-FLAG antibody. Stains used: CEP-1::FLAG expressing animals in
1217 control wildtype background (Ctrl), in *ilc-17.1* background, and in *ilc-17.1* rescued from dauer with
1218 *ilc-17.1; unc-54p::ilc-17.1* CDS. n=4 experiments. *$p < 0.05$. (unpaired t-test).
1219
1220 **f**. Percent dauers in *ilc-17.1* larvae and *ilc-17.1;phg-1* double mutants. **$p < 0.05$, ***$p<0.001$ (n=6
1221 experiments, Chi-squared = 826.95, df = 3, p-value< 2.2e-16). Individual points in the bar graph
1222 represent the % dauers/experiment, Pearson's Chi-squared test with Yates' continuity correction.
1223
1224 **g**. **Top:** Representative micrographs of wildtype (N2) animals and animals overexpressing CEP-
1225 1 driven by the *pax*-3 promoter or 25°C. Scale bar, 50µm. **Bottom:** Percent larvae that displayed
1226 body morphology defects. **$p<0.01$, (unpaired t-test)
1227
1228 **h**. **Top:** Schematic showing homeobox gene expression patterns during post-embryonic
1229 development. **Bottom:** Heatmap depicting expression levels ($\log_2$ normalized counts) of the
1230 homeobox genes on Chromosome III, 32 hrs post-hatching at 25°C, in *ilc-17.1* deletion mutants
1231 and CEP-1 overexpressing larvae that enter dauer, compared to *ilc-17.1; cep-1* double mutants
1232 and wildtype (N2) larvae that continue development. (Also see **Supplementary Table 12**).
1233
1234 Bars show the mean ± S.E.M.
1235
1236

1237 **Figure 5. Impaired glucose utilization in ILC-17.1 deficient larvae activates CEP-1/p53**
1238 **and decreases the expression of Cytochrome C.**
1239 **a. Left**: Schematic of experimental design. **Right**: Percent dauers at 25°C amongst wildtype (N2),
1240 *ilc-17.* deletion mutants, and *ilc-17.1* deletion mutants rescued by expressing *unc-54p::ilc-17.1* on
1241 Control (L4440) and *fgt-1* RNAi. ***p < 0.001, **p < 0.01, ns, not significant. (n= 5 experiments,
1242 Chi-squared = 1817.1, df = 5, p-value < 2.2e-16).
1243
1244 **b. Left**: Schematic of experimental design. **Right**: Percent SDS (1%)-resistant dauers that
1245 accumulate amongst wildtype (N2) and *ilc-17.1* deletion mutants growing on Control (L4440) and
1246 *fgt-1* RNAi under optimal growth conditions of 20°C. ***p < 0.001, **p < 0.01, ns, not significant.
1247 (n= 3 experiments, Chi-squared = 206.82, df = 7, p-value < 2.2e-16).
1248
1249 **c. Left**: Schematic of experimental design. **Right**: Percent dauers amongst wildtype (N2) larvae,
1250 *ilc-17.1* deletion mutants and CEP-1/p53 overexpressing animals on Control (H_2O) and 50mM
1251 glucose at 25°C. **p < 0.01, ns, not significant. (n= 3-6 experiments, Chi-squared = 2882.3, df =
1252 5, p-value < 2.2e-16).
1253
1254 **d**. Fluorescent intensity (arbitrary units; AU) measured in P cells in L1 larvae on Control (H_2O)
1255 and 50mM glucose, 15 hrs. post-hatching at 25°C. Strains: *cep-1* (lg12501); CEP-1::GFP and
1256 CEP-1/p53 overexpressing larvae. n=2-3 experiments, 3-5 larvae/experiment. ***p < 0.001,
1257 **p < 0.01, ns, not significant (unpaired t-test). Each data point indicates the average fluorescence
1258 intensity value across five P cells in one animal.
1259
1260 **e.** Average *phg-1, sod-3 and mtl-1* mRNA levels in 32-36 hr. larvae that arrest as dauers (on H_2O,
1261 control) and larvae that bypass dauer (50mM glucose) at 25°C. mRNA levels were determined

1262 relative to *pmp-3* and normalized to wildtype (N2) values. n=3 experiments. ***$p < 0.001$, **
1263 $p < 0.01$, ns, not significant (unpaired t-test).
1264
1265 **f**. Average *cyc-2.2* mRNA levels in 32-36 hr. larvae grown at 25°C. mRNA levels were determined
1266 relative to *pmp-3* and normalized to the wildtype (N2) values. n=4-6 experiments. ***$p < 0.001$,
1267 **$p < 0.01$, *$p < 0.05$. (unpaired t-test).
1268
1269 Bars show the mean ± S.E.M. Individual points in the bar graphs in **a, b, c** represent the %
1270 dauers/experiment, Pearson's Chi-squared test with Yates' continuity correction.
1271

1272 **Figure 6: ILC-17.1 suppresses CEP-1/p53 in *C. elegans* and mammalian epithelial cells.**

1273 **a. Top:** Representative Western blot showing p53 levels in A459 epithelial cells stimulated for
1274 18hrs. with increasing doses of rIL-17. β-actin was used as a loading control and Nutlin was used
1275 as a positive control. **Bottom:** Quantification of p53 levels normalized to actin levels. n= 4
1276 independent experiments. **p<0.01. (One-Way ANOVA with uncorrected Fisher's LSD; df=2).

1277

1278 **b.** Percent dauers upon overexpressing ILC-17.1 (expression under the *unc-54* promoter) in *cep-*
1279 *1* overexpressing larvae at 25°C. ***p < 0.001. (n=4 experiments, Chi-squared = 1245.4, df = 2,
1280 p-value < 2.2e-16).

1281

1282 **c. Top:** Schematic of germline apoptosis (apoptotic cells in red) scored with Acridine Orange.
1283 **Bottom:** Average numbers of apoptotic cells in day-two adult animals under control, non-
1284 irradiated conditions, and upon irradiation with 75 Gy (day-one adults were irradiated). n= 3
1285 experiments, and 12 gonad arms/experiment. ***p < 0.001, **p < 0.01 (analysis of variance
1286 (ANOVA) with Tukey's correction, df=13). Note: p values between N2 vs *ilc-17.1* OE (*unc-54p*),
1287 non-irradiated and irradiated are p=0.0192 and p=0.0623, if compared by themselves (unpaired
1288 t-test), but do not rise to significance when corrected for the multiple comparisons.

1289

1290 **d**. Working model: ILC-17.1 secretion from larval amphid neurons that occurs in response to food
1291 availability links cell fate decisions with glucose metabolism and DAF-16, DAF-3/DAF-5 activation
1292 through CEP-1/p53.

1293

1294 Data in all graphs show mean ± S.E.M.

1295 **Supplementary Figure S1: ILC-17.1 modulates *C. elegans* developmental diapause.**

1296 **a.** Schematic of *ilc-17.1* gene depicting the syb5296 and syb5297 deletions made by
1297 CRISPR/Cas9 editing using two distinct guide RNAs. *ilc-17.1* (syb5296) X deletion mutants were
1298 used in all future experiments.

1299

1300 **b.** Average mRNA expression in *ilc-17.1* deletion mutants relative to wildtype (N2). n=4-8
1301 experiments. ***$p < 0.001$ (unpaired t-test,).

1302

1303 **c.** Schematic of experiment leveraging the resistance of dauers to 1% SDS used to identify
1304 dauers developing under optimal growth conditions at 20°C.

1305

1306 **d.** Percent *ilc-17.1* larvae that transiently enter the dauer state as seen by SDS-resistance 48 hrs
1307 and 72 hrs. post-hatching under optimal conditions at 20°C. ***$p < 0.001$, **$p < 0.01$ (n=4
1308 experiments, Chi-squared = 166.53, df = 3, p-value < 2.2e-16).

1309

1310 **e-i.** Representative micrographs showing DIC images of **e**, whole *ilc-17.1* deletion mutant dauer
1311 larvae (inset shows alae), **f,** pharyngeal region and **h,** arrested germline 72 hr. post-hatching at
1312 25°C. Wildtype (N2) larval stage 2 (L2) animals used as comparisons: **g**, pharyngeal region and
1313 **i**, germline. Scale bar, a=50µm, f-i, 5 µm.

1314

1315 **j**. Average pharyngeal pumping rates/minute in *ilc-17.1* deletion mutants relative to wildtype (N2)
1316 larval stage 2 (L2) animals. n=4-8 experiments. ***$p < 0.001$, (unpaired t-test).

1317

1318 **k**. Percent F25D1.3, syb7367, and 2X backcrossed *ilc-17.1* larvae that arrest as dauers at 25°C.
1319 ***$p < 0.001$, (n=3 experiments; 50-100 larvae each).

1320

1321

1322 **l. Top:** Schematic of experiment. **Bottom:** Percent wildtype (N2) larvae that arrest as dauers as

1323 determined by SDS-resistance, 48 hrs post-hatching on control (Ctrl; L4440) and *ilc-17.1* RNAi at

1324 25°C. *$p < 0.05$. (n=5 experiments, Chi-squared = 5.1712, df = 1, p-value = 0.02296).

1325 Bars show the mean ± S.E.M**.** Individual points in the bar graphs in **d, k** represent the %

1326 dauers/experiment, Pearson's Chi-squared test with Yates' continuity correction.

1327

1328 **Supplementary Figure S2: Characterization of ILC-17.1 signaling pathway components in**
1329 ***C. elegans*.**
1330 **a. Top:** Schematic of CRISPR insertion of SL2::GFP into *ilcr-2* locus to identify sites of *ilcr-2*
1331 expression. **Bottom, Upper panels:** Representative micrographs showing GFP expression in
1332 cells of the pharynx (**left**), epidermis (**middle**; arrows) and gonad (**right**). **Bottom, lower panels:**
1333 Control, wildtype (N2) non-transgenic animals not expressing GFP confirm specificity of GFP
1334 expression. Scale bar=5μm.
1335
1336 **b.** Average expression in *ilc-17.1* mRNA in 32-26 hr. larvae of wildtype (N2), *ilc-17.1* deletion
1337 mutants rescued with *ilc-17.1p::ilc-17.1* and *unc-54p::ilc-17.1*. Values normalized to *pmp-3* and
1338 shown relative to wildtype (N2) values. *$p<0.05$ (unpaired t-test).
1339
1340 **c.** Percentage of wildtype (N2) and *ilc-17.1* larvae that arrest as dauers on control HT115
1341 (L4440) bacteria. ***$p < 0.001$ (n=10-20 experiments, Chi-squared = 3206, df = 3, p-value <
1342 2.2e-16). Representative average numbers of embryos/plates of wildtype (N2), *ilc-17.1*, *ilc-17.1*
1343 rescued with *ilc-17.1p::ilc-17.1*, and *ilc-17.1* rescued with *unc-54p::ilc-17.1* on HT115 (L4440)
1344 bacteria are 59, 66, 66, 46 respectively. Individual points in the bar graphs represent the %
1345 dauers/experiment, Pearson's Chi-squareddtest with Yates' continuity correction.
1346
1347 **d. Top:** Schematic of CRISPR insertion of SL2::mCherry into *ilc-17.1* locus. **Bottom, upper**
1348 **panel**: Representative z-section micrographs showing mCherry expression in amphid neurons
1349 of *C. elegans* expressing mCherry as a bicistronic SL2 cassette along with the endogenous *ilc-*
1350 *17.1* gene to report on sites of *ilc-17.1* mRNA expression. Amphid neurons were identified by
1351 DiO dye filling (green); mCherry overlapped with a subset of DiO filled neurons. **Bottom, lower**
1352 **panel**: Control, wildtype (N2) animals not expressing mCherry confirm specificity of mCherry
1353 expression. Scale bar=5μm.

1354

1355 **e. Top:** Schematic of *ilc-17.1::*flag driven by the *unc-54* promoter [*ilc-17.1* OE *(unc-54p)*] that
1356 was used to rescue *ilc-17.1* deletion mutants to assess ILC-17.1 protein localization. **Bottom:**
1357 Representative micrographs showing a z-section of these animals immunostained with α-FLAG
1358 antibody, and α-actin (to show expression in body wall muscle cells). Scale bar=5μm

1359

1360 **f. Top:** Representative Western blots showing (**upper panel**) expression of ILC-17.1::FLAG
1361 rescue constructs under the *ilc-17.1* promoter (1) and under the *unc-54* promoter (2) in *ilc-17.1*
1362 deletion mutants. Wildtype (N2) were used to show specificity of α-FLAG antibody. (**lower**
1363 **panel**), tubulin. **Bottom:** Quantification of ILC-17.1::FLAG levels in *ilc-17.1* deletion mutant
1364 animals relative to tubulin, and normalized to FLAG levels in (1). n=3 experiments. ***$p < 0.001$
1365 (unpaired t-test).

1366

1367 **g.** Quantification of fluorescent intensity in pharynx versus background (arbitrary units; AU), in
1368 larvae harboring CRISPR tagged endogenous ILC-17.1::HA**,** immunostained with anti-HA
1369 (**Figure 1f)**. n=3 experiments. 5-6 larvae/experiment. ***$p < 0.001$, (unpaired t-test).

1370

1371 Representative micrographs showing z-sections through animals overexpressing ILC-17.1::FLAG
1372 in their body wall muscle cells as in **e**. Note: ILC-17.1::FLAG is detected at the amphid
1373 commissures near the pharynx (**top panel**; arrow) and in the epidermis (**bottom panel**; arrows)
1374 in addition to the body wall muscle cells (**e**), Scale bar=5μm

1375

1376 Bars show the mean ± S.E.M.

1377

1378

1379 **Supplementary Figure S3: RNA-seq analysis of ILC-17.1 deficient larvae.**

1380 **a.** Pair-wise distance matrix of RNA-seq samples shows the expected clustering of total RNA of
1381 the biological triplicates of each strain [Strains used: wildtype (N2), *ilc-17.1*, and *ilc-17.1* rescued
1382 with *unc-54p::ilc-17.1* CDS]

1383

1384 **b.** Spearman correlation between all genes in a microarray analysis of dauer larvae that were
1385 induced by starvation and *ilc-17.1* deleted larvae *en route* to dauer arrest grown for 32-36 hrs. at
1386 25°C.

1387

1388 **c**. Spearman correlation between all genes in L1 larvae exposed to ascarosides and *ilc-17.1*
1389 deleted larvae *en route* to dauer arrest grown for 32-36 hrs. at 25°C.

1390

1391 **Supplementary Figure S4: ILC-17.1 loss does not affect the animal's chemotaxis or**
1392 **pumping and is associated with changes in *daf-16* target gene expression.**
1393 **a. Top:** Schematic of experimental design. **Bottom:** Average chemotaxis index towards OP50,
1394 0.01% v/v diacetyl, and 1M lysine for *ilc-17.1* deletion mutants and wildtype (N2) day-one adults
1395 at 20°C. n= 5-8 experiments. ns, not significant (unpaired t-test). Data points: average
1396 chemotaxis/experiment.
1397
1398 **b.** Number of pharyngeal pumps/min in *ilc-17.1* deletion mutants and wildtype (N2) day-one adults
1399 at 20°C, on OP50 lawns, and on plates without food. n=3 experiments, with at least 5
1400 animals/experiment scored. Data points: pumping rates of individual animals. ns, not significant
1401 (unpaired t-test).
1402
1403 **c.** Average numbers of fluorescent latex beads in similar areas of distal gut lumen of 40-hour *ilc-*
1404 *17.1* deletion mutants and wildtype (N2) larvae at 20°C. n=3 experiments, with at least 10
1405 animals/experiment. Data points: the numbers of beads in individual animals. ns, not significant
1406 (unpaired t-test).
1407
1408 **d.** Percent dauers amongst wildtype (N2) and *ilc-17.1* deletion mutants raised on Control (H_2O)
1409 and 5mM 8-bromo-cGMP at 25°C. ***$p < 0.001$, Pearson's Chi-squared test with Yates
1410 correction, (n=3 experiments. Chi squared = 798, df = 3, p-value <2e-16.). Individual points in
1411 the bar graphs represent the % dauers/experiment,
1412
1413 **e.** Average *sod-3, mtl-1, and lys-7* mRNA levels in 40 hr. old larvae grown at 20°C. mRNA levels
1414 were determined relative to *pmp-3* and normalized to wildtype (N2) values. n=3 experiments.
1415 ***$p < 0.001$, **$p < 0.01$, ns, not significant (unpaired t-test).
1416

1417 Data in all graphs show mean ± S.E.M.

1418

1419 **Supplementary Figure S5: ILC-17.1 deficiency does not alter the expression levels of**
1420 **Insulin signaling- or TGFβ signaling- pathway components.**

1421 **a.** Percent dauers in *ilc-17.1* deletion mutant larvae following RNAi-mediated downregulation of
1422 several genes known to interact with DAF-16 and DAF3/DAF-5. *daf-16* RNAi was used as a
1423 positive control. ***p < 0.001, ns, not significant. (*n=3*-5 experiments, Chi-squared = 156.66, df =
1424 3, p-value < 2.2e-16).

1425

1426 **b.** Heatmap depicting expression levels (log_2 normalized counts) of *daf-2* (boxed) and insulin
1427 ligands in the *ilc-17.1* deletion mutants, *ilc-17.1* deletion mutants rescued by *unc-54p::ilc-17.1* and
1428 wildtype (N2). Arrows highlight lack of changes in *ins-1* and *ins-18* mRNA. RNA-seq data from
1429 larvae grown for 32-36 hrs. at 25°C.

1430

1431 **c.** Average mRNA levels (insulins) in 32-36 hr. larvae grown at 25°C. mRNA levels were
1432 determined relative to *pmp-3* and normalized to wildtype (N2) values. n=3 experiments.
1433 **p < 0.001, ns, not significant (unpaired t-test).

1434

1435 **d. Left**: Representative micrographs showing DAF-28::GFP expression in the last intestinal cell
1436 of 32-36hr. larvae at 25°C of *ilc-17.1* deletion mutants and wildtype (N2). Images are projections
1437 of confocal z-sections. Scale bar: 5μm. **Right:** Quantification of fluorescent intensity (arbitrary
1438 units, AU) of DAF-28::GFP. n=3 experiments. Data points: the fluorescence intensity of DAF-
1439 28::GFP in individual animals. ns, not significant (unpaired t-test).

1440

1441 **e. Top**: Representative micrographs showing INS-4::GFP expression in the pharynx and
1442 neurons of 32-36 hr. larvae at 25°C in *ilc-17.1* deletion mutants and wildtype (N2). Images are
1443 projections of confocal z-sections. Scale bar: 5μm. **Bottom:** Bars represent percent larvae that

1444 express GFP in the different tissues where INS-4 is known to be expressed. n=3 experiments of
1445 5-10 larvae of each strain. ns, not significant (unpaired t-test).
1446
1447 **f.** Overexpressing ILC-17.1 under *unc-54p::ilc-17.1* CDS [*ilc-17.1* OE (*unc-54p)*] in *daf-2*
1448 (e1370) III strains does not rescue their dauer arrest. ***$p < 0.001$, ns, not significant (n=3
1449 experiments, Chi-squared = 521, df = 3, p-value < 2.2e-16).
1450
1451 **g.** Heatmap depicting expression levels ($\log_2$ normalized counts) of TGFβ signaling pathway
1452 components in the *ilc-17.1* deletion mutants, *ilc-17.1* deletion mutants rescued by *unc-54p::ilc-*
1453 *17.1*, and wildtype (N2).
1454
1455 Data in all graphs show mean ± S.E.M. Individual points in the bar graphs in **e**, **g**, represent the
1456 % dauers/experiment, Pearson's Chi-squared test with Yates' continuity correction.
1457

1458 **Supplementary Figure S6: CEP-1/p53 overexpression induces dauer arrest.**

1459 **a. Top:** Schematic of *cep-1* mRNA, isoform b. **Bottom:** Average *cep-1* isoform b mRNA levels in
1460 32-36 hr. larvae grown at 25°C. mRNA levels were determined relative to *pmp-3* and normalized
1461 to wildtype (N2) values. *n*=3 experiments. **p < 0.001, *p < 0.05 (unpaired t-test).

1462

1463 **b. Top:** Schematic of SDS treatment to assess dauer formation at 20°C. **Bottom:** Percent of
1464 wildtype (N2) and *cep-1* overexpressing larvae (*cep-1* OE) that enter a dauer state during
1465 development, 48 hrs. and 72 hrs. post-hatching at 20°C. ***p < 0.001, (n=3 experiments, Chi-
1466 squared = 414.65, df = 3, p-value < 2.2e-16). Individual points in the bar graphs represent the %
1467 dauers/experiment, Pearson's Chi-squared test with Yates' continuity correction.

1468

1469 **c**. Venn diagram depicting overlap between significantly differentially expressed genes (p<0.05)
1470 in *ilc-17.1* deletion mutants and CEP-1/p53 overexpressing larvae, 32-36 hr. post-hatching at
1471 25°C *en route* to dauer entry. p=0.0; hypergeometric test (Also see **Supplementary Tables 9,**
1472 **10**)

1473

1474 **d**. Heatmap comparing expression levels (log_2 normalized counts) of the major dauer-specific
1475 collagens in the *ilc-17.1* deletion mutants, CEP-1/p53 overexpressing larvae, *ilc-17.1; cep-1*
1476 double mutants, *ilc-17.1* deletion mutants rescued by *unc-54p::ilc-17.1,* and wildtype (N2).

1477

1478 **e.** KEGG enrichments associated with differentially downregulated genes (p.adjust <0.05) in CEP-
1479 1/p53 overexpressing larvae [RNA-seq: 32-36 hr. larvae grown at 25°C; **Supplementary Tables**
1480 **9**].

1481

1482 **f**. KEGG enrichments associated with differentially upregulated genes (padjust <0.05) in CEP-
1483 1/p53 overexpressing larvae [RNA-seq: 32-36 hr. larvae grown at 25°C; **Supplementary Tables**
1484 **9**].
1485
1486 **g.** Principle Component Analysis **(PCA)** of the observed variance in the triplicate RNA-seq
1487 samples collected during development, 15 hrs. and 32 hrs. post-hatching at 25°C, of *ilc-17.1*
1488 deletion mutants, CEP-1/p53 overexpressing larvae, *ilc-17.1; cep-1* double mutants and
1489 wildtype (N2) larvae (**Supplementary Tables 9).**.
1490
1491 Data in all graphs show mean ± S.E.M.

1492 **Supplementary Figure S7: CEP-1/p53 overexpression upregulates DAF-16/FOXO targets**
1493 **and cell cycle inhibitors to induce dauer arrest.**
1494 Average *sod-3, mtl-1, and lys-7* mRNA levels in 40 hr. larvae grown at 20°C. mRNA levels were
1495 determined relative to *pmp-3* and normalized to wildtype (N2) values. Strains used are on X-axis.
1496 n=6-10 experiments. ***$p < 0.001$, **$p < 0.01$, ns, not significant. (unpaired t-test).
1497
1498 **b.** Percent dauers in *daf-2* and *cep-1;daf-2* double mutants. Note: no rescue. n=3 experiments.
1499 ns, not significant. (Chi-squared = Not appropriate, df = 1, p-value = no significant)
1500
1501 **c.** Percent high temperature (27.5°C; HID phenotype) dauers in wildtype (N2) and *cep-1* deletion
1502 mutants. ns, not significant. (n=4 experiments, Chi-squared = 0.67295, df = 1, p-value = 0.412).
1503
1504 **d.** Average *egl-1* and *ced-13* mRNA levels in 40 hr. larvae grown at 20°C. mRNA levels were
1505 determined relative to *pmp-3* and normalized to wildtype (N2) values. n=6-7 experiments.
1506 ***$p < 0.001$, **$p < 0.01$, ns, not significant (unpaired t-test).
1507
1508 **e.** CEP-1 occupancy (expressed as percent input) in 32-36 hr. larvae grown at 25°C, measured
1509 at three promoter proximal regions of *cki-1* (Schematic on **top**). Strains used: CEP-1::FLAG
1510 expressing animals in wildtype background (Ctrl), in *ilc-17.1* deletion background. n=4
1511 experiments. ns, not significant. (unpaired t-test).
1512
1513 **f.** Percent dauers in *ilc-17.1* larvae, CEP-1/p53 overexpressing larvae and *daf-2* larvae upon RNAi
1514 induced downregulation of *cki-1* and *phg-1.* ***$p < 0.001$, **$p < 0.01$, ns, not significant (n=6
1515 experiments, Chi-squared = 7443.7, df = 14, p-value < 2.2e-16).
1516

1517 **g**. Representative micrograph of *ilc-17.1; phg-1* double mutants showing the dauer rescue of
1518 some individuals but not others (dauers marked with arrow).
1519
1520 **h.** Average pumps/minute in *ilc-17.1, cep-1 and daf-2* dauers when subjected to control (L4440;
1521 Ctrl), *cki-1* and *phg-1* RNAi. n= 4 experiments, and 10 dauers were scored per experiment.
1522 *$p < 0.05$, ns, not significant (unpaired t-test). Pumping rates in wildtype (N2), L2 larvae are shown
1523 for comparison.
1524
1525 Data in all graphs show mean ± S.E.M. Individual points in the bar graphs in **b**, **c**, **f**, represent
1526 the % dauers/experiment, Pearson's Chi-squared test with Yates' continuity correction.
1527

1528 **Supplementary Figure S8: CEP-1/p53 activity can be repressed by glucose**
1529 **supplementation.**

1530 **a.** Percent dauers amongst *ilc-17.1* deletion mutants, CEP-1/p53 overexpressing larvae and
1531 wildtype (N2) larvae on 5 mM, 10mM and 50 mM glucose at 25°C. ***p < 0.001, **p < 0.01, ns, not
1532 significant. (*n*= 5-9 experiments, Chi-squared = 5263.6, df = 11, p-value < 2.2e-16)

1533

1534 **b.** Percent dauers amongst *ilc-17.1* deletion mutants and wildtype (N2) larvae on 50mM glucose
1535 on Control (Ctrl; L4440) and *fgt-1* RNAi. **p < 0.01, *p < 0.05, ns, not significant. (*n*=6 experiments,
1536 Chi-squared = 299.36, df = 3, p-value < 2.2e-16).

1537

1538 **c.** Percent dauers amongst *ilc-17.1* deletion mutants and wildtype (N2) larvae upon exposure to
1539 50mM DOG, 50mM glucose, and 0.1mM MitoTEMPO at 25°C (see X-axis for different conditions).
1540 ***p < 0.001, ns, not significant, (n=3- experiments, Chi-squared = 1251.7, df = 9, p-value < 2.2e-
1541 16).

1542

1543 **d.** Percent dauers amongst *ilc-17.1* deletion mutants and wildtype (N2) larvae on 20mM Skim
1544 Milk powder and 0.26 mM L-Glutamine at 25°C. ns, not significant, (n=3 experiments, Chi-squared
1545 = 648.89, df = 5, p-value < 2.2e-16).

1546

1547 **e.** Average mRNA levels of *egl-1* and *ced-13* in wildtype (N2) larvae subjected to Control (Ctrl;
1548 L4440) and *fgt-1* RNAi. mRNA levels were determined relative to *pmp-3* and normalized to
1549 wildtype (N2) values. *n=3* experiments, *p < 0.05, ns, not significant (unpaired t-test).

1550

1551 Data in all graphs show mean ± S.E.M. Individual points in the bar graphs in **a-d** represent the %
1552 dauers/experiment, Pearson's Chi-squared test with Yates' continuity correction.

1553

1554 **Supplementary Figure S9: ILC-17.1 deficiency and CEP-1/p53 overexpression modulate**
1555 **key glucose metabolic enzymes.**
1556 **a-f**. Heatmap depicting expression levels (log_2 normalized counts) of glycolysis and mitochondrial
1557 OXPHOS genes in the *ilc-17.1* deletion mutants, CEP-1/p53 overexpressing animals, *ilc-17.1;*
1558 *cep-1* double mutants, *ilc-17.1* rescued with *unc-54p::ilc-17.1*, and wildtype (N2). Arrows:
1559 highlight decreases in *pfk-1.2* and *cyc-2.2* mRNA levels in *ilc-17.1* deleted and CEP-1/p53
1560 overexpressing larvae (Boxed). RNA-seq data was collected as previously described.
1561
1562 **g**. Average *pfk-1.2* mRNA levels in 32-36 hr. old larvae grown at 25°C. mRNA levels were
1563 determined relative to *pmp-3* and normalized to wildtype (N2) values. Strain names on X-axis.
1564 n=4-6 experiments. ***$p < 0.001$, **$p < 0.01$, *$p < 0.05$. (unpaired t-test).
1565
1566 **h. Top:** Schematic of SDS treatment to assess dauer formation at 20°C. **Bottom:** Percent of
1567 wildtype (N2) and *ilc-17.1* deletion mutant larvae that enter a dauer state at 20°C, 48 hr. post-
1568 hatching, when subjected to control (Ctrl; L4440), *cyc-2.2* and *pfk-1.2* RNAi. **$p < 0.01$, ns, not
1569 significant (*n*=3-4 experiments, Chi-squared = 213.38, df = 5, p-value < 2.2e-16) . Individual
1570 points in the bar graphs represent the % dauers/experiment, Pearson's Chi-squared test with
1571 Yates' continuity correction.
1572
1573 Data in all graphs show mean ± S.E.M.

1574 **Supplementary Figure S10: rIL-17 induces the expected cytokine response in human**
1575 **epithelial cells.**
1576 **a.** Soluble CXCL5 levels in the supernatant of A459 epithelial cells stimulated for 18hrs. with rIL-
1577 17 measured by ELISA. Data is a summary of 2 independent experiments, performed in
1578 triplicates. *$p<0.05$, (unpaired t-test). Data show mean ± S.E.M.
1579
1580 b. Percent wild-type (N2) and *npr-1*(ad609); *ilc-17.1*(tm5218) double mutant larvae that arrest
1581 as dauers at 25°C. ns, not significant (n=3 experiments; 50-100 larvae each).
1582
1583
1584
1585
1586

1587 References

1588

1589 1. Golden, J.W. & Riddle, D.L. The Caenorhabditis elegans dauer larva: developmental effects of
1590 pheromone, food, and temperature. *Dev Biol* **102**, 368-78 (1984).

1591 2. Swanson, M.M. & Riddle, D.L. Critical periods in the development of the Caenorhabditis elegans
1592 dauer larva. *Dev Biol* **84**, 27-40 (1981).

1593 3. Hu, P.J. Dauer. *WormBook*, 1-19 (2007).

1594 4. Karp, X. Working with dauer larvae. *WormBook* **2018**, 1-19 (2018).

1595 5. Fielenbach, N. & Antebi, A. C. elegans dauer formation and the molecular basis of plasticity. *Genes*
1596 *Dev* **22**, 2149-65 (2008).

1597 6. Burnell, A.M., Houthoofd, K., O'Hanlon, K. & Vanfleteren, J.R. Alternate metabolism during the
1598 dauer stage of the nematode Caenorhabditis elegans. *Exp Gerontol* **40**, 850-6 (2005).

1599 7. Rashid, S., Wong, C. & Roy, R. Developmental plasticity and the response to nutrient stress in
1600 Caenorhabditis elegans. *Dev Biol* **475**, 265-276 (2021).

1601 8. Cohen, S.M., Wrobel, C.J.J., Prakash, S.J., Schroeder, F.C. & Sternberg, P.W. Formation and
1602 function of dauer ascarosides in the nematodes Caenorhabditis briggsae and Caenorhabditis
1603 elegans. *G3 (Bethesda)* **12**(2022).

1604 9. Braendle, C., Milloz, J. & Felix, M.A. Mechanisms and evolution of environmental responses in
1605 Caenorhabditis elegans. *Curr Top Dev Biol* **80**, 171-207 (2008).

1606 10. Diaz, S.A. & Viney, M. The evolution of plasticity of dauer larva developmental arrest in the
1607 nematode Caenorhabditis elegans. *Ecol Evol* **5**, 1343-53 (2015).

1608 11. Ewald, C.Y., Landis, J.N., Porter Abate, J., Murphy, C.T. & Blackwell, T.K. Dauer-independent
1609 insulin/IGF-1-signalling implicates collagen remodelling in longevity. *Nature* **519**, 97-101 (2015).

1610 12. Harvey, S.C., Shorto, A. & Viney, M.E. Quantitative genetic analysis of life-history traits of
1611 Caenorhabditis elegans in stressful environments. *BMC Evol Biol* **8**, 15 (2008).
1612 13. Zhu, J. & Thompson, C.B. Metabolic regulation of cell growth and proliferation. *Nat Rev Mol Cell*
1613 *Biol* **20**, 436-450 (2019).
1614 14. Altan-Bonnet, G. & Mukherjee, R. Cytokine-mediated communication: a quantitative appraisal of
1615 immune complexity. *Nat Rev Immunol* **19**, 205-217 (2019).
1616 15. Mills, K.H.G. IL-17 and IL-17-producing cells in protection versus pathology. *Nat Rev Immunol*
1617 (2022).
1618 16. Li, X., Bechara, R., Zhao, J., McGeachy, M.J. & Gaffen, S.L. IL-17 receptor-based signaling and
1619 implications for disease. *Nat Immunol* **20**, 1594-1602 (2019).
1620 17. Douglas, A., Stevens, B. & Lynch, L. Interleukin-17 as a key player in neuroimmunometabolism.
1621 *Nat Metab* **5**, 1088-1100 (2023).
1622 18. Hall, P.A. & Lane, D.P. Tumor suppressors: a developing role for p53? *Curr Biol* **7**, R144-7 (1997).
1623 19. Jain, A.K. & Barton, M.C. p53: emerging roles in stem cells, development and beyond.
1624 *Development* **145**(2018).
1625 20. Levine, A.J. p53: 800 million years of evolution and 40 years of discovery. *Nat Rev Cancer* **20**, 471-
1626 480 (2020).
1627 21. Rutkowski, R., Hofmann, K. & Gartner, A. Phylogeny and function of the invertebrate p53
1628 superfamily. *Cold Spring Harb Perspect Biol* **2**, a001131 (2010).
1629 22. Lu, W.J., Amatruda, J.F. & Abrams, J.M. p53 ancestry: gazing through an evolutionary lens. *Nat*
1630 *Rev Cancer* **9**, 758-62 (2009).
1631 23. Bowen, M.E., Mulligan, A.S., Sorayya, A. & Attardi, L.D. Puma- and Caspase9-mediated apoptosis
1632 is dispensable for p53-driven neural crest-based developmental defects. *Cell Death Differ* **28**,
1633 2083-2094 (2021).

1634 24. Van Nostrand, J.L. *et al.* Inappropriate p53 activation during development induces features of
1635 CHARGE syndrome. *Nature* **514**, 228-32 (2014).
1636 25. Chen, C. *et al.* IL-17 is a neuromodulator of Caenorhabditis elegans sensory responses. *Nature*
1637 **542**, 43-48 (2017).
1638 26. Flynn, S.M. *et al.* MALT-1 mediates IL-17 neural signaling to regulate C. elegans behavior,
1639 immunity and longevity. *Nat Commun* **11**, 2099 (2020).
1640 27. Lillis, M., Zaccardi, N.J. & Heiman, M.G. Axon-dendrite and apical-basolateral sorting in a single
1641 neuron. *Genetics* **221**(2022).
1642 28. Golden, J.W. & Riddle, D.L. A pheromone-induced developmental switch in Caenorhabditis
1643 elegans: Temperature-sensitive mutants reveal a wild-type temperature-dependent process. *Proc*
1644 *Natl Acad Sci U S A* **81**, 819-23 (1984).
1645 29. Thomas, J.H., Birnby, D.A. & Vowels, J.J. Evidence for parallel processing of sensory information
1646 controlling dauer formation in Caenorhabditis elegans. *Genetics* **134**, 1105-17 (1993).
1647 30. Vowels, J.J. & Thomas, J.H. Genetic analysis of chemosensory control of dauer formation in
1648 Caenorhabditis elegans. *Genetics* **130**, 105-23 (1992).
1649 31. Ailion, M. & Thomas, J.H. Isolation and characterization of high-temperature-induced Dauer
1650 formation mutants in Caenorhabditis elegans. *Genetics* **165**, 127-44 (2003).
1651 32. Li, W. & Ou, G. The application of somatic CRISPR-Cas9 to conditional genome editing in
1652 Caenorhabditis elegans. *Genesis* **54**, 170-81 (2016).
1653 33. Paix, A. *et al.* Scalable and versatile genome editing using linear DNAs with microhomology to
1654 Cas9 Sites in Caenorhabditis elegans. *Genetics* **198**, 1347-56 (2014).
1655 34. Xu, S. The application of CRISPR-Cas9 genome editing in Caenorhabditis elegans. *J Genet Genomics*
1656 **42**, 413-21 (2015).

1657 35. Holt, S.J. Staying alive in adversity: transcriptome dynamics in the stress-resistant dauer larva.
1658 *Funct Integr Genomics* **6**, 285-99 (2006).
1659 36. Cohen, S.M., Sun, J.J., Schroeder, F.C. & Sternberg, P.W. Transcriptional Response to a Dauer-
1660 Inducing Ascaroside Cocktail in Late L1 in C. elegans. *MicroPubl Biol* **2021**(2021).
1661 37. Wang, J. & Kim, S.K. Global analysis of dauer gene expression in Caenorhabditis elegans.
1662 *Development* **130**, 1621-34 (2003).
1663 38. Wirick, M.J. *et al.* daf-16/FOXO blocks adult cell fate in Caenorhabditis elegans dauer larvae via
1664 lin-41/TRIM71. *PLoS Genet* **17**, e1009881 (2021).
1665 39. Kyani-Rogers, T. *et al.* Developmental history modulates adult olfactory behavioral preferences
1666 via regulation of chemoreceptor expression in Caenorhabditiselegans. *Genetics* **222**(2022).
1667 40. Ow, M.C., Borziak, K., Nichitean, A.M., Dorus, S. & Hall, S.E. Early experiences mediate distinct
1668 adult gene expression and reproductive programs in Caenorhabditis elegans. *PLoS Genet* **14**,
1669 e1007219 (2018).
1670 41. Bargmann, C.I. Chemosensation in C. elegans. *WormBook*, 1-29 (2006).
1671 42. Motola, D.L. *et al.* Identification of ligands for DAF-12 that govern dauer formation and
1672 reproduction in C. elegans. *Cell* **124**, 1209-23 (2006).
1673 43. Vowels, J.J. & Thomas, J.H. Multiple chemosensory defects in daf-11 and daf-21 mutants of
1674 Caenorhabditis elegans. *Genetics* **138**, 303-16 (1994).
1675 44. Lin, K., Dorman, J.B., Rodan, A. & Kenyon, C. daf-16: An HNF-3/forkhead family member that can
1676 function to double the life-span of Caenorhabditis elegans. *Science* **278**, 1319-22 (1997).
1677 45. Libina, N., Berman, J.R. & Kenyon, C. Tissue-specific activities of C. elegans DAF-16 in the
1678 regulation of lifespan. *Cell* **115**, 489-502 (2003).
1679 46. Lee, S.S., Kennedy, S., Tolonen, A.C. & Ruvkun, G. DAF-16 target genes that control C. elegans life-
1680 span and metabolism. *Science* **300**, 644-7 (2003).

1681 47. Kenyon, C. & Murphy, C.T. Enrichment of regulatory motifs upstream of predicted DAF-16 targets.
1682 *Nat Genet* **38**, 397-8; author reply 398 (2006).
1683 48. da Graca, L.S. *et al.* DAF-5 is a Ski oncoprotein homolog that functions in a neuronal TGF beta
1684 pathway to regulate C. elegans dauer development. *Development* **131**, 435-46 (2004).
1685 49. Pierce, S.B. *et al.* Regulation of DAF-2 receptor signaling by human insulin and ins-1, a member of
1686 the unusually large and diverse C. elegans insulin gene family. *Genes Dev* **15**, 672-86 (2001).
1687 50. Ritter, A.D. *et al.* Complex expression dynamics and robustness in C. elegans insulin networks.
1688 *Genome Res* **23**, 954-65 (2013).
1689 51. Gems, D. *et al.* Two pleiotropic classes of daf-2 mutation affect larval arrest, adult behavior,
1690 reproduction and longevity in Caenorhabditis elegans. *Genetics* **150**, 129-55 (1998).
1691 52. Zecic, A. & Braeckman, B.P. DAF-16/FoxO in Caenorhabditis elegans and Its Role in Metabolic
1692 Remodeling. *Cells* **9**(2020).
1693 53. Oh, S.W. *et al.* JNK regulates lifespan in Caenorhabditis elegans by modulating nuclear
1694 translocation of forkhead transcription factor/DAF-16. *Proc Natl Acad Sci U S A* **102**, 4494-9
1695 (2005).
1696 54. Greer, E.L. *et al.* An AMPK-FOXO pathway mediates longevity induced by a novel method of
1697 dietary restriction in C. elegans. *Curr Biol* **17**, 1646-56 (2007).
1698 55. Leiser, S.F., Begun, A. & Kaeberlein, M. HIF-1 modulates longevity and healthspan in a
1699 temperature-dependent manner. *Aging Cell* **10**, 318-26 (2011).
1700 56. Perrin, A.J. *et al.* Noncanonical control of C. elegans germline apoptosis by the insulin/IGF-1 and
1701 Ras/MAPK signaling pathways. *Cell Death Differ* **20**, 97-107 (2013).
1702 57. Gurkar, A.U. *et al.* Dysregulation of DAF-16/FOXO3A-mediated stress responses accelerates
1703 oxidative DNA damage induced aging. *Redox Biol* **18**, 191-199 (2018).

1704 58. Baruah, A. *et al.* CEP-1, the Caenorhabditis elegans p53 homolog, mediates opposing longevity
1705 outcomes in mitochondrial electron transport chain mutants. *PLoS Genet* **10**, e1004097 (2014).
1706 59. Ewald, C.Y., Castillo-Quan, J.I. & Blackwell, T.K. Untangling Longevity, Dauer, and Healthspan in
1707 Caenorhabditis elegans Insulin/IGF-1-Signalling. *Gerontology* **64**, 96-104 (2018).
1708 60. Derry, W.B., Putzke, A.P. & Rothman, J.H. Caenorhabditis elegans p53: role in apoptosis, meiosis,
1709 and stress resistance. *Science* **294**, 591-5 (2001).
1710 61. Schumacher, B., Hofmann, K., Boulton, S. & Gartner, A. The C. elegans homolog of the p53 tumor
1711 suppressor is required for DNA damage-induced apoptosis. *Curr Biol* **11**, 1722-7 (2001).
1712 62. Schumacher, B. *et al.* Translational repression of C. elegans p53 by GLD-1 regulates DNA damage-
1713 induced apoptosis. *Cell* **120**, 357-68 (2005).
1714 63. Levi-Ferber, M. *et al.* It's all in your mind: determining germ cell fate by neuronal IRE-1 in C.
1715 elegans. *PLoS Genet* **10**, e1004747 (2014).
1716 64. Hicks, T. *et al.* R-loop-induced irreparable DNA damage evades checkpoint detection in the C.
1717 elegans germline. *Nucleic Acids Res* **50**, 8041-8059 (2022).
1718 65. Arum, O. & Johnson, T.E. Reduced expression of the Caenorhabditis elegans p53 ortholog cep-1
1719 results in increased longevity. *J Gerontol A Biol Sci Med Sci* **62**, 951-9 (2007).
1720 66. Lee, C.C. *et al.* Mutation of a Nopp140 gene dao-5 alters rDNA transcription and increases germ
1721 cell apoptosis in C. elegans. *Cell Death Dis* **5**, e1158 (2014).
1722 67. Gartner, A., Boag, P.R. & Blackwell, T.K. Germline survival and apoptosis. *WormBook*, 1-20 (2008).
1723 68. Greiss, S., Schumacher, B., Grandien, K., Rothblatt, J. & Gartner, A. Transcriptional profiling in C.
1724 elegans suggests DNA damage dependent apoptosis as an ancient function of the p53 family. *BMC*
1725 *Genomics* **9**, 334 (2008).
1726 69. Schumacher, B. *et al.* C. elegans ced-13 can promote apoptosis and is induced in response to DNA
1727 damage. *Cell Death Differ* **12**, 153-61 (2005).

1728 70. Schertel, C. & Conradt, B. C. elegans orthologs of components of the RB tumor suppressor
1729 complex have distinct pro-apoptotic functions. *Development* **134**, 3691-701 (2007).
1730 71. Sendoel, A., Kohler, I., Fellmann, C., Lowe, S.W. & Hengartner, M.O. HIF-1 antagonizes p53-
1731 mediated apoptosis through a secreted neuronal tyrosinase. *Nature* **465**, 577-83 (2010).
1732 72. Sulston, J.E. & Horvitz, H.R. Post-embryonic cell lineages of the nematode, Caenorhabditis
1733 elegans. *Dev Biol* **56**, 110-56 (1977).
1734 73. Sternberg, P.W. Vulval development. *WormBook*, 1-28 (2005).
1735 74. Horvitz, H.R. & Sternberg, P.W. Nematode postembryonic cell lineages. *J Nematol* **14**, 240-8
1736 (1982).
1737 75. Chisholm, A.D. & Hardin, J. Epidermal morphogenesis. *WormBook*, 1-22 (2005).
1738 76. Herman, M.A. Hermaphrodite cell-fate specification. *WormBook*, 1-16 (2006).
1739 77. Costa, M., Weir, M., Coulson, A., Sulston, J. & Kenyon, C. Posterior pattern formation in C. elegans
1740 involves position-specific expression of a gene containing a homeobox. *Cell* **55**, 747-56 (1988).
1741 78. Euling, S. & Ambros, V. Reversal of cell fate determination in Caenorhabditis elegans vulval
1742 development. *Development* **122**, 2507-15 (1996).
1743 79. Braendle, C. & Felix, M.A. Plasticity and errors of a robust developmental system in different
1744 environments. *Dev Cell* **15**, 714-24 (2008).
1745 80. Karp, X. & Greenwald, I. Control of cell-fate plasticity and maintenance of multipotency by DAF-
1746 16/FoxO in quiescent Caenorhabditis elegans. *Proc Natl Acad Sci U S A* **110**, 2181-6 (2013).
1747 81. Tenen, C.C. & Greenwald, I. Cell Non-autonomous Function of daf-18/PTEN in the Somatic Gonad
1748 Coordinates Somatic Gonad and Germline Development in C. elegans Dauer Larvae. *Curr Biol* **29**,
1749 1064-1072 e8 (2019).

1750 82. Hong, Y., Roy, R. & Ambros, V. Developmental regulation of a cyclin-dependent kinase inhibitor
1751 controls postembryonic cell cycle progression in Caenorhabditis elegans. *Development* **125**, 3585-
1752 97 (1998).
1753 83. Karp, X. & Ambros, V. Dauer larva quiescence alters the circuitry of microRNA pathways regulating
1754 cell fate progression in C. elegans. *Development* **139**, 2177-86 (2012).
1755 84. O'Keeffe, C. & Greenwald, I. EGFR signal transduction is downregulated in C. elegans vulval
1756 precursor cells during dauer diapause. *Development* **149**(2022).
1757 85. Colella, E., Li, S. & Roy, R. Developmental and Cell Cycle Quiescence Is Mediated by the Nuclear
1758 Hormone Receptor Coregulator DIN-1S in the Caenorhabditis elegans Dauer Larva. *Genetics* **203**,
1759 1763-76 (2016).
1760 86. Narbonne, P. & Roy, R. Inhibition of germline proliferation during C. elegans dauer development
1761 requires PTEN, LKB1 and AMPK signalling. *Development* **133**, 611-9 (2006).
1762 87. Wong, C., Kadekar, P., Jurczak, E. & Roy, R. Germline stem cell integrity and quiescence are
1763 controlled by an AMPK-dependent neuronal trafficking pathway. *PLoS Genet* **19**, e1010716
1764 (2023).
1765 88. Vousden, K.H. & Ryan, K.M. p53 and metabolism. *Nat Rev Cancer* **9**, 691-700 (2009).
1766 89. van den Heuvel, S. Cell-cycle regulation. *WormBook*, 1-16 (2005).
1767 90. Derry, W.B. *et al.* Regulation of developmental rate and germ cell proliferation in Caenorhabditis
1768 elegans by the p53 gene network. *Cell Death Differ* **14**, 662-70 (2007).
1769 91. Cameron, S., Clark, S.G., McDermott, J.B., Aamodt, E. & Horvitz, H.R. PAG-3, a Zn-finger
1770 transcription factor, determines neuroblast fate in C. elegans. *Development* **129**, 1763-74 (2002).
1771 92. Thompson, K.W. *et al.* The Paired-box protein PAX-3 regulates the choice between lateral and
1772 ventral epidermal cell fates in C. elegans. *Dev Biol* **412**, 191-207 (2016).

1773 93. Salser, S.J. & Kenyon, C. Patterning C. elegans: homeotic cluster genes, cell fates and cell
1774 migrations. *Trends Genet* **10**, 159-64 (1994).
1775 94. Sternberg, P.W. Genetic control of cell type and pattern formation in Caenorhabditis elegans. *Adv*
1776 *Genet* **27**, 63-116 (1990).
1777 95. Burglin, T.R. & Ruvkun, G. The Caenorhabditis elegans homeobox gene cluster. *Curr Opin Genet*
1778 *Dev* **3**, 615-20 (1993).
1779 96. Jones, R.G. *et al.* AMP-activated protein kinase induces a p53-dependent metabolic checkpoint.
1780 *Mol Cell* **18**, 283-93 (2005).
1781 97. Feng, Y., Williams, B.G., Koumanov, F., Wolstenholme, A.J. & Holman, G.D. FGT-1 is the major
1782 glucose transporter in C. elegans and is central to aging pathways. *Biochem J* **456**, 219-29 (2013).
1783 98. Schulz, T.J. *et al.* Glucose restriction extends Caenorhabditis elegans life span by inducing
1784 mitochondrial respiration and increasing oxidative stress. *Cell Metab* **6**, 280-93 (2007).
1785 99. Wu, Z. *et al.* Dietary Restriction Extends Lifespan through Metabolic Regulation of Innate
1786 Immunity. *Cell Metab* **29**, 1192-1205 e8 (2019).
1787 100. Walker, M.D. *et al.* WormPaths: Caenorhabditis elegans metabolic pathway annotation and
1788 visualization. *Genetics* **219**(2021).
1789 101. Li, Q. *et al.* IL-17 induces radiation resistance of B lymphoma cells by suppressing p53 expression
1790 and thereby inhibiting irradiation-triggered apoptosis. *Cell Mol Immunol* **12**, 366-72 (2015).
1791 102. Chen, K. *et al.* IL-17 Receptor Signaling in the Lung Epithelium Is Required for Mucosal Chemokine
1792 Gradients and Pulmonary Host Defense against K. pneumoniae. *Cell Host Microbe* **20**, 596-605
1793 (2016).
1794 103. Liu, Y. *et al.* p53 regulates hematopoietic stem cell quiescence. *Cell Stem Cell* **4**, 37-48 (2009).
1795 104. Cheung, T.H. & Rando, T.A. Molecular regulation of stem cell quiescence. *Nat Rev Mol Cell Biol* **14**,
1796 329-40 (2013).

1797 105. Das, S., Min, S. & Prahlad, V. Gene bookmarking by the heat shock transcription factor programs
1798 the insulin-like signaling pathway. *Mol Cell* **81**, 4843-4860 e8 (2021).
1799 106. Das, S. *et al.* Serotonin signaling by maternal neurons upon stress ensures progeny survival. *Elife*
1800 **9**(2020).
1801 107. Tatum, M.C. *et al.* Neuronal serotonin release triggers the heat shock response in C. elegans in
1802 the absence of temperature increase. *Curr Biol* **25**, 163-174 (2015).
1803 108. Ooi, F.K. & Prahlad, V. Olfactory experience primes the heat shock transcription factor HSF-1 to
1804 enhance the expression of molecular chaperones in C. elegans. *Sci Signal* **10**(2017).
1805 109. Venkatesh, H. & Monje, M. Neuronal Activity in Ontogeny and Oncology. *Trends Cancer* **3**, 89-112
1806 (2017).
1807 110. Curry, R.N. & Glasgow, S.M. The Role of Neurodevelopmental Pathways in Brain Tumors. *Front*
1808 *Cell Dev Biol* **9**, 659055 (2021).
1809 111. Gibson, D.G. *et al.* Enzymatic assembly of DNA molecules up to several hundred kilobases. *Nat*
1810 *Methods* **6**, 343-5 (2009).
1811 112. Nonet, M.L. *et al.* Caenorhabditis elegans rab-3 mutant synapses exhibit impaired function and
1812 are partially depleted of vesicles. *J Neurosci* **17**, 8061-73 (1997).
1813 113. Nika, L., Gibson, T., Konkus, R. & Karp, X. Fluorescent Beads Are a Versatile Tool for Staging
1814 Caenorhabditis elegans in Different Life Histories. *G3 (Bethesda)* **6**, 1923-33 (2016).
1815 114. Krueger, F. TrimGalore. (2021).
1816 115. Kopylova, E., Noe, L. & Touzet, H. SortMeRNA: fast and accurate filtering of ribosomal RNAs in
1817 metatranscriptomic data. *Bioinformatics* **28**, 3211-7 (2012).
1818 116. Yates, A.D. *et al.* Ensembl Genomes 2022: an expanding genome resource for non-vertebrates.
1819 *Nucleic Acids Res* **50**, D996-D1003 (2022).
1820 117. Dobin, A. *et al.* STAR: ultrafast universal RNA-seq aligner. *Bioinformatics* **29**, 15-21 (2013).

1821 118. Liao, Y., Smyth, G.K. & Shi, W. The R package Rsubread is easier, faster, cheaper and better for
1822 alignment and quantification of RNA sequencing reads. *Nucleic Acids Research* **47**, e47-e47 (2019).
1823 119. Love, M.I., Huber, W. & Anders, S. Moderated estimation of fold change and dispersion for RNA-
1824 seq data with DESeq2. *Genome Biol* **15**, 550 (2014).
1825 120. Davis, P. *et al.* WormBase in 2022-data, processes, and tools for analyzing Caenorhabditis elegans.
1826 *Genetics* **220**(2022).
1827 121. Cohen, S.M., Sun, J.J., Schroeder, F.C. & Sternberg, P.W. Transcriptional Response to a Dauer-
1828 Inducing Ascaroside Cocktail in Late L1 in C. elegans. (microPublication Biology, 2021).
1829 122. Hu, M., Crossman, D., Prasain, J.K., Miller, M.A. & Serra, R.A. Transcriptomic Profiling of DAF-
1830 7/TGFβ Pathway Mutants in C. elegans. *Genes* **11**, 288 (2020).
1831 123. Shen, L. & Sinai, M. GeneOverlap: Test and visualize gene overlaps. (2019).
1832 124. Chen, H. VennDiagram: Generate High-Resolution Venn and Euler Plots. (2018).
1833 125. Wu, T. *et al.* clusterProfiler 4.0: A universal enrichment tool for interpreting omics data.
1834 *Innovation (N Y)* **2**, 100141 (2021).
1835 126. Carlson, M. org.Ce.eg.db: Genome wide annotation for Worm. (2019).
1836 127. Kanehisa, M., Furumichi, M., Sato, Y., Kawashima, M. & Ishiguro-Watanabe, M. KEGG for
1837 taxonomy-based analysis of pathways and genomes. *Nucleic Acids Res* (2022).
1838 128. Gu, Z. Complex heatmap visualization. *iMeta* **1**, e43 (2022).
1839 129. Kolde, R. pheatmap: Pretty Heatmaps. (2019).
1840 130. Chikka, M.R., Anbalagan, C., Dvorak, K., Dombeck, K. & Prahlad, V. The Mitochondria-Regulated
1841 Immune Pathway Activated in the C. elegans Intestine Is Neuroprotective. *Cell Rep* **16**, 2399-414
1842 (2016).
1843
1844

1845 A**cknowledgements**

1846 We thank the V.P. laboratory, Drs. Sarit Smolikove, Josep Comeron, Anna Malkova and Michael
1847 Petrascheck for comments, Dr. Peter Ratcliffe, Oxford, for his generous gift of *CeHIF-1* antibody,
1848 and Dr. Mario de Bono, Institute of Science and Technology Austria (ISTA) for *C. elegans* strains.
1849 Nematode strains were provided by the Caenorhabditis Genetics Center (CGC) (funded by the
1850 NIH Infrastructure Programs P40 OD010440). This work was supported by NIH R01 AG060616
1851 (V.P.).

1852 **Author Contributions**

1853 All authors designed the study, performed experiments, analyzed data, and drafted the

1854 manuscript. P.D.I coordinated the mammalian experiments; V.P. coordinated *C. elegans*

1855 experiments and the project. All authors approved the final version of the manuscript.

1856

1857 **Declaration of Interests**

1858 The authors declare no competing interests

1859

Figure 1

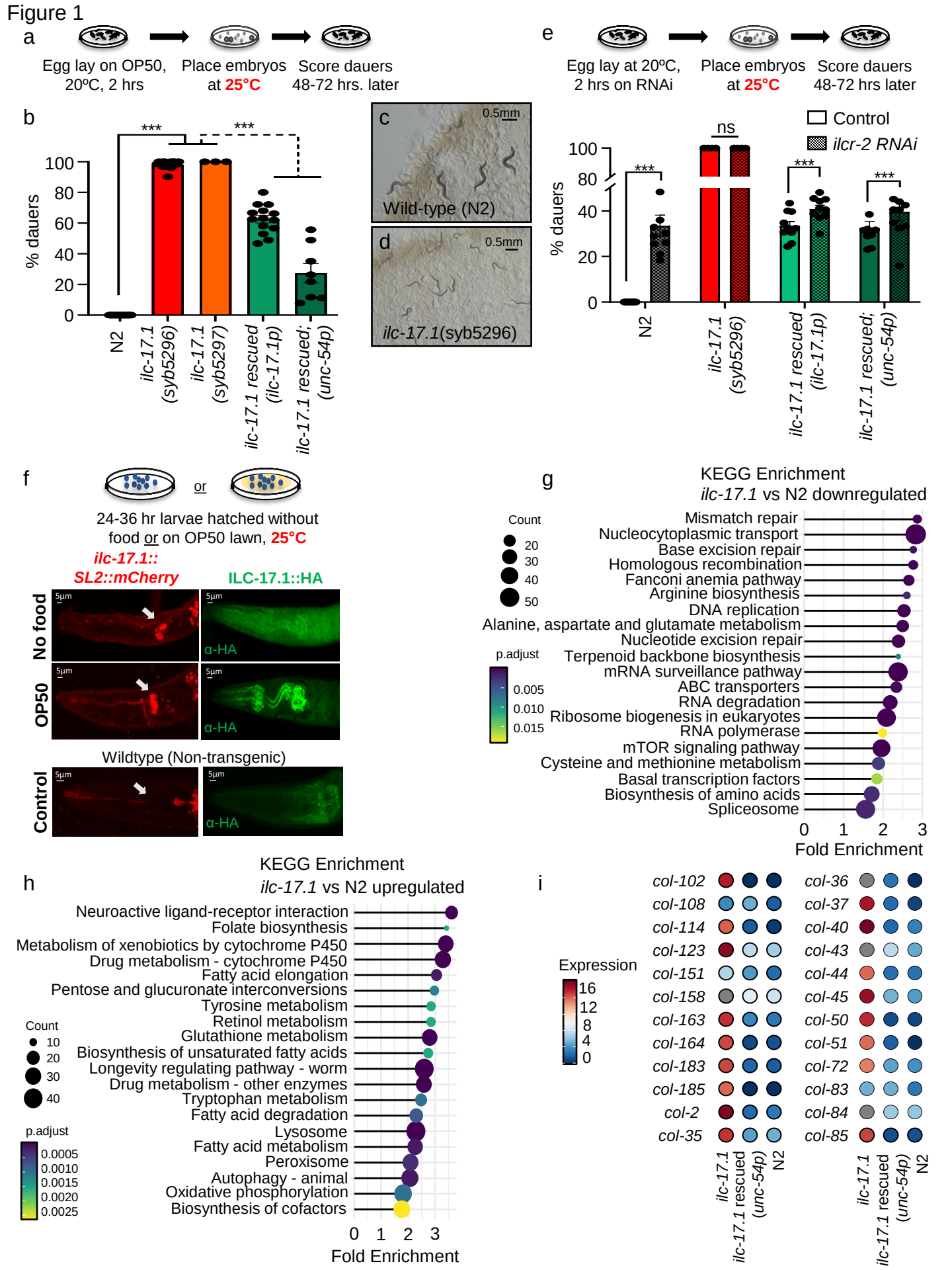
a
Egg lay on OP50, 20ºC, 2 hrs
Place embryos at 25°C
Score dauers 48-72 hrs. later
b
% dauers
***
***
N2
ilc-17.1 (syb5296)
ilc-17.1 (syb5297)
ilc-17.1 rescued (ilc-17.1p)
ilc-17.1 rescued; (unc-54p)
c
0.5mm
Wild-type (N2)
d
0.5mm
ilc-17.1(syb5296)
e
Egg lay at 20ºC, 2 hrs on RNAi
Place embryos at 25°C
Score dauers 48-72 hrs later
Control
ilcr-2 RNAi
ns
% dauers
f
or
24-36 hr larvae hatched without food or on OP50 lawn, 25°C
ilc-17.1:: SL2::mCherry
ILC-17.1::HA
No food
OP50
Wildtype (Non-transgenic)
Control
α-HA
g
KEGG Enrichment
ilc-17.1 vs N2 downregulated
Count
p.adjust
Mismatch repair
Nucleocytoplasmic transport
Base excision repair
Homologous recombination
Fanconi anemia pathway
Arginine biosynthesis
DNA replication
Alanine, aspartate and glutamate metabolism
Nucleotide excision repair
Terpenoid backbone biosynthesis
mRNA surveillance pathway
ABC transporters
RNA degradation
Ribosome biogenesis in eukaryotes
RNA polymerase
mTOR signaling pathway
Cysteine and methionine metabolism
Basal transcription factors
Biosynthesis of amino acids
Spliceosome
Fold Enrichment
h
KEGG Enrichment
ilc-17.1 vs N2 upregulated
Count
p.adjust
Neuroactive ligand-receptor interaction
Folate biosynthesis
Metabolism of xenobiotics by cytochrome P450
Drug metabolism - cytochrome P450
Fatty acid elongation
Pentose and glucuronate interconversions
Tyrosine metabolism
Retinol metabolism
Glutathione metabolism
Biosynthesis of unsaturated fatty acids
Longevity regulating pathway - worm
Drug metabolism - other enzymes
Tryptophan metabolism
Fatty acid degradation
Lysosome
Fatty acid metabolism
Peroxisome
Autophagy - animal
Oxidative phosphorylation
Biosynthesis of cofactors
Fold Enrichment
i
Expression
col-102
col-108
col-114
col-123
col-151
col-158
col-163
col-164
col-183
col-185
col-2
col-35
col-36
col-37
col-40
col-43
col-44
col-45
col-50
col-51
col-72
col-83
col-84
col-85
ilc-17.1
ilc-17.1 rescued (unc-54p)
N2

Figure 2

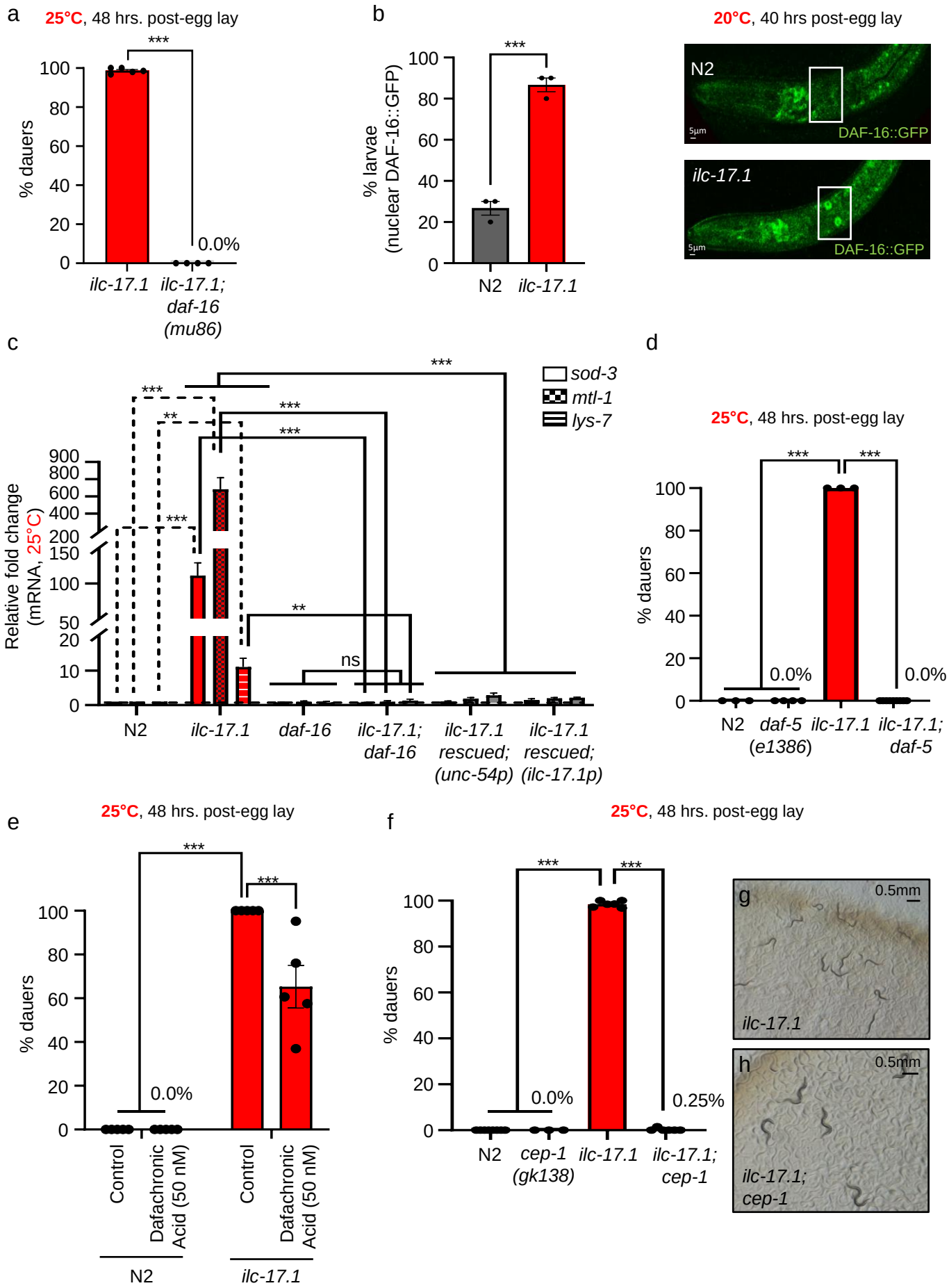
a
25°C, 48 hrs. post-egg lay
% dauers
0.0%
ilc-17.1
ilc-17.1; daf-16 (mu86)
b
% larvae (nuclear DAF-16::GFP)
N2
ilc-17.1
20°C, 40 hrs post-egg lay
DAF-16::GFP
5µm
c
Relative fold change (mRNA, 25°C)
sod-3
mtl-1
lys-7
N2
daf-16
ilc-17.1; daf-16
ilc-17.1 rescued; (unc-54p)
ilc-17.1 rescued; (ilc-17.1p)
ns
d
25°C, 48 hrs. post-egg lay
daf-5 (e1386)
ilc-17.1; daf-5
e
Control
Dafachronic Acid (50 nM)
f
cep-1 (gk138)
ilc-17.1; cep-1
0.25%
g
h
0.5mm

Figure 3

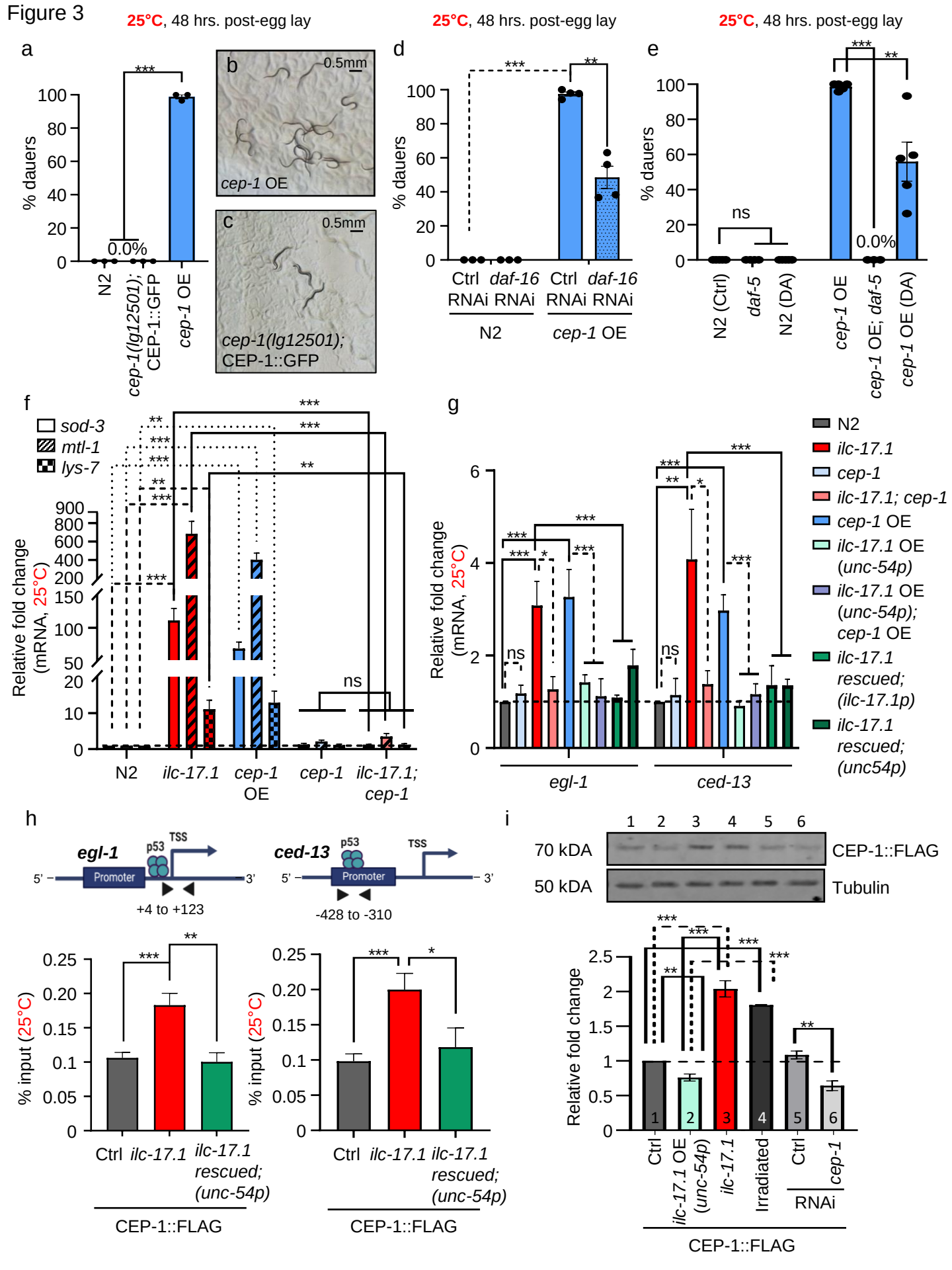
25°C, 48 hrs. post-egg lay
a
% dauers
0.0%
N2
cep-1(lg12501); CEP-1::GFP
cep-1 OE
b
0.5mm
cep-1 OE
c
0.5mm
cep-1(lg12501); CEP-1::GFP
d
Ctrl RNAi
daf-16 RNAi
N2
cep-1 OE
e
ns
N2 (Ctrl)
daf-5
N2 (DA)
cep-1 OE; daf-5
cep-1 OE (DA)
f
sod-3
mtl-1
lys-7
Relative fold change (mRNA, 25°C)
ilc-17.1
cep-1 OE
cep-1
ilc-17.1; cep-1
g
N2
ilc-17.1
cep-1
ilc-17.1; cep-1
cep-1 OE
ilc-17.1 OE (unc-54p)
ilc-17.1 OE (unc-54p); cep-1 OE
ilc-17.1 rescued; (ilc-17.1p)
ilc-17.1 rescued; (unc54p)
egl-1
ced-13
h
p53
TSS
Promoter
5'
3'
+4 to +123
-428 to -310
% input (25°C)
Ctrl
ilc-17.1
ilc-17.1 rescued; (unc-54p)
CEP-1::FLAG
i
70 kDA
50 kDA
CEP-1::FLAG
Tubulin
Relative fold change
Irradiated
RNAi

Figure 4

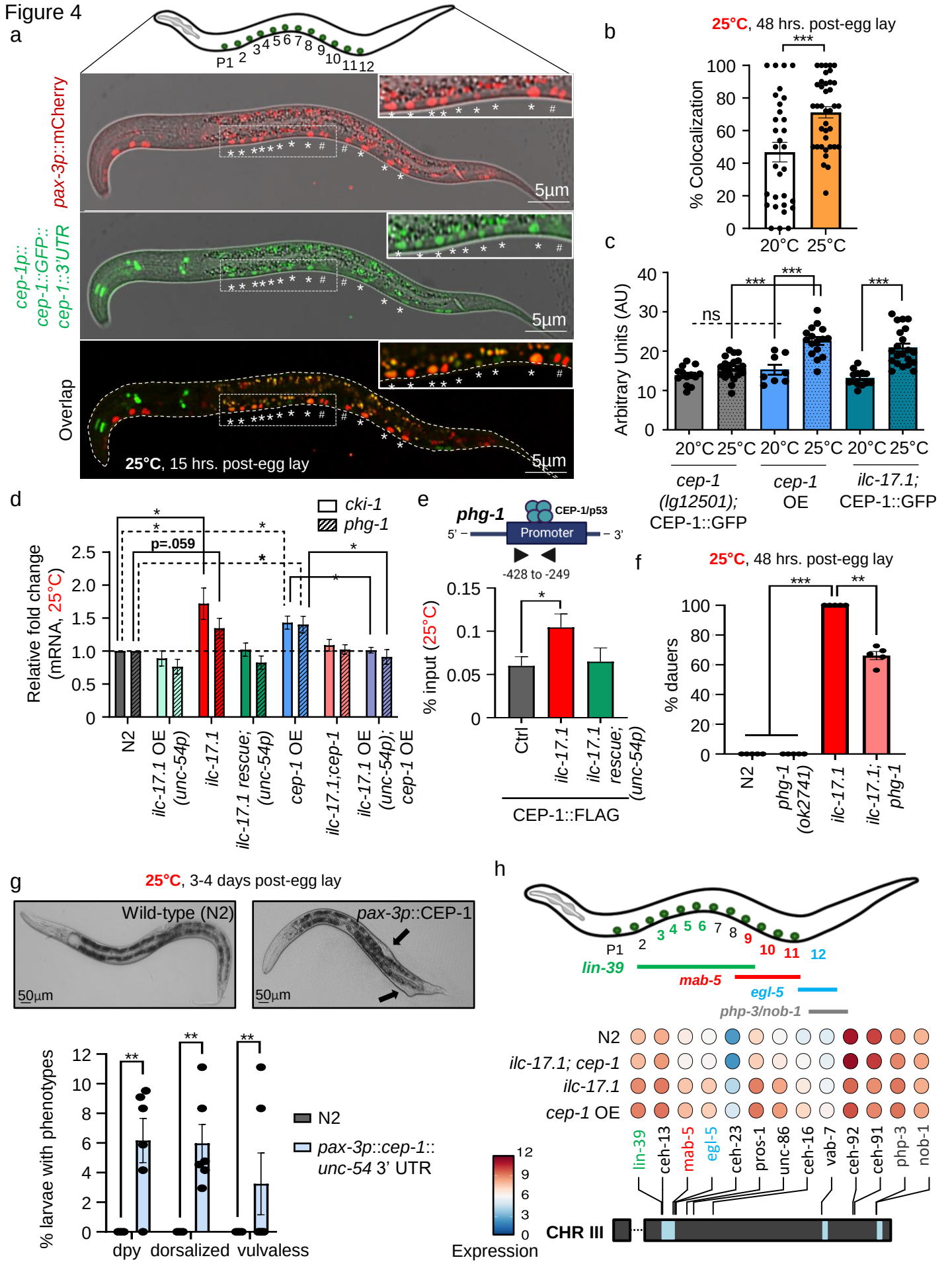
a
P1 2 3 4 5 6 7 8 9 10 11 12
pax-3p::mCherry
cep-1p::
cep-1::GFP::
cep-1::3'UTR
Overlap
5µm
25°C, 15 hrs. post-egg lay
b
25°C, 48 hrs. post-egg lay
% Colocalization
20°C 25°C
c
Arbitrary Units (AU)
ns
20°C 25°C 20°C 25°C 20°C 25°C
cep-1 (lg12501); CEP-1::GFP
cep-1 OE
ilc-17.1; CEP-1::GFP
d
cki-1
phg-1
Relative fold change (mRNA, 25°C)
p=.059
N2
ilc-17.1 OE (unc-54p)
ilc-17.1
ilc-17.1 rescue; (unc-54p)
cep-1 OE
ilc-17.1;cep-1
ilc-17.1 OE (unc-54p); cep-1 OE
e
phg-1
CEP-1/p53
Promoter
5' 3'
-428 to -249
% input (25°C)
Ctrl
ilc-17.1
ilc-17.1 rescue; (unc-54p)
CEP-1::FLAG
f
25°C, 48 hrs. post-egg lay
% dauers
N2
phg-1 (ok2741)
ilc-17.1
ilc-17.1; phg-1
g
25°C, 3-4 days post-egg lay
Wild-type (N2)
pax-3p::CEP-1
50µm
% larvae with phenotypes
dpy
dorsalized
vulvaless
N2
pax-3p::cep-1:: unc-54 3' UTR
h
P1 2 3 4 5 6 7 8 9 10 11 12
lin-39
mab-5
egl-5
php-3/nob-1
N2
ilc-17.1; cep-1
ilc-17.1
cep-1 OE
lin-39 ceh-13 mab-5 egl-5 ceh-23 pros-1 unc-86 ceh-16 vab-7 ceh-92 ceh-91 php-3 nob-1
CHR III
Expression

Figure 5

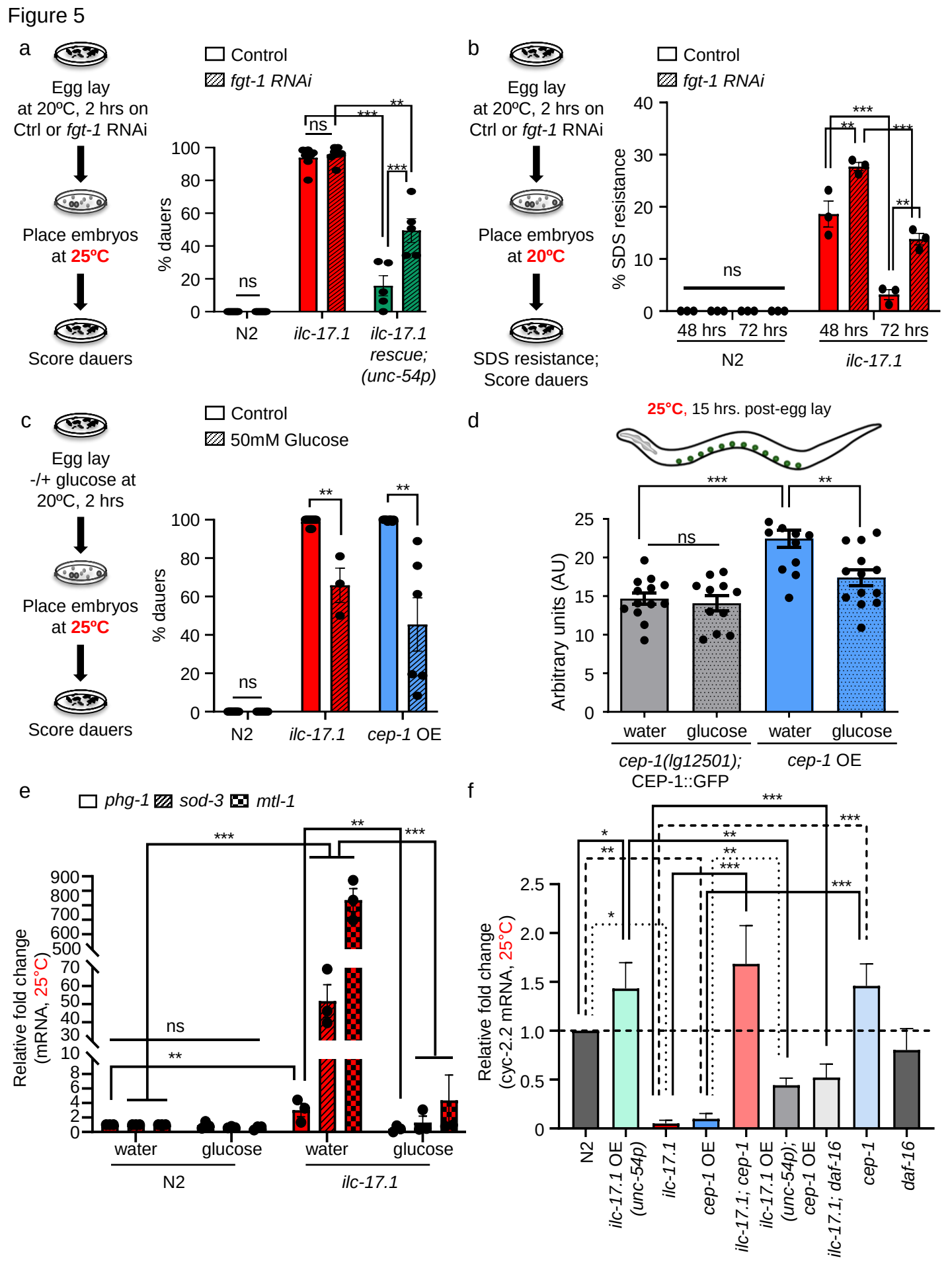
a
Egg lay
at 20ºC, 2 hrs on
Ctrl or fgt-1 RNAi
Place embryos
at 25ºC
Score dauers
Control
fgt-1 RNAi
% dauers
ns
***
**
N2
ilc-17.1
ilc-17.1
rescue;
(unc-54p)
b
Egg lay
at 20ºC, 2 hrs on
Ctrl or fgt-1 RNAi
Place embryos
at 20ºC
SDS resistance;
Score dauers
Control
fgt-1 RNAi
% SDS resistance
48 hrs
72 hrs
N2
ilc-17.1
c
Egg lay
-/+ glucose at
20ºC, 2 hrs
Place embryos
at 25ºC
Score dauers
Control
50mM Glucose
% dauers
N2
ilc-17.1
cep-1 OE
d
25°C, 15 hrs. post-egg lay
Arbitrary units (AU)
water
glucose
cep-1(lg12501);
CEP-1::GFP
cep-1 OE
e
phg-1
sod-3
mtl-1
Relative fold change
(mRNA, 25°C)
water
glucose
N2
ilc-17.1
f
Relative fold change
(cyc-2.2 mRNA, 25°C)
N2
ilc-17.1 OE
(unc-54p)
ilc-17.1
cep-1 OE
ilc-17.1; cep-1
ilc-17.1 OE
(unc-54p);
cep-1 OE
ilc-17.1; daf-16
cep-1
daf-16

Figure 6

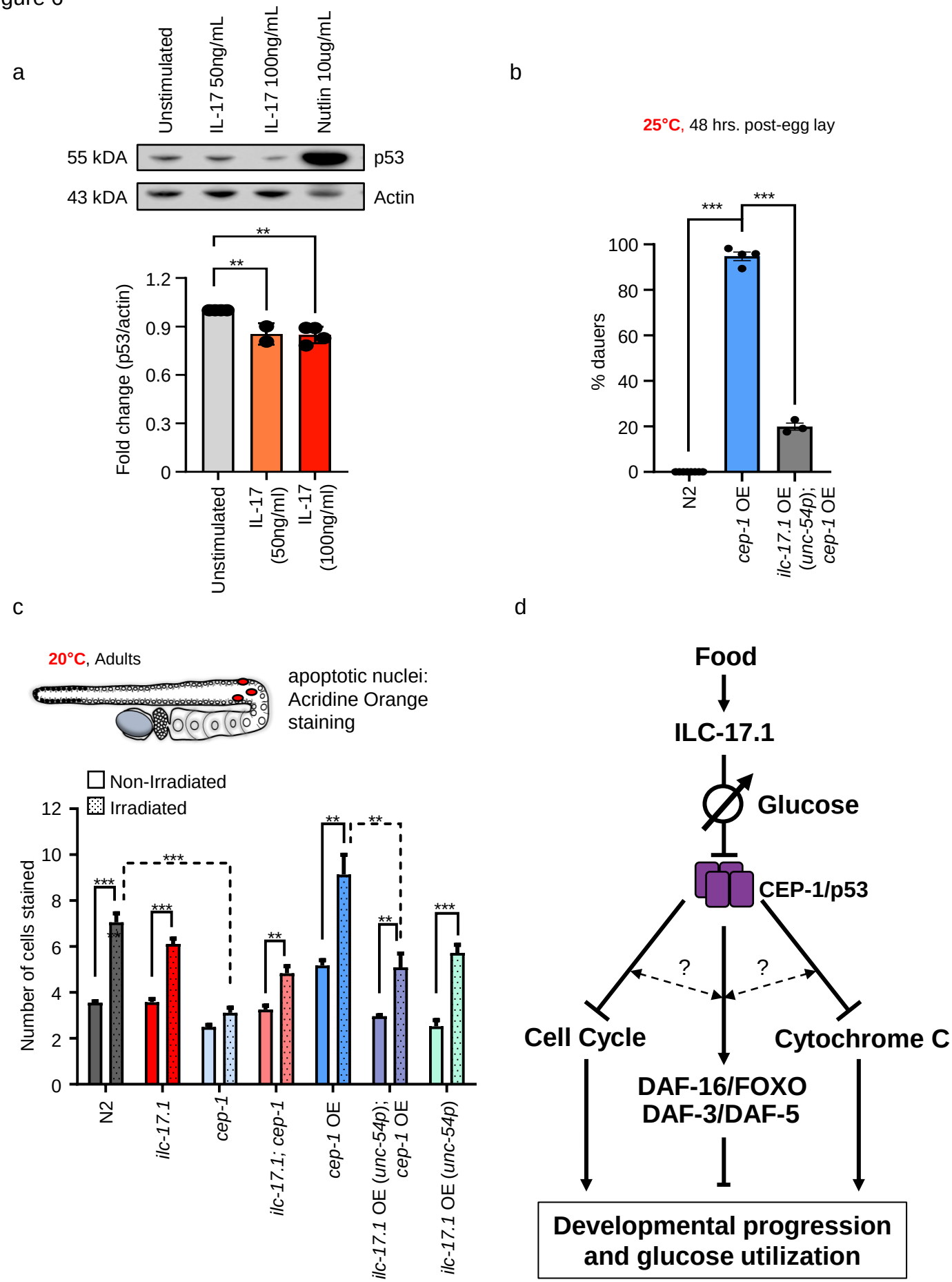
a
Unstimulated
IL-17 50ng/mL
IL-17 100ng/mL
Nutlin 10ug/mL
55 kDA
p53
43 kDA
Actin
Fold change (p53/actin)
1.2
0.9
0.6
0.3
0
**
**
Unstimulated
IL-17 (50ng/ml)
IL-17 (100ng/ml)
b
25°C, 48 hrs. post-egg lay
% dauers
100
80
60
40
20
0
***
***
N2
cep-1 OE
ilc-17.1 OE (unc-54p); cep-1 OE
c
20°C, Adults
apoptotic nuclei: Acridine Orange staining
Non-Irradiated
Irradiated
Number of cells stained
12
10
8
6
4
2
0
N2
ilc-17.1
cep-1
ilc-17.1; cep-1
cep-1 OE
ilc-17.1 OE (unc-54p); cep-1 OE
ilc-17.1 OE (unc-54p)
d
Food
ILC-17.1
Glucose
CEP-1/p53
?
?
Cell Cycle
Cytochrome C
DAF-16/FOXO
DAF-3/DAF-5
Developmental progression and glucose utilization

Figure S1

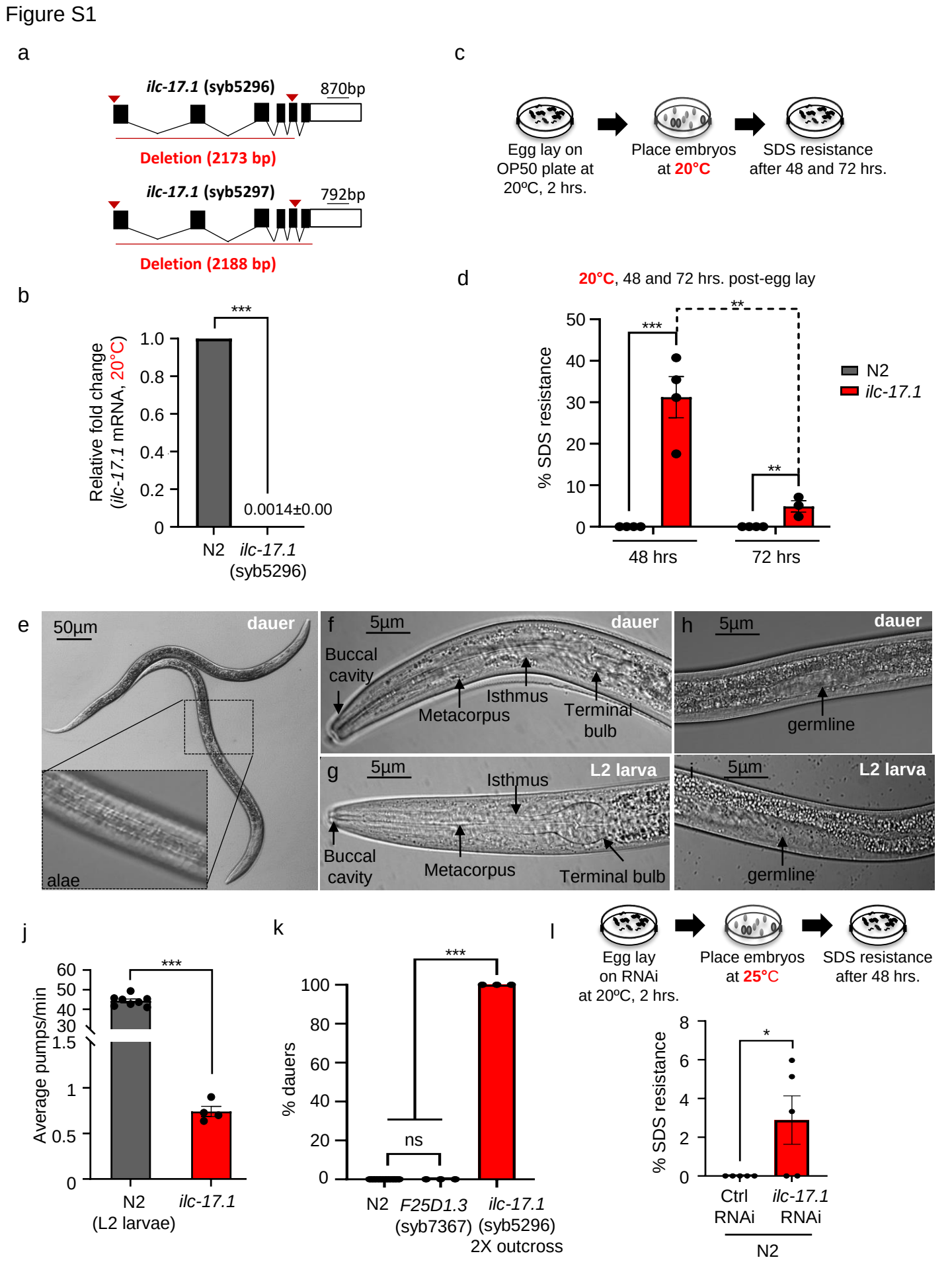
a
ilc-17.1 (syb5296)
870bp
Deletion (2173 bp)
ilc-17.1 (syb5297)
792bp
Deletion (2188 bp)
b
Relative fold change (ilc-17.1 mRNA, 20°C)
1.0
0.8
0.6
0.4
0.2
0
***
0.0014±0.00
N2
ilc-17.1 (syb5296)
c
Egg lay on OP50 plate at 20ºC, 2 hrs.
Place embryos at 20°C
SDS resistance after 48 and 72 hrs.
d
20°C, 48 and 72 hrs. post-egg lay
% SDS resistance
50
40
30
20
10
0
***
**
**
48 hrs
72 hrs
N2
ilc-17.1
e
50µm
dauer
alae
f
5µm
dauer
Buccal cavity
Isthmus
Metacorpus
Terminal bulb
h
5µm
dauer
germline
g
5µm
L2 larva
Isthmus
Buccal cavity
Metacorpus
Terminal bulb
i
5µm
L2 larva
germline
j
Average pumps/min
60
50
40
30
1.5
1
0.5
0
***
N2
ilc-17.1
(L2 larvae)
k
% dauers
100
80
60
40
20
0
***
ns
N2
F25D1.3 (syb7367)
ilc-17.1 (syb5296)
2X outcross
l
Egg lay on RNAi at 20ºC, 2 hrs.
Place embryos at 25°C
SDS resistance after 48 hrs.
% SDS resistance
8
6
4
2
0
*
Ctrl RNAi
ilc-17.1 RNAi
N2

Figure S2

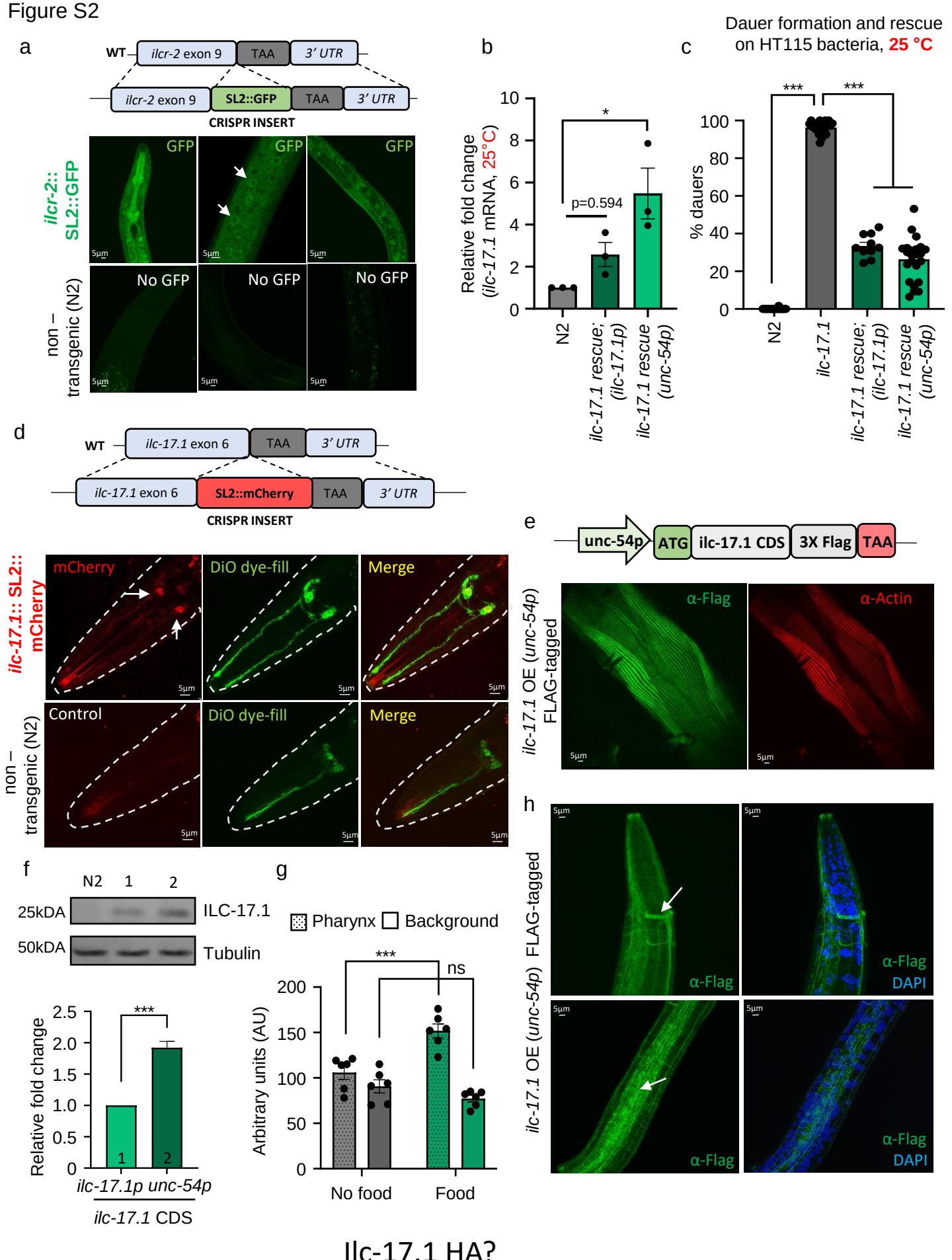

Ilc-17.1 HA?

Figure S3

a

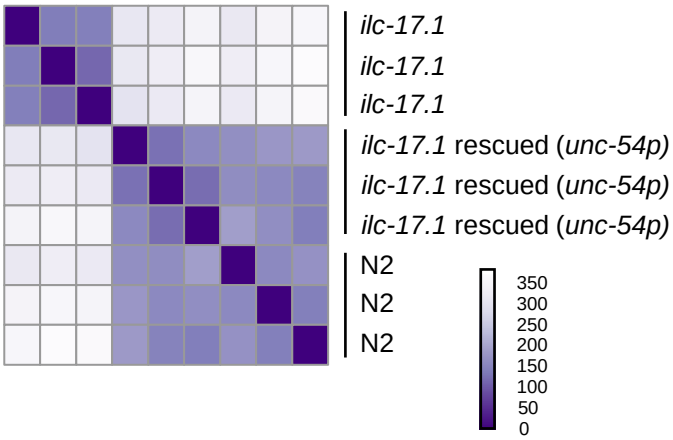

b

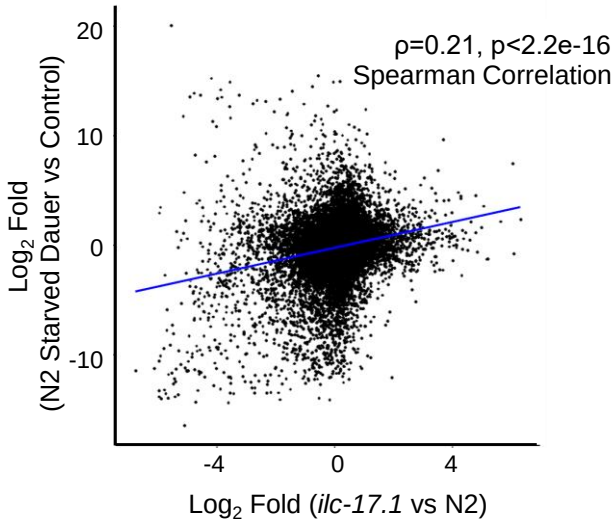

c

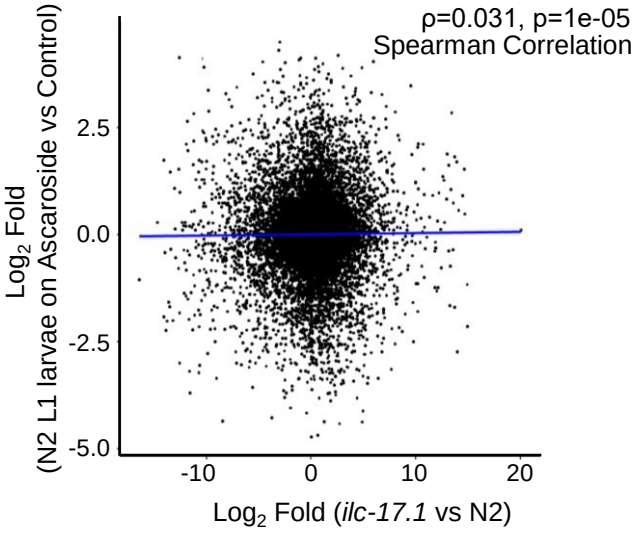

Figure S4

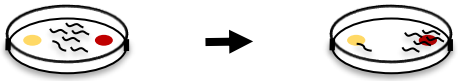

a

Day-one adults placed at center of plate and control (H_2O), OP50, or odor placed at opposite end. Chemotaxis index, after 1 hour

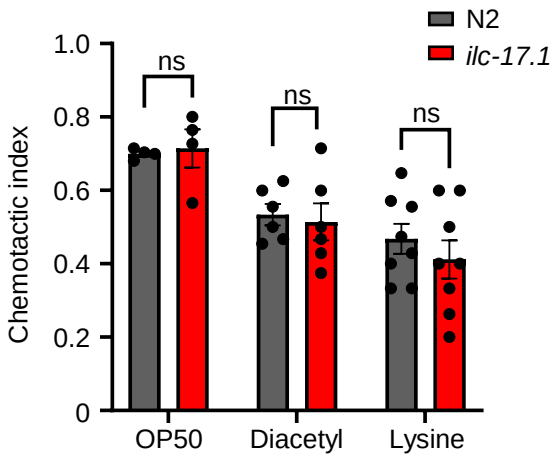

b

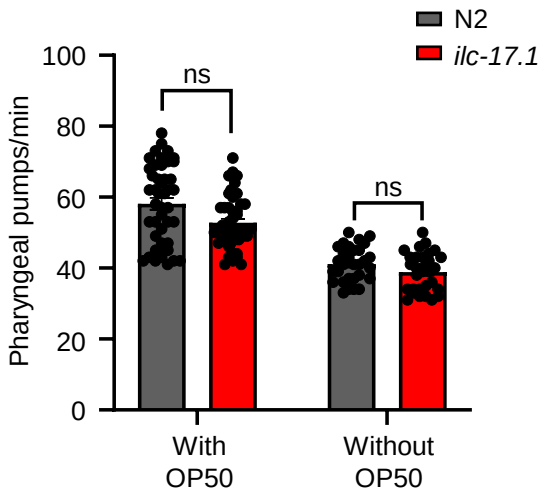

c

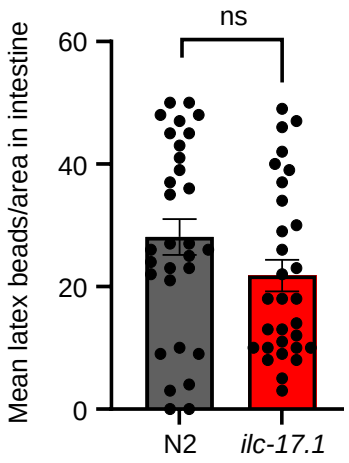

d

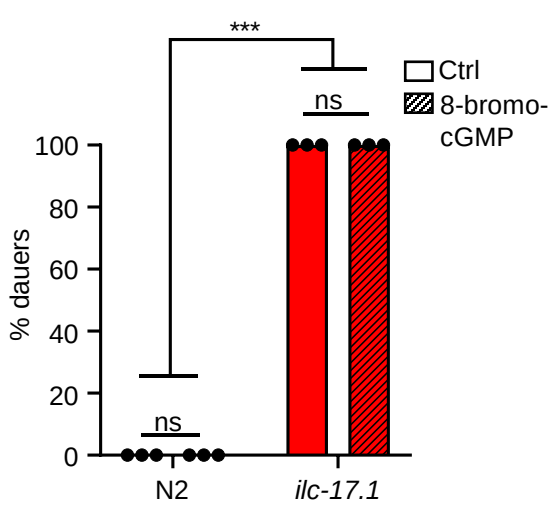

e

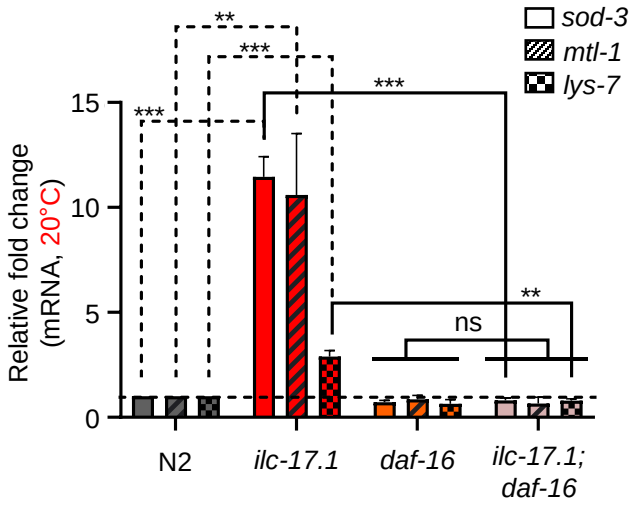

Figure S5

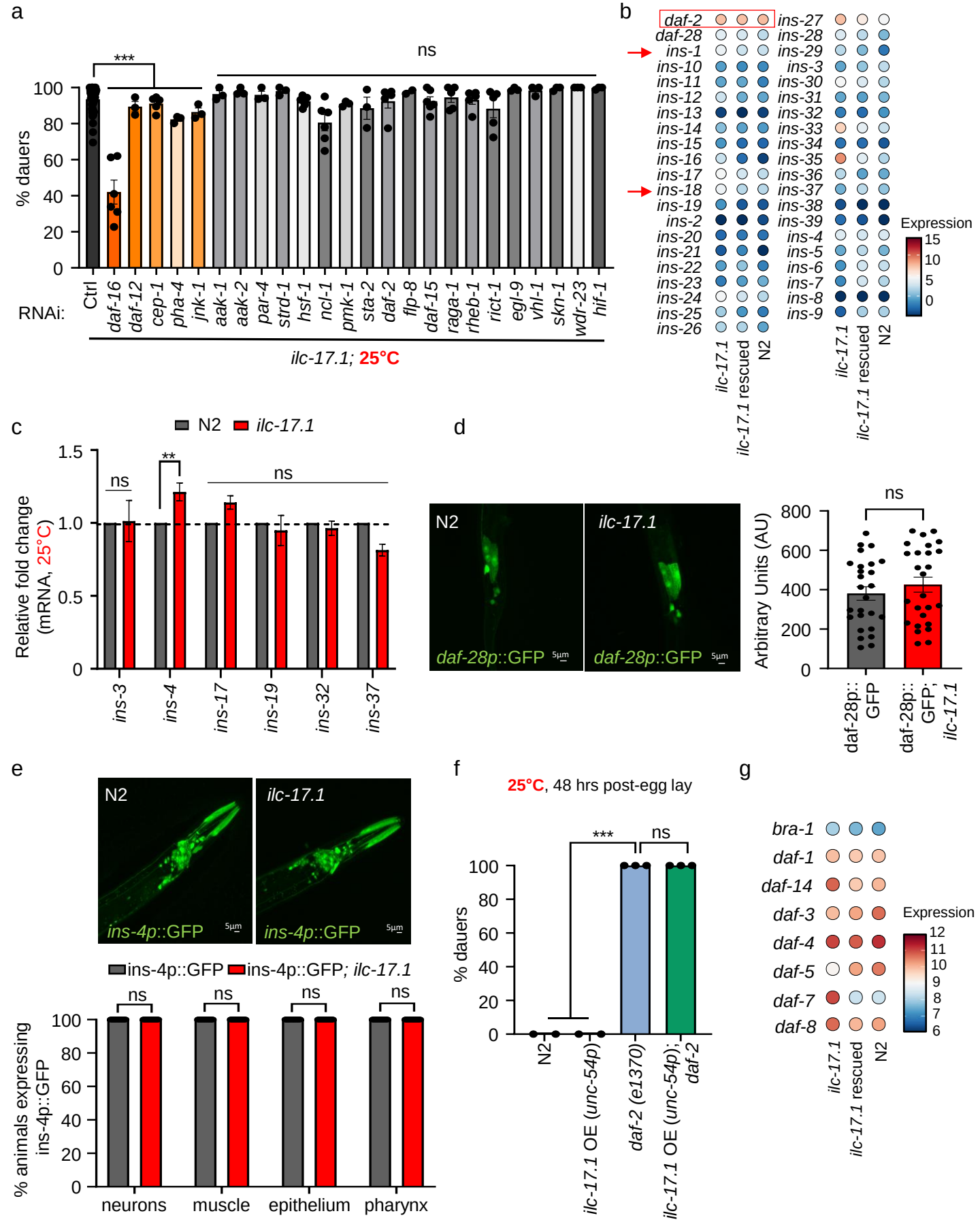
a
***
ns
% dauers
RNAi:
Ctrl
daf-16
daf-12
cep-1
pha-4
jnk-1
aak-1
aak-2
par-4
strd-1
hsf-1
ncl-1
pmk-1
sta-2
daf-2
flp-8
daf-15
raga-1
rheb-1
rict-1
egl-9
vhl-1
skn-1
wdr-23
hif-1
ilc-17.1; 25°C
b
daf-2
daf-28
ins-1
ins-10
ins-11
ins-12
ins-13
ins-14
ins-15
ins-16
ins-17
ins-18
ins-19
ins-2
ins-20
ins-21
ins-22
ins-23
ins-24
ins-25
ins-26
ins-27
ins-28
ins-29
ins-3
ins-30
ins-31
ins-32
ins-33
ins-34
ins-35
ins-36
ins-37
ins-38
ins-39
ins-4
ins-5
ins-6
ins-7
ins-8
ins-9
ilc-17.1
ilc-17.1 rescued
N2
Expression
c
N2
ilc-17.1
Relative fold change (mRNA, 25°C)
ins-3
ins-4
ins-17
ins-19
ins-32
ins-37
d
N2
ilc-17.1
daf-28p::GFP
Arbitrary Units (AU)
daf-28p::GFP
daf-28p::GFP; ilc-17.1
e
N2
ilc-17.1
ins-4p::GFP
ins-4p::GFP; ilc-17.1
% animals expressing ins-4p::GFP
neurons
muscle
epithelium
pharynx
f
25°C, 48 hrs post-egg lay
% dauers
N2
ilc-17.1 OE (unc-54p)
daf-2 (e1370)
ilc-17.1 OE (unc-54p); daf-2
g
bra-1
daf-1
daf-14
daf-3
daf-4
daf-5
daf-7
daf-8
ilc-17.1
ilc-17.1 rescued
N2
Expression

Figure S6

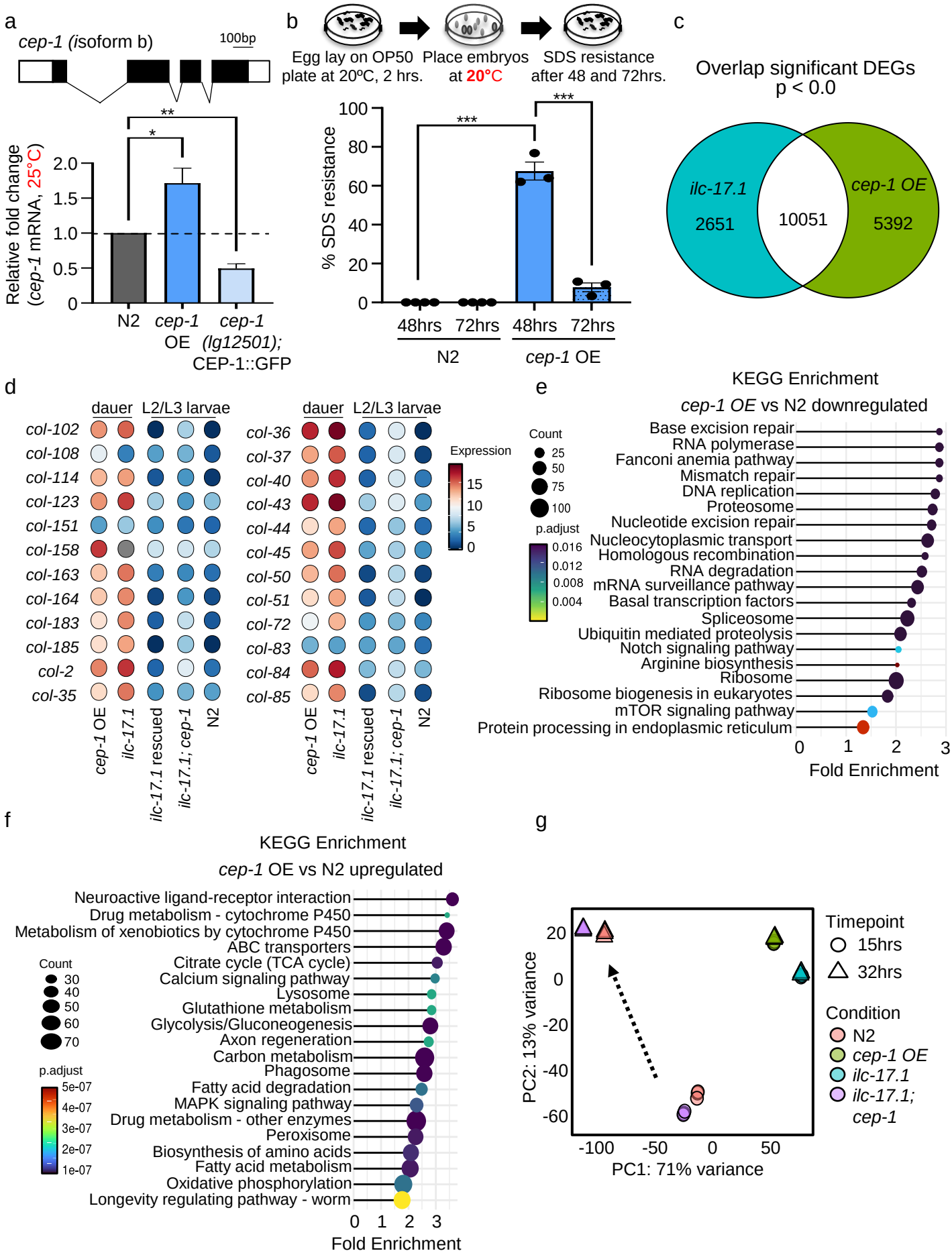
a
cep-1 (isoform b)
100bp
Relative fold change (cep-1 mRNA, 25°C)
2.0
1.5
1.0
0.5
0
**
*
N2
cep-1 OE
cep-1 (lg12501); CEP-1::GFP
b
Egg lay on OP50 plate at 20ºC, 2 hrs.
Place embryos at 20°C
SDS resistance after 48 and 72hrs.
% SDS resistance
100
80
60
40
20
0
***
***
48hrs
72hrs
48hrs
72hrs
N2
cep-1 OE
c
Overlap significant DEGs
p < 0.0
ilc-17.1
2651
10051
cep-1 OE
5392
d
dauer
L2/L3 larvae
col-102
col-108
col-114
col-123
col-151
col-158
col-163
col-164
col-183
col-185
col-2
col-35
col-36
col-37
col-40
col-43
col-44
col-45
col-50
col-51
col-72
col-83
col-84
col-85
cep-1 OE
ilc-17.1
ilc-17.1 rescued
ilc-17.1; cep-1
N2
Expression
15
10
5
0
e
KEGG Enrichment
cep-1 OE vs N2 downregulated
Count
25
50
75
100
p.adjust
0.016
0.012
0.008
0.004
Base excision repair
RNA polymerase
Fanconi anemia pathway
Mismatch repair
DNA replication
Proteosome
Nucleotide excision repair
Nucleocytoplasmic transport
Homologous recombination
RNA degradation
mRNA surveillance pathway
Basal transcription factors
Spliceosome
Ubiquitin mediated proteolysis
Notch signaling pathway
Arginine biosynthesis
Ribosome
Ribosome biogenesis in eukaryotes
mTOR signaling pathway
Protein processing in endoplasmic reticulum
0
1
2
3
Fold Enrichment
f
KEGG Enrichment
cep-1 OE vs N2 upregulated
Count
30
40
50
60
70
p.adjust
5e-07
4e-07
3e-07
2e-07
1e-07
Neuroactive ligand-receptor interaction
Drug metabolism - cytochrome P450
Metabolism of xenobiotics by cytochrome P450
ABC transporters
Citrate cycle (TCA cycle)
Calcium signaling pathway
Lysosome
Glutathione metabolism
Glycolysis/Gluconeogenesis
Axon regeneration
Carbon metabolism
Phagosome
Fatty acid degradation
MAPK signaling pathway
Drug metabolism - other enzymes
Peroxisome
Biosynthesis of amino acids
Fatty acid metabolism
Oxidative phosphorylation
Longevity regulating pathway - worm
0
1
2
3
Fold Enrichment
g
PC2: 13% variance
20
0
-20
-40
-60
-100
-50
0
50
PC1: 71% variance
Timepoint
15hrs
32hrs
Condition
N2
cep-1 OE
ilc-17.1
ilc-17.1; cep-1

Figure S7

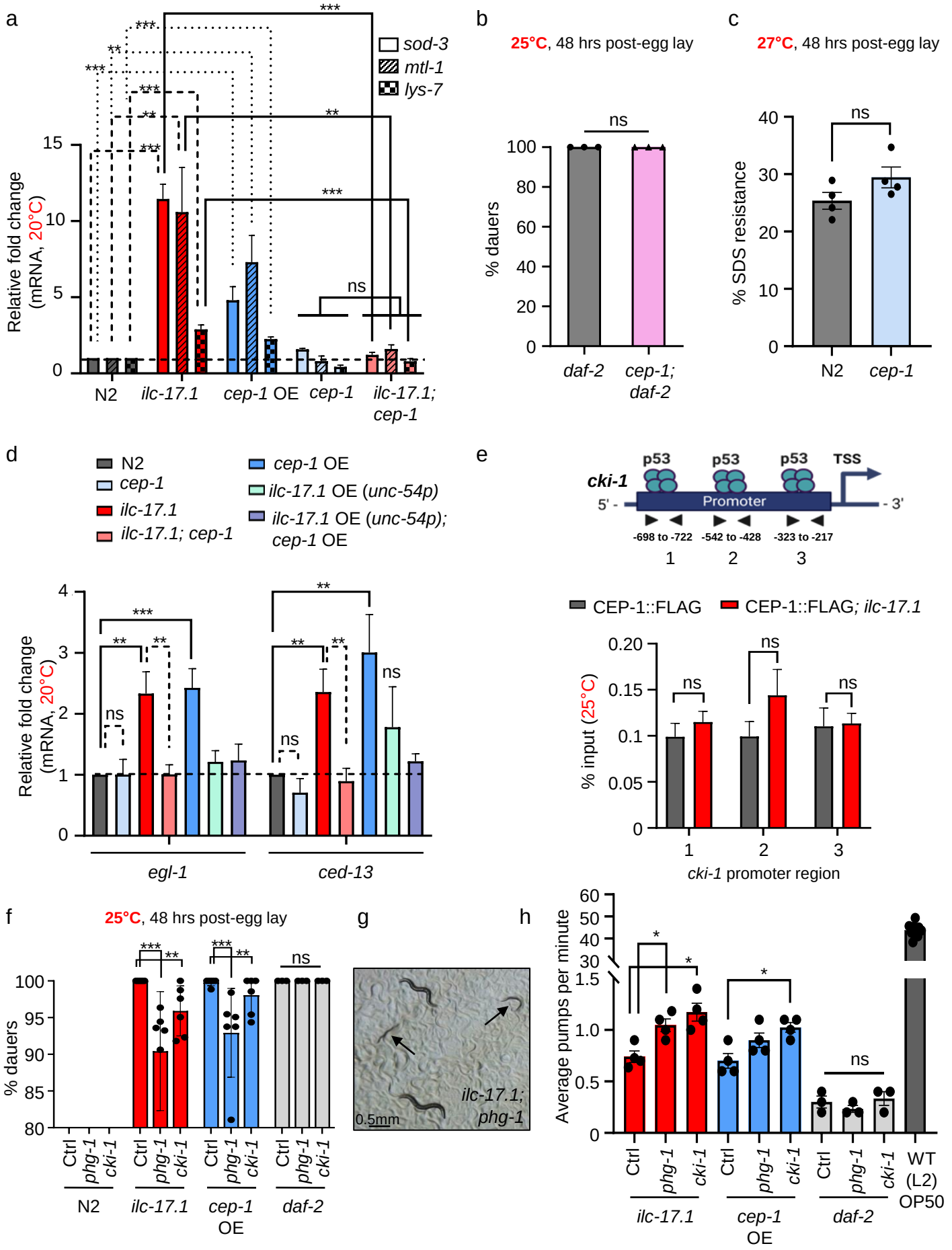
a
sod-3
mtl-1
lys-7
Relative fold change (mRNA, 20°C)
N2
ilc-17.1
cep-1 OE
cep-1
ilc-17.1; cep-1
ns
b
25°C, 48 hrs post-egg lay
% dauers
daf-2
cep-1; daf-2
c
27°C, 48 hrs post-egg lay
% SDS resistance
N2
cep-1
d
N2
cep-1
ilc-17.1
ilc-17.1; cep-1
cep-1 OE
ilc-17.1 OE (unc-54p)
ilc-17.1 OE (unc-54p); cep-1 OE
egl-1
ced-13
e
cki-1
p53
TSS
Promoter
5' -
- 3'
-698 to -722
-542 to -428
-323 to -217
CEP-1::FLAG
CEP-1::FLAG; ilc-17.1
% input (25°C)
cki-1 promoter region
f
25°C, 48 hrs post-egg lay
% dauers
Ctrl
phg-1
cki-1
N2
ilc-17.1
cep-1 OE
daf-2
g
0.5mm
ilc-17.1; phg-1
h
Average pumps per minute
WT (L2) OP50

Figure S8

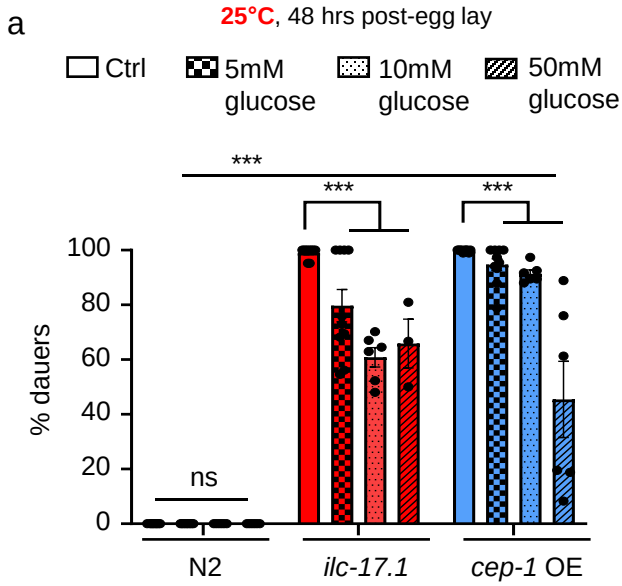
a
25°C, 48 hrs post-egg lay
Ctrl
5mM glucose
10mM glucose
50mM glucose
***
***
***
ns
% dauers
100
80
60
40
20
0
N2
ilc-17.1
cep-1 OE

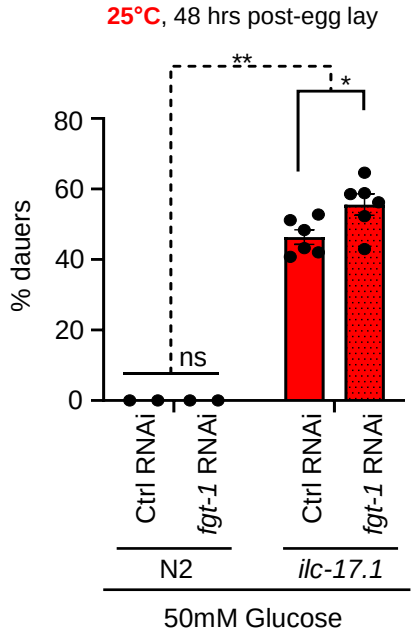
25°C, 48 hrs post-egg lay
b
**
*
ns
% dauers
80
60
40
20
0
Ctrl RNAi
fgt-1 RNAi
Ctrl RNAi
fgt-1 RNAi
N2
ilc-17.1
50mM Glucose

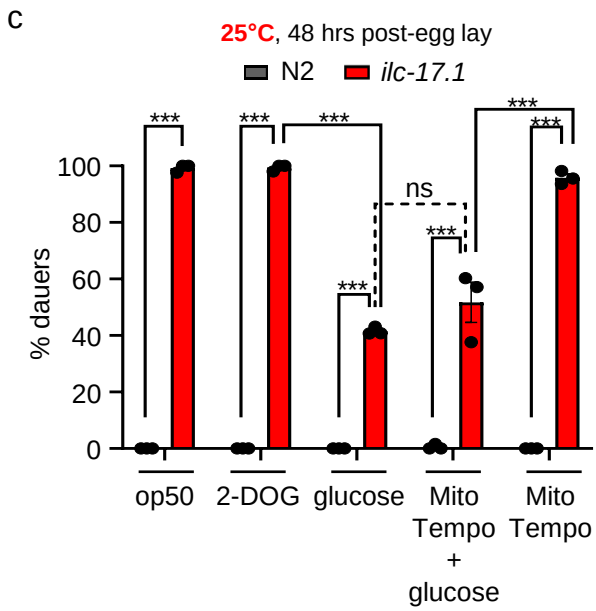
c
25°C, 48 hrs post-egg lay
N2
ilc-17.1
***
***
***
***
***
***
ns
% dauers
100
80
60
40
20
0
op50
2-DOG
glucose
Mito Tempo + glucose
Mito Tempo

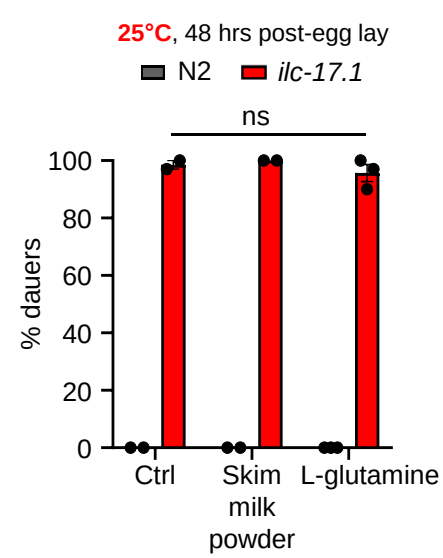
d
25°C, 48 hrs post-egg lay
N2
ilc-17.1
ns
% dauers
100
80
60
40
20
0
Ctrl
Skim milk powder
L-glutamine

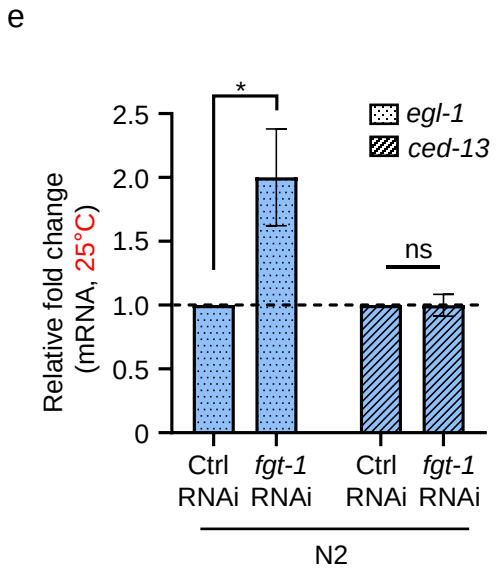
e
*
egl-1
ced-13
ns
Relative fold change (mRNA, 25°C)
2.5
2.0
1.5
1.0
0.5
0
Ctrl RNAi
fgt-1 RNAi
Ctrl RNAi
fgt-1 RNAi
N2

Figure S9

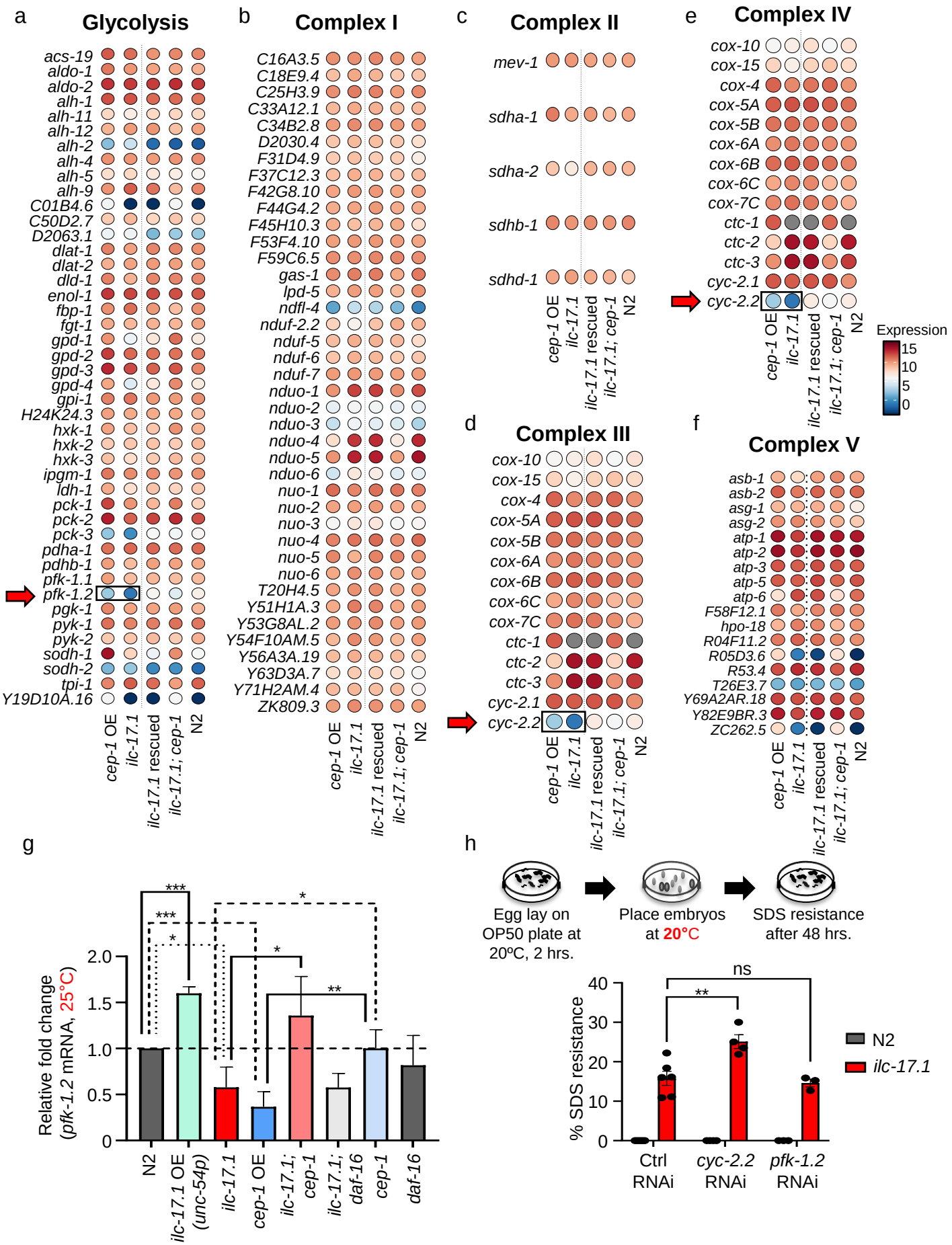
a
Glycolysis
acs-19
aldo-1
aldo-2
alh-1
alh-11
alh-12
alh-2
alh-4
alh-5
alh-9
C01B4.6
C50D2.7
D2063.1
dlat-1
dlat-2
dld-1
enol-1
fbp-1
fgt-1
gpd-1
gpd-2
gpd-3
gpd-4
gpi-1
H24K24.3
hxk-1
hxk-2
hxk-3
ipgm-1
ldh-1
pck-1
pck-2
pck-3
pdha-1
pdhb-1
pfk-1.1
pfk-1.2
pgk-1
pyk-1
pyk-2
sodh-1
sodh-2
tpi-1
Y19D10A.16
cep-1 OE
ilc-17.1
ilc-17.1 rescued
ilc-17.1; cep-1
N2
b
Complex I
C16A3.5
C18E9.4
C25H3.9
C33A12.1
C34B2.8
D2030.4
F31D4.9
F37C12.3
F42G8.10
F44G4.2
F45H10.3
F53F4.10
F59C6.5
gas-1
lpd-5
ndfl-4
nduf-2.2
nduf-5
nduf-6
nduf-7
nduo-1
nduo-2
nduo-3
nduo-4
nduo-5
nduo-6
nuo-1
nuo-2
nuo-3
nuo-4
nuo-5
nuo-6
T20H4.5
Y51H1A.3
Y53G8AL.2
Y54F10AM.5
Y56A3A.19
Y63D3A.7
Y71H2AM.4
ZK809.3
c
Complex II
mev-1
sdha-1
sdha-2
sdhb-1
sdhd-1
e
Complex IV
cox-10
cox-15
cox-4
cox-5A
cox-5B
cox-6A
cox-6B
cox-6C
cox-7C
ctc-1
ctc-2
ctc-3
cyc-2.1
cyc-2.2
Expression
15
10
5
0
d
Complex III
f
Complex V
asb-1
asb-2
asg-1
asg-2
atp-1
atp-2
atp-3
atp-5
atp-6
F58F12.1
hpo-18
R04F11.2
R05D3.6
R53.4
T26E3.7
Y69A2AR.18
Y82E9BR.3
ZC262.5
g
Relative fold change
(pfk-1.2 mRNA, 25°C)
2.0
1.5
1.0
0.5
0
***
***
*
*
*
**
N2
ilc-17.1 OE
(unc-54p)
ilc-17.1
cep-1 OE
ilc-17.1;
cep-1
ilc-17.1;
daf-16
cep-1
daf-16
h
Egg lay on
OP50 plate at
20ºC, 2 hrs.
Place embryos
at 20°C
SDS resistance
after 48 hrs.
% SDS resistance
40
30
20
10
0
ns
**
N2
ilc-17.1
Ctrl
RNAi
cyc-2.2
RNAi
pfk-1.2
RNAi

Figure S10

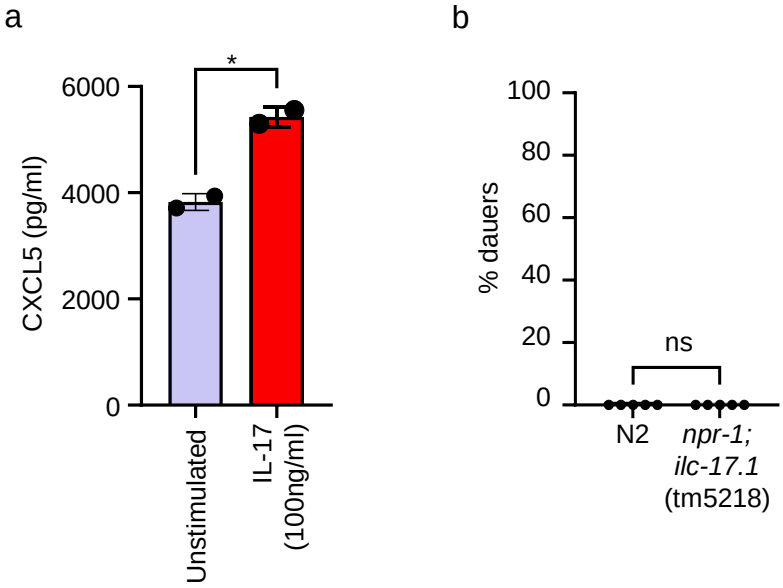
a
*
6000
4000
2000
0
CXCL5 (pg/ml)
Unstimulated
IL-17
(100ng/ml)
b
100
80
60
40
20
0
% dauers
ns
N2
npr-1;
ilc-17.1
(tm5218)